University of Stavanger

Faculty of Science and Technology

MASTER'S THESIS

Study program/ Specialization: MSc Petroleum Technology Production Technology	Spring semester, 2010 Open / ~~Restricted access~~
Writer: Barbro Ramstad	…… (Writer's signature)

Faculty supervisor: Rune Wiggo Time

Laboratory supervisor: Hermonja Andrianifaliana Rabenjafimanantsoa

External supervisor(s): Vidar Alstad, Atle Gyllensten

Title of thesis:

Effect of Water Flow in Gravel Pack with Regards to Heavy Oil Production

Credits (ECTS): 30

Key words: - 1D flow in gravel pack - Physical and experimental modelling of gravel pack - Fluid and gravel pack properties	Pages: …… + enclosure: …… Stavanger, June 15, 2010

Effect of Water Flow in Gravel Pack with Regards to Heavy Oil Production

Master Thesis
By
Barbro Ramstad
Production Technology

Faculty of Science and Technology
Department of Petroleum Engineering
2010

Acknowledgements

I would like to give thanks to Prof. Rune Wiggo Time for providing me with an interesting and challenging master thesis and for his experimental and theoretical guidance.

I would also like to thank Hermonja Andrianifaliana Rabenjafimanantsoa for his excellent guidance through laboratory experiments and providing tools for experiments.
A great thank you to Statoil ASA for help and useful information throughout this study.. Thank you to Ruben Schulkes, Vidar Alstad and Atle Gyllensten from Statoil ASA.

I would also like to say thank you to the Senior Engineers and professors at Departement of Petroleum Engineering, Inger Johanne Munthe-Kaas Olsen for help with different fluids and HSSE data sheets for the different fluids and Svein Myhren for his help with data installations.

Also a great thank you to the other master students in production and reservoir, both at the University of Stavanger and Techniche Universität (TU) Clausthal, Germany, for cooperation during this semester.

I really appreciate the work done by Cristma Plastic, Forus, have done when helping me with building the gravel pack-model.

And last but not the least, I want to say thank you to the great students at multiphase laboratories for excellent team spirit.

Barbro Ramstad,
Master Student Petroleum Technology,
Production Technology
University of Stavanger,
22nd of June, 2010

ABSTRACT

The objective of the thesis is to see how the effect of water is displacing the oil through gravel pack. Experimental solutions have been developed for displacement performance of two vertical displacements and one horizontal. The two vertical displacements were done to calculate the absolute permeability, relative permeabilities and saturations. Production performance and displacement efficiency was also determined to find out the recovery of the vertical displacement. The horizontal displacement was performed to see the occurrence of viscous fingering. It was assumed that after a certain time, water started to cone upwards towards the well and entered the gravel pack. Then the experimental part was to see on how the water was fingering through the gravel pack.
Viscous fingering appeared in both horizontal and vertical displacement. The vertical displacement was also affected by gravity segregation. This was because the displacing water is denser than the displaced oil and the displacing direction is vertical upwards.
Two models have been designed for modeling the gravel pack. The original model was based on experimental setup of the formation and the gravel pack, to see water coning effect in gravel pack. The revised model is the horizontal model used for experimental visualization of the water flow through gravel pack.

Both of the displacements had viscous fingering. The breakthrough of water occurred earlier than anticipated. For the vertical displacement 99% of the oil was displaced while, for the horizontal

INTRODUCTION

Petroleum is the most economical source of energy at the present time. The reservoir is the source of fluids for the productions system. It is the porous, permeable media in which the reservoir fluids are stored and through which the fluids will flow to the wellbore through the gravel pack (1).

Two phase flow in porous media are related to many important industrial and geological applications, such as recovery, ground water flow modelling and effect of water coning. For immiscible flow, a wide range of behaviours are observed depending on the wetting properties of the two fluids, their viscosity ratio, their resepective density and their flowing rate.

In this thesis, the reader will be introduced to the different displacement mechanisms that can occur when water has coned upwards and entered the gravel pack.

This thesis is based on the assumption that somewhere in the production a water cone has started to grow. In a certain time, the water will start to be produced and the production of oil will decline. The behaviour of water is incremental and after a while it will take over the production, and no oil will be produced.

In this study, its adressed which effects a water cone has in a porous medium, where the porous medium is given as a gravel pack. At a certain time, the water cone has occured and production of water will start. The effect of water coning consists of immiscible displacement of less viscous water by a highly viscous oil. There are several effects happening during the displacement.

The gravel pack consists of large grained sand that prevents sand production from the formation. Even if it prevents sand from the formation, it nevertheless allows fluids to flow through. The design of the gravel pack is important and the beads used are sized to be 5 to 6 times larger than the formation sand. The gravel pack will also maintain its permeability under a broad range of producing conditions.

DEFINITIONS AND ABBREVIATIONS

Table 1-1 Definitions

Heterogeneities	Degree of uniformity in porous media
Wettability	The tendency of one fluid to spread on, or adhere to the solid's surface in the presence of another immiscible fluid
Permeability	A medium's fluid-transmission capacity
Relative Permeability	Relative permeability relates the absolute permeability of the porous system with the effective permeability of a particular fluid in the system.
Porosity	Fluid-storage capacity, the void part of the rock's total volume
Saturation	Fraction of pore space that is occupied by a phase
Connate water saturation	Saturation of water when water is displaced by oil
Roundness of porous medium	Degree of angularity of the particle
Sphericity of porous medium	Degree of which the particles approaches a spherical shape
Darcy	The permeability of a porous medium is 1 Darcy if a fluid with viscosity of 1 cP and a pressure difference of 1atm/cm is flowing through the medium's cross-section of 1cm2 at a rate of 1cm3/s
Interstitial water saturation	Saturation at which the water is immobile which means that the permeability to water, krw is zero
Mesh	Number of openings per inch, counting from the center of any wire in the sieve to a point exactly 1-in. distant
Cohesion	The molecules of a fluid are attracted to each other by an electrostatic force
Adhesion	The molecules to a fluid are to some degree attracted to the molecules of an adjoining solid, an electrostatic force
Capillary pressure	The molecular pressure difference across the interface of two fluids

Table 1-2 Abbreviations

α	Interfacial tension
ΔP	Pressure drop
ρ_o	Oil density
ρ_w	Water density
θ	Wetting contact angle
μ	Viscosity of oil or water
Φ	Effective porosity
$\|\Phi\|$	Absolute porosity
$(\lambda_D)_{\bar{S}D}$	Mobility of the displacing phase measured at the average displacing phase saturation at breakthrough
$(\lambda_d)_{\bar{S}d}$	Mobility of the displaced phase measured at the average saturation ahead of the displacement front, just before breakthrough
λ_w	Mobility water
λ_o	Mobility oil
$\bar{v}$	Average velocity of fluid in the pores of the medium
σ_{os}	Surface tension between the oil and the fluid
σ_{ow}	Interfacial tension between water and oil
σ_{ow}	Interfacial Tension between oil and water
σ_{ws}	Surface tension between the water and solid
ω_b	???

A	Interface area
A_d	Surface area of the water-oil contact
A_{glass}	Cross sectional area of glass plate
A_s	Surface area of the water-solid contact
Bt	Breakthrough
d	Diameter
D	Darcy
dP_D	Darcy Pressure Drop
dP_f	Frictional Pressure Drop
dP_h	Hydrostatic Pressure Drop
dP_{tot}	Total Pressure Drop
dX	Delta length
E_A	Area Efficiency
E_D	Displacement Efficiency
E_I	Vertical Efficiency
E_V	Volumetric Displacement Efficiency
f_w	Fractional Flow of Water
G	Gibbs free energy
g	Gravity
H	Height
h_1	Fluid height
H_{glass}	Height of glass plate
k	Absolute permeability
k_e	Effective permeability
k_j	Permeability in layer j
k_o	Permeability oil
k_{ro}	Relative permeability oil
k_{rw}	Relative Permeability water
k_w	Permeability water
L	Length
M	Mass
M	Mobility ratio
$M_{average}$	Average momentum on glass plate
n	Total number of layers
n_i	Number of flooded layers
N_{pBt}	Cumulative oil production
P	Pressure
P_A	Pressure at point A
p_{atm}	Atmospheric pressure, 1.0 bara
P_B	Pressure at point B
P_c	Pressure difference between the wetting and the non-wetting fluid
P_{cow}	Capillary pressure
P_o	Pressure oil
p_o	Oil-phase pressure at a point just above the oil/water interface
P_w	Pressure water
p_w	Water-phase pressure just below the interface
q	Flow rate
q_o	Flow rate oil
q_{real}	Actual flow rate
q_t	Total flow rate
q_w	Flow rate water

r	Radius
R	Pore throat dimension
R	Regression factor
Re	Reynolds number
RF	Recovery efficiency
S_{iw}	Interstitial water saturation
S_{or}	Reducable oil saturation after displacement by water
S_{oi}	Initial oil saturation
S_{owr}	Critical oil saturation in oil/water system
S_w	Saturation water
S_{wc}	Saturation water connate
S_{wi}	Saturation water irreducible
T	Temperature
t	Time
t_{glass}	Thickness of glass plate
u	Fluid velocity
V_b	Bulk volume
V_g	Volume gas
V_o	Volume oil
V_{oi}	Initial oil volume
V_p	Total volume of interconnected voids (pore volume)
V_{pa}	Total void volume
V_t	Total volume produced
V_w	Volume water
X_{sw}	Location of water saturation

LIST OF FIGURES

LIST OF PLOTS

LIST OF TABLES

TABLE OF CONTENTS

1 OBJECTIVES

1.1 Objectives of the project

The objective of this project is to find out how flow is behaving in gravel pack with 1D displacement of oil. This thesis is given by the Production Technology, TNE RD RCP, Statoil ASA, department Porsgrunn.

The assignment is prepared to give an understanding of fluid flow through gravel pack. The reader will be introduced to some of the different reservoir conditions like porosity, permeability, saturation and other important reservoir conditions needed for a proper modelling of gravel pack. Water coning in horizontal wells will be introduced to some extent, since the main problem from the beginning of was to see the effect of flow in gravel pack with influence from water coning in oil reservoir.

Further on the reader will be introduced to modelling of gravel pack and horizontal displacement of oil in a porous medium.

The different parts discussed in this thesis are, as mentioned before, reservoir conditions, 1D displacement of oil through a porous medium, Modelling of gravel pack, properties of test cell and gravel pack model, horizontal displacement efficiency, displacement mechanisms, production of oil, and determination of fluid properties.

Tools and software used will be mentioned in one chapter, but among them are tools for determining viscosity, density and porosity. The software used, Lab View, was together with Rosemount dP logger, measuring the pressure difference for the flow rate in the gravel pack.

The different results have been reviewed and discussed in the discussion part.

1.2 Laboratory Study

The thesis Effect of Water Flow in Gravel Pack with Regards to Heavy Oil Production is a laboratory study where there have been performed laboratory experiments and analysis of actual measured data. Many different literature sources to obtain the information needed have been used. Society of Petroleum Engineers (SPE) has many of the articles and research done by different companies and professors. International Journal of Multiphase flow, Science Direct, Springer Link and the Petroleum Engineering Handbooks have been effectively used together with different reservoir literature. In these different books and web pages it is possible to find papers, definitions, abbreviations and documents needed for this thesis. Other books, assignments and documents related to this thesis have been used.

The author of this thesis had the chance to talk with the representatives from Statoil where they presented high understanding of the field of this thesis, everything from the design to simulation of the gravel pack. The information provided gave the author a satisfactory understanding of the thesis.

The laboratory experiments were performed at the multiphase laboratory, University of Stavanger (UiS). The tools and software used have been presented further in this thesis.

Several experiments have been done to get the overall result. The modelled gravel pack is for a horizontal well and the flow is modelled in 1 dimension.

1.3 Share of Work

This assignment is done by one master thesis in Production Technology with specialization in Production Technology. The writer built and modelled her own gravel pack model, did several experiments on displacement and made a discussion out of the obtained results.

2 GRAVEL PACK CONDITIONS

2.1 Properties of gravel pack

2.1.1 Porosity

The rock's porosity, or fluid-storage capacity, is the void part of the rock's total volume, unoccupied by the rock grains and mineral cement. Absolute porosity,$|\Phi|$, is defined as the ratio of the total void volume, V_{pa}, to the bulk volume, V_b, of a rock sample, irrespective of whether the voids are interconnected or not(2).

$$|\phi| = \frac{V_{pa}}{V_b} \tag{2-1}$$

Effective porosity,Φ, means the ratio of the total volume of interconnected voids, V_p, to the bulk volume, V_b, of the sample (2).

$$\phi = \frac{V_p}{V_b} \tag{2-2}$$

Effective porosity depends on several factors, such as the rock type, grain size range, packing and orientation, content and hydration of clay minerals. Porosity is a static parameter, comparing to permeability which defines the rock's fluid-transmission capability and relates to the condition where the fluid is moving through a porous medium (3).

2.1.2 Permeability

The permeability of a medium is an expression of the medium's fluid-transmission capacity and can be considered as a reverse of the medium's resistivity to an internal flow of fluids (2) Permeability in a reservoir rock is associated with its capacity to transport fluids through a system of interconnected pores (4). Only single phase permeability is considered in this thesis.

In order to calculate the absolute permeability the medium must be 100% saturated with oil and neither the fluid nor the medium should react chemically, or by adsorption or absorption.

In general terms the permeability is a tensor, since the resistance towards fluid flow will vary, depending on the flow direction (3).

Relative permeability together with capillary pressure relationships is used to measure the amount of oil and for predicting the capacity for flow of oil and water (5). The relative permeability and the capillary pressure can vary from place to place in the gravel pack. The relative permeability have not been considered for the modelling of gravel pack because of its complexity, but have been calculated for finding the fractional flow in the reservoir and for the front velocity of the displacement. Capillary pressure has been neglected in this thesis, but will be mentioned because of its importance in measuring interfacial tension in the gravel pack.

The relative permeability represents the flow through a porous medium. Relative permeability relates the absolute permeability of the porous system with the effective permeability of a

particular fluid in the system. In this case the absolute permeability is measured with oil and the displacing fluid is water. For 100% saturation, the effective permeability is equal to the absolute permeability, $k_e = k$. When measuring the flow rate, q, of a fluid versus the pressure difference, it is possible to obtain, for single phase flow (2);

Darcy Equation $$q = \frac{k_e A}{\mu} \frac{\Delta P}{L} \quad \textbf{(2-3)}$$

Maximum effective permeability is found from:

Oil $$k_o(S_w=S_{wc}) = k \times k_{ro}' \quad \textbf{(2-4)}$$

Water $$k_w(S_w=S_{wc}) = k \times k_{rw}' \quad \textbf{(2-5)}$$

Relative permeability of water and oil

It is important to consider that permeability only can be regarded as a constant property of a porous medium if there is a single fluid flowing through it. This is an absolute permeability, which is constant for a particular medium, and independent of the fluid type (2). When several phases or mixtures of fluids are passing through a rock simultaneously, each fluid phase will counteract the free flow of the other phases and reduced the effective permeability (3). The effective permeability of each fluid strongly depends upon the relative saturation and may be much lower than the absolute permeability of the medium. The relative permeability to a fluid is the ratio of the rock's effective permeability to a particular fluid over its absolute permeability (2).

To have an increased capacity of flow, the permeability needs to be high. The following relative permeabilities are defined below, where they are specifically written for water and oil flow in horizontal direction. Gravitational effects have been neglected (5).

Oil $$q_o = \frac{k k_{ro} A}{\mu_o} \frac{\partial p_o}{\partial x} \quad \textbf{(2-6)}$$

Water $$q_w = \frac{k k_{rw} A}{\mu_w} \frac{\partial p_w}{\partial x} \quad \textbf{(2-7)}$$

The relative permeabilities can also be found from the effective and absolute permeability (6):

Oil $$k_{ro} = \frac{k_o}{k} \quad \textbf{(2-8)}$$

Water $$k_{rw} = \frac{k_w}{k} \quad \textbf{(2-9)}$$

The difference in pressure between the two phases is called capillary pressure:

$$P_{cow} = p_o - p_w \quad \textbf{(2-10)}$$

The relationship between the two pressures can range from large negative values to large positive. Normally the relative permeabilities and the capillary pressures are functions of saturations of phases in the porous media and this will be for oil and water flow, $k_{ro}(S_w)$, $k_{rw}(S_w)$:

$$k_{rw}(S_w) = \frac{k_w(S_w)}{k} \quad \textbf{(2-11)}$$

$$k_{ro}(S_w) = \frac{k_o(S_w)}{k} \quad \textbf{(2-12)}$$

The model considered in this thesis will be capable of simulating the flow in two phases, oil and water. At a reservoir location where several phases are flowing simultaneously, the effective permeability k_e of the phases will normally be smaller than the absolute permeability k. The relative permeability for both water and oil are calculated in the result part, and the equations are shown above (6). The value of relative permeability lies normally in between 0 and 1 (6).

$$0 \le k_{ro,w} \le 1 \quad \textbf{(2-13)}$$

Where $k_{ro,w}$ are the relative permeability for oil and water. Since the system in this model is a water/oil system the relative permeability of water, k_{rw}, and oil, k_{row}, are measured as functions of water saturation S_w. The number of water saturation will influence the amount of water initially. The , S_{owr}, is 0.2, referred to as the largest oil saturation for which oil relative permeability is zero. The maximal water saturation is 1.00, which means that there is only water below the water/oil contact (6).

2.1.3 Saturation

Saturation is defined as the "fraction of pore space that is occupied by a phase" (7). For oil and water flow the saturation will be:

$$P_{cow} = p_o - p_w \quad \textbf{(2-14)}$$

$$S_o + S_w = 1 \quad \textbf{(2-15)}$$

A representative elementary volume of particles is considered. The pores are filled with oil. The pore's contents can be written as follows (2):

$$V_p = V_o + V_g + V_w \quad \textbf{(2-16)}$$

Let's take two fluids, oil and water. The fluids are distributed unevenly in the pore space due to the wettability preferences. The adhesive forces of one fluid against the pore walls and on the surface of the grains are always stronger than those of the other fluid (2).

The fluid saturation, S_o and S_w, in the reservoir will vary in space. This is most notably from the water-oil contact to the reservoir top. During production the fluid saturation will also vary (2).

Residual Saturation

Not all of the oil present in the reservoir rock's pores can be removed from the reservoir during production. The oil recovery factor can be as low as 5-10% and high as 99.99%.

Higher than 70% is rarely, and it depends on the reservoir quality and the oil-recovery method (2).
The remaining oil in the reservoir is a residue, and can be called residual oil. The fluid saturation and the oil-recovery factor needs to be estimated (2). When the pore volume, V_p, is estimated, then it is possible to calculate the residual oil (2):

$$S_{or} = \frac{V_{oi} - V_o}{V_p} \quad \textbf{(2-17)}$$

Irreducible Water Saturation

Irreducible water saturation, S_{wi}, is the lowest saturation water can have when it is displaced by oil in the test model. The state is achieved when oil is displacing water in a water wet medium (8). The relative permeabilities can also be termed as the effective permeability. The effective permeability of oil at irreducible water saturation, $k_o(S_{wi})$ is used to normalize relative permeabilities (7).

$$S_{wi} = \frac{V_{wi} - V_w}{V_p} \quad \textbf{(2-18)}$$

Endpoint Saturations

The most encountered saturation endpoints are residual oil saturation and irreducible water saturation. The residual oil and the irreducible water refers to the remaining saturation after first displacing oil by water and then by oil again, which means displacing one phase with another phase (7).

Residual oil relationships

Residual oil saturation refers to the remaining oil saturation after displacing by water, where the displacement starts near the maximum initial oil saturation: $= 1 - S_{wi}$ (7).

Residual irreducible water saturation

The residual or irreducible water saturation is the lowest water saturation that can be achieved by displacement of oil. The water saturation also depends on the extent of displacement and its displacement efficiency, and also by how many pore volumes of the displacing fluid that is injected. S_{wi} also varies with increasing breadth of grain size distribution. S_{wi} should occur when small clusters of consolidated media of one grain size are surrounded by media of another grain size. If the grains of the clusters are larger than those of the surrounding media, S_{wi} decreases, if it is smaller S_{wi} increases (7).

Connate water saturation, S_{wc}, is the saturation of water when water is displaced by oil. S_{wc} differentiate from S_{wi}, because if the processes that produced connate water can be replicated, then S_{wi} should be the same as S_{wc}. It is also significant to its connection with initial oil or gas saturation in a saturated model. For an oil saturated model:

$$S_o = 1 - S_{wc} \quad \textbf{(2-19)}$$

The connate water saturation will also affect the relative permeability, in that way that gravel pack with a low permeability compare to one with high permeability, the relative permeability

to oil are higher for the gravel pack with a low permeability than it is for the one with high permeability (7).

2.1.4 Interfacial tension

Interfacial tension is the tension between two interfaces of two fluids. Depending on the magnitude of the intra- and interfluid cohesive forces, the interfacial tension might be either positive or negative. When the molecules of each fluid are strongly attracted to the molecules of their own kind and the fluids are immiscible, the interfacial tension is positive, $\sigma > 0$.

The reservoir fluids used belong to the immiscible category, but even water and oil can be miscible and developed to a certain extent by use of chemical techniques. The interface between two immiscible fluids can be considered as a membrane- like equilibrium surface separating phases with relatively strong intermolecular cohesion and little or no molecular exchange. The cohesive force is stronger on the denser' fluid side and this means that there is a sharper change in molecular pressure across the boundary surface. The boundary surface is in a state of tangential tension called the interfacial tension, σ.

At the interface of water and oil, the molecules of each fluid are attracted symmetrically to one side of the boundary and are therefore less free to move and accelerate. On the average they have less kinetic energy than the molecules on either side of the boundary . Since the energy of molecules is a function of temperature, and since the temperature is uniform, the potential energy of the molecules in the boundary zone is greater than that of the bulk-fluid molecules on either side.

A molecule at surface of the fluid has a higher potential energy than the bulk of the phase's molecules, because of the anisotropy of intermolecular attractions and dynamic interactions (collisions). The energy or work that is required to move a molecule from interior of the liquids phase to the surface and to increase the surface area.

The surface area is proportional to the potential energy of the fluids phases' energy, the surface area of the fluid phase is always minimized.

The interfacial tension can be formulated as follows:

$$\sigma = \left(\frac{\partial G}{\partial A}\right)_{T,P,M,_{1,2}} \quad \textbf{(2-20)}$$

The stronger the intermolecular attractions in the fluid phase, the greater the work needed to bring its molecules to the surface and the greater the interfacial tension, σ. The interfacial tension between a liquid and its vapour phase, the liquids surface tension, is in the range of 10-80 mN/m.

2.1.5 Capillary Forces

A petroleum reservoir, saturated with more than one fluid is a complex system of mutual static interaction of water, oil, gas and the rock mineral solids. A combined effect of these phenomena controls the saturation distribution and contacts of fluids in a reservoir. The effect of these phenomena controls the saturation distribution and contacts of fluids in a reservoir. The molecules of a fluid are attracted to each other by an electrostatic force, called *cohesion*. All the fluids have intrafluid molecular attraction, and if this attraction is stronger than the interfluid attraction, the two fluids are immiscible (2). The intrafluid molecular attraction is

the inner forces between molecules in the fluid, and the interfluid attraction means the force between the fluids. This gives a respectable understanding that the two fluids will be immiscible, like water and oil. The molecules to a fluid are to some degree attracted to the molecules of an adjoining solid, an electrostatic force called *adhesion*. If one or more fluid is present in the reservoir the most adhesive one sticks to the solid's surface and is called the wetting fluid.

The interfacial tension between two immiscible fluids in contact with each other depends on the chemical composition of the fluids and is very sensitive to chemical changes at the fluid contact (2).

2.1.6 Wettability

Wettability can be defined as "*the tendency of one fluid to spread on, or adhere to the solid's surface in the presence of another immiscible fluid*". The wettability can be measured by finding the contact angle between the liquid-liquid interface and the solids surface. The wetting angle, θ, is reflecting the equilibrium between the interfacial tension of the two fluid phases, and individual adhesive attraction to the solid. The angle is measured on the denser fluids side of the interface. If the angle is less than 90º, the denser fluid is the wetting phase. If the angle is above 90º, the lighter fluid is considered to be the wetting phase. The wettability of a solid's pore walls depends upon the chemical composition of the solid and fluid and the solids mineral composition (2).

Wetting Angle

For oil and water as two immiscible fluids, there are three types of interfacial tension to consider, σ_{os}, σ_{ws}, σ_{wo}, but they are not independent of each other (2).

2.1.7 Capillary Pressure

The consideration of the wettability of pores leads us to the concept of wettability. This is the phenomenon whereby liquid is drawn up a capillary tube (9). When two immiscible fluids are in contact with each other in a narrow capillary tube, glass pipe, or a glass basin, the stronger adhesive force of the wetting fluid causes their interface to curve. There will be an axisymmetric meniscus developed, convex towards the wetting fluid, and the angle of the meniscus contact with the pipe's wall is the wetting angle, θ (9).

The capillary pressure is the difference between the ambient pressure and the pressure exerted by the column of liquid. It is possible to say that the capillary pressure can be defined as "*the molecular pressure difference across the interface of two fluids"* (9). The pressure difference can be calculated from the external (adhesive) and internal (cohesive) electrostatic forces that is acting on the two fluids (9). Capillary pressure increases with decreasing tube diameter, or with a decreasing pore size (9).

Capillary pressure is also related to the surface tension generated by the two adjacent fluids. In this case it is water and oil.

Capillary pressure can be tested by which samples of 100% of one fluid are injected with another (oil, gas, water). The injected fluid begins to invade the reservoir and we have the displacement pressure. As the pressure increase, the proportions of the two fluids gradually reverse until the irreducible saturation point is reached, and no further invasion by the second fluid is possible at any pressure (9).

The capillary pressure in tubes is little bit different. If the pipe is vertical and the fluids are water and oil, the greater pressure of the water will displace the oil in the pipe to some height, until equilibrium is reached between the pressure difference and the fluid gravity. P_c is the pressure difference between the wetting and the non-wetting fluid (9).

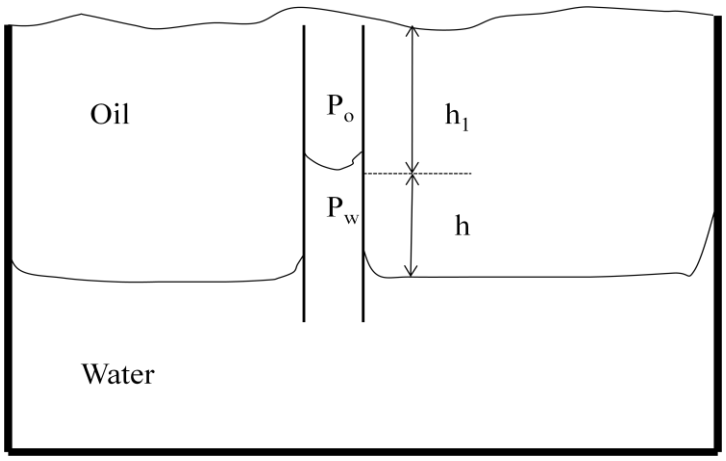

Figure 2-1 Capillary pressure resulting from interfacial forces in a capillary tube. This is an oil wet system, where the meniscus is concave.

Figure 2-1 shows water rise in a glass capillary. The fluid being displaced is oil, and the water saturate the glass and there is a capillary rise. The two pressures of oil and water, p_o and p_w are identified.

Force balance:

Oil $$p_o = p_{atm} + \rho_o g h_1 \quad \textbf{(2-21)}$$

Water $$p_w = p_{atm} + \rho_w g(h_1 + h) - \rho_w g h \quad \textbf{(2-22)}$$

$$p_o - p_w = h(\rho_w - \rho_o)g = P_c \quad \textbf{(2-23)}$$

From the equation it is possible to see that there exists a pressure difference across the interface, which is the capillary pressure P_c.

Interfacial tension between oil and water:

$$\sigma_{ow} = \frac{rgh(\rho_w - \rho_o)}{2 \cdot \cos\theta} \quad \textbf{(2-24)}$$

Equation (2-23) and equation (2-24) gives:

$$\sigma_{ow} = \frac{rP_c}{2 \cdot \cos\theta} \quad \textbf{(2-25)}$$

$$P_c = \frac{2\sigma_{ow}\cos\theta}{r} \quad \textbf{(2-26)}$$

The capillary pressure is then related to the interfacial tension of the fluid and the relative wettability of the fluids θ, and the radius of the channel, r.

2.2 Relationship between permeability and porosity

Permeability is directly related to porosity, and the factors controlling the permeability will also affect the porosity. If a sample or rock is without any connections between pores it will be considered impermeable (2). It is therefore natural to assume that there exist certain correlations between permeability and effective porosity. As rock permeability is difficult to measure in a reservoir, porosity correlated permeabilities are often used in extrapolating reservoir permeability between wells (3).

The texture of sediment is closely correlated to its porosity and permeability (9).

The permeability can be considered to be a property of pore space geometry. It can be found to be proportional to ($R\Phi^2$) (4).

$$k \sim R\phi^2 \tag{2-27}$$

R is a pore throat dimension and Φ is porosity (4). For an intergranular medium, the small pore space at the point where two grains meet and connects two larger pore volumes is defined as the pore throat (10) (Figure 2-2). The volume of a pore throat is very small relative to volumes of pore bodies. So an eventually movement of the interface through a pore throat is assumed to occur instantaneously. The flow in the pore throat is laminar and is given by Poiseuille's law:

$$\Delta P = \frac{8\mu LQ}{\pi r^4} \tag{2-28}$$

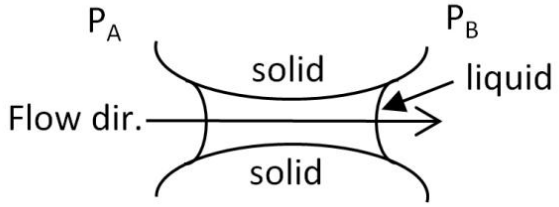

Figure 2-2 Pore throat between two glass beads

The pore throats can be assumed to be cylindrical and then the interface movement is instantaneous, and only the fluid can occupy a given pore throat at a given time (11).
The pores and the pore throat size together control the initial and residual flow distribution and fluid flow through the reservoir (12).

A measure of the pore throat dimension R is not possible unless capillary pressure have been made (4).

2.3 Petro-physical Controls

The most important textural parameters of unconsolidated sediment that may affect porosity and permeability are (13):

- Grain shape – roundness and sphericity
- Grain size
- Sorting
- Packing

Of the parameters listed above, grain size and sorting are most importantant. With respect to porosity and permeability is the grain shape and roundness of less importance. Packing is difficult to measure with respect to its influence on porosity and permeability (13). The permeability can also depend on the size ratio of particles as well as particles size, and porosity depend on size ratio of particles and also particle size.

2.3.1 Relationship between Porosity, Permeability and Grain shape

Roundness and sphericity are two aspects to consider. These two properties are quite distinct. Roundness describes the degree of angularity of the particle, and sphericity describes the degree to which the particle approaches a spherical shape (9). It is easy to distinguish between them. Sharpness to edges and corners of a grain refers to roundness. It is difficult to separate angularity from sphericity. Porosity and permeability can be higher as the angularity increases. This may also be due to brigding of pores by other angular grains and then looser packing. Sphericity might be defined as the *"ratio of the surface area of a sphere of the same volume to the surface area of the object in question"* (13). Sand grains of high sphericity can pack with a minimum of pore space, and from that porosity and permeability increases depending on orientation of grains. This is due to bridging of pores of lowest sphericity and looser original packing. The effect of low sphericity and high angularity (grain shape and roundness) is to increase porosity and permeability of unconsolidated sand (13).

Porosity might decrease with sphericity because spherical grains may be more tightly packed than subspherical (9).

It is difficult to separate the effects of grain shape and roundness for natural sand. It is then difficult to obtain irregular shaped grains of the same grain size (13). But for laboratory purposes this is simpler, because the size can be measured with sieves and the sphericity can be obtained from microscope.

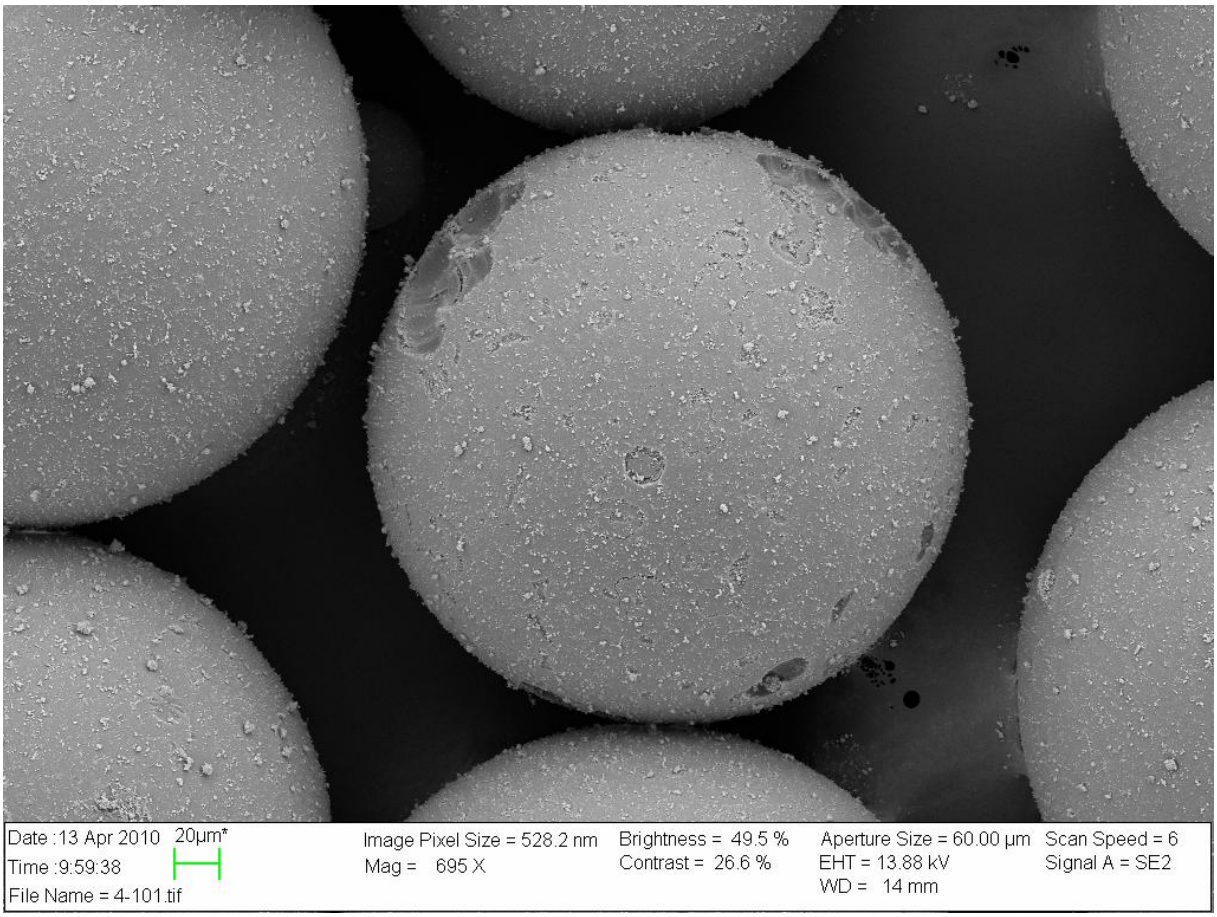

Figure 2-3 Microscopic visualization of a well rounded glass bead

2.3.2 Relationship between Porosity, Permeability and Grain Size

The permeability, *k*, will have a large value for coarse grain size, where Φ will decrease. Very fine grains, like for silt, can produce low *k* at high porosity. Theoretically, porosity is independent on grain size for uniformly packed and graded sands. Coarser sands sometimes have higher porosities than the finer sands or vice versa. This disparity may be due to separate, but correlative factors such as sorting and cementation. Permeability declines with decreasing grain size because pore diameter decreases and the capillary pressure increases.

A common and accepted method for determining grain size is a combination of sieving and by the use of electron microscope. The sieves give an average size of the grain sizes, where a more exact determination of sizes can be given with the electron microscope. Sieving is most accurate for finding the size interval, and the electron microscope can measure sphericity, roundness, angularity and size. The sieving is time consuming and with the electron microscope it is only a small part of the sample that will be measured.

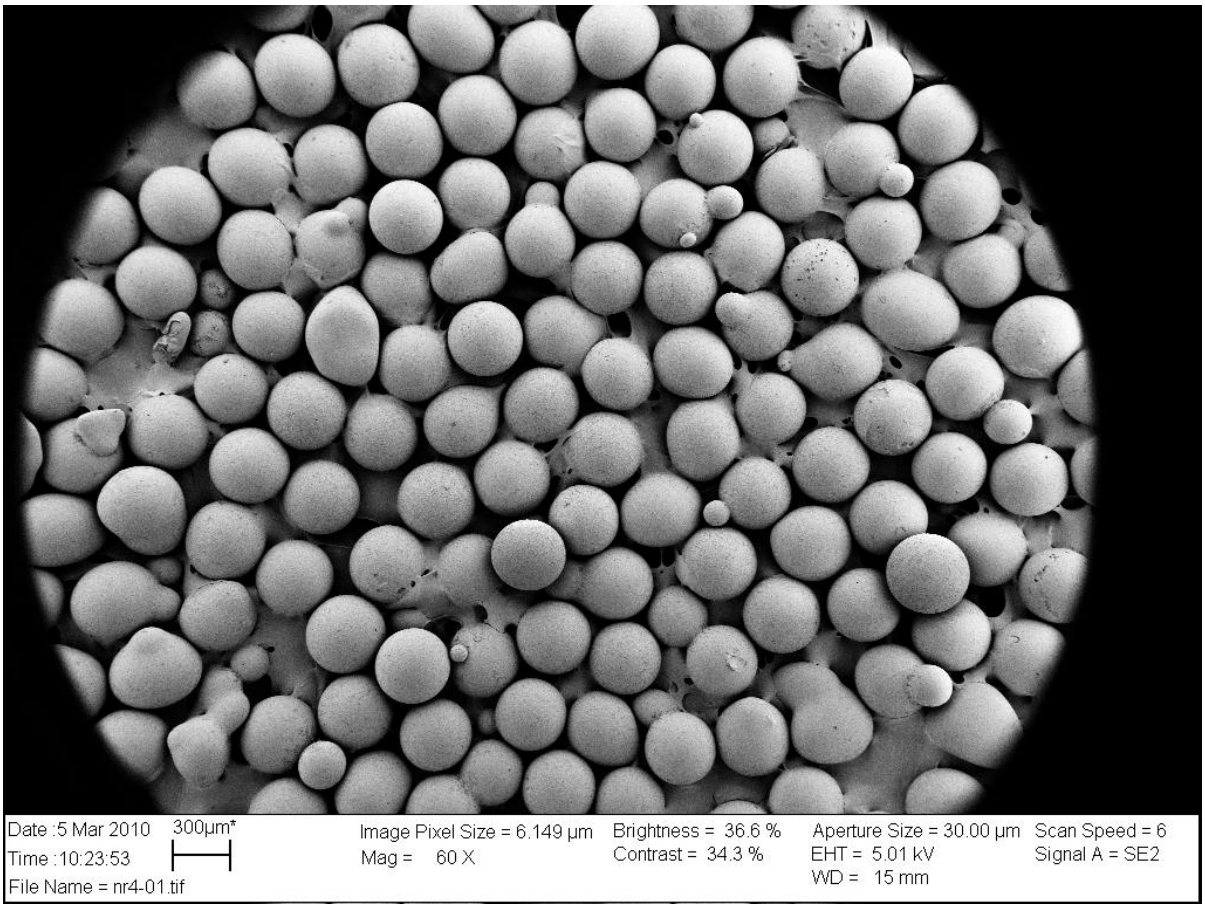

Figure 2-4 Microscopic view of glass beads with a size of approximately 300µm

2.3.3 Relationship between Porosity, Permeability and Grain Sorting

Consider that better sorting increases both Φ and k. This means that porosity increases with improved sorting (4). If there is a bad sorting the small particles will fill in the larger, framework-forming grains. For the same reason, the permeability will decrease (9). As mentioned earlier, sorting sometimes varies with the grain size of particular reservoir sand, thus indicating possible correlation between porosity and grain size. Sand with grain diameter between 250-500µm can be classed as medium grained sand, because grain size correlates with pore size and is a control on permeability (4). The size classes can be labeled to $D = 2^{-phi}$, where it will be in mm. The glass beads used, the range in diameter is between 250-355 µm, and the size class can be, $D = 2^{-2}$ for 200µm and $D = 2^{-1.5}$ for 350µm.

For samples that do not have a good sorting, where an increase in coarse grain content can result in decreased Φ and k increases. Beard and Weyl (13) also stated that permeability is proportional to the square of grain size and it can be said that their data demonstrate that pore size is proportional to grain size. Very poorly sorted sand indicates that dry unconsolidated sand is more difficult to pack uniformly as grain size becomes finer and sorting becomes poorer (13). Permeability of unconsolidated sand decreases as grain size becomes finer and as sorting becomes poorer.

2.3.4 Relationship between Porosity, Permeability and Grain Packing

Two important characteristics of the fabrics of a sediment are how the grains are packed and how they are oriented. It is possible that the packing geometries can be divided into six parts. The geometries are ranging from the loosest cubic style with a porosity, $\Phi = 48\%$, down to the tightest rombohedral style with porosity, $\Phi = 26\%$. Porosity of packed sand is for same sorting independent of grain size, but porosity varies with sorting. When comparing compaction studies of sandstones, there must always be a comparison between the same sorting (13). Packing is obviously a major influence on porosity of the glass beads (13).

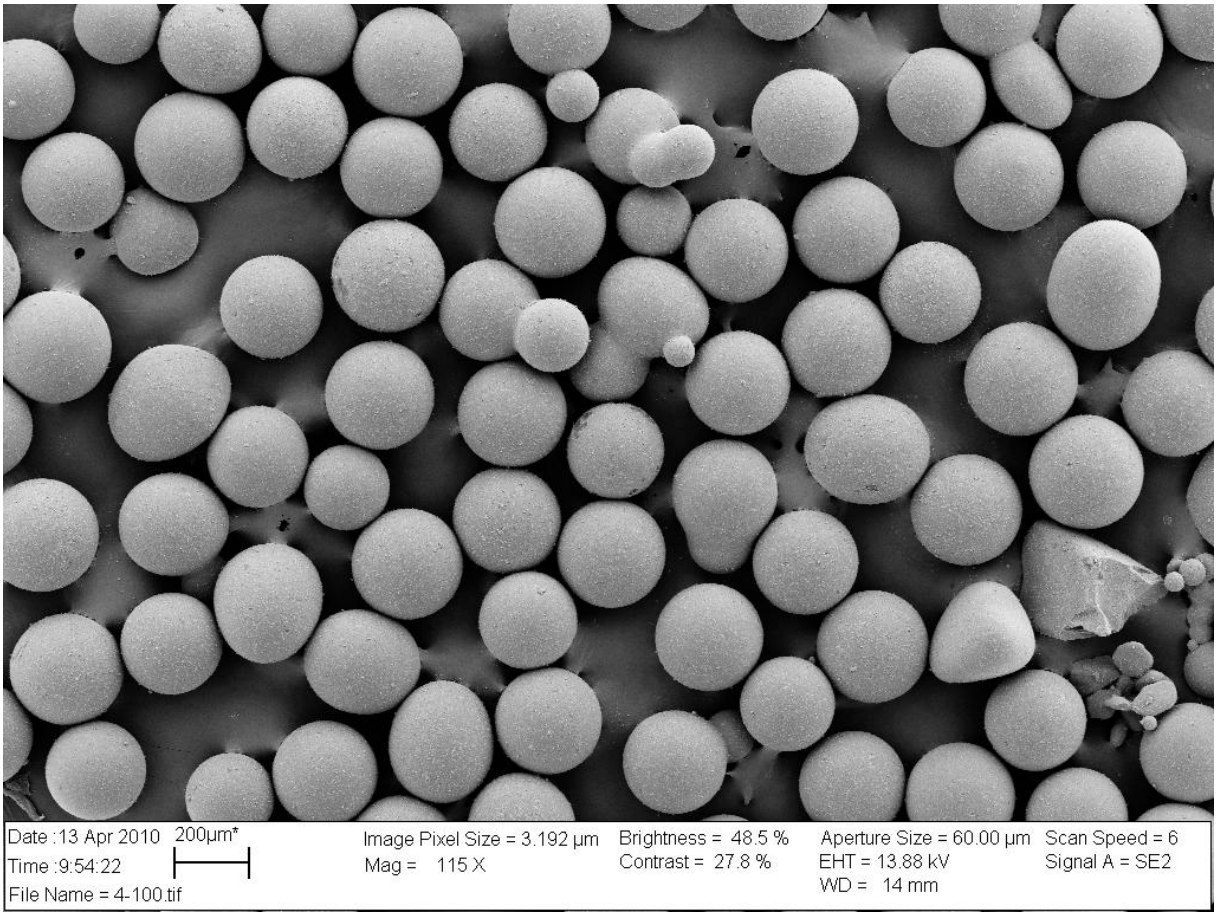

Figure 2-5 Well sorted glass beads of approximately 200µm

2.4 Vertical permeability variation

Vertical variation in permeability in a gravel pack is relatively common. The vertical variation in permeability will lead to a reduction of the vertical displacement efficiency at breakthrough, because of uneven flow in the different layers. This would occur at idealized conditions of mobility ratio and in the abscense of gravity segregation. (14)

2.5 Effects of Water Coning

Oil reservoirs which have a high water drive will exhibit high oil recovery due to supplementary energy impacted in the aquifer. A large oil production rate may cause water to be produced by upward flow. This is a phenomena that is known as water coning and refers to deformation of water-oil interface which was initially horizontal. Several researchers has investigated several issues as critical rate and/or breakthrough time calculations. The maximum water-free oil production rate corresponds to the critical rate and the breakthrough time which represents the period required by bottom water to reach the well's oil perforation. If oil production rate is above this critical value, water breakthrough occurs. (15)

After breakthrough the water phase may dominate the total production rate to the extent thatfurther operation of the well becomes economically not valuable and the well must be shut down. (15)

There are several ways of keeping the unwanted water from the oil wells;

- Keeping production rate below the critical value
- Have the perforation far away from the initial water-oil contact (WOC)

The use of horizontal wells can also minimize water coning, but they are of course not free for water influx(15).

Several factors affecting water coning are(15):

- Oil production rate
- Mobility ratio between oil and water (displaced and displacing fluid)
- Porosity
- Density between fluids

There are three forces that may affect fluid flow distribution around the wellbore;

- Capillary forces
- Gravity forces
- Viscous forces

Capillary forces have been neglected, because it does not have so much affection on water cone. Gravity forces are directed in vertical way and arise from the water and oils' fluid density differences. Viscous forces refers to pressure drop associated with fluids flowing through the porous gravel pack model. At a given time there is a balance between gravitational forces and viscous forces. When the viscous forces exceed the gravitational forces, a cone will break into the well. If the pressure is at unsteady state condition a unstable cone will occur and water will flow through the gravel pack and into the well(15).

2.6 1D displacement through a porous medium

Displacement methods involve the displacement of one fluid by another (16). Displacement of oil by water from a porous medium is one of the processes of primary importance in connection with oil production.

Displacement of oil in a porous medium by water depends both on heterogeneities and the interaction of several forces. The acting forces include gravity forces driven by fluid density gradients, capillary forces due to interfacial tension between immiscible fluids and viscous forces driven by adverse viscosity ratios

Under a wide variety of circumstances a thin layered porous media can provide a suitable method of investigate the stability of displacement fronts (17). A porous medium is any solid phase that is permeable. The flow is going through the connected pores in the porous medium. The porous medium contains oil, where water will displace the oil. Usually the flow models are based on direct extensions of one-phase flow equations like Darcy's law and conservation of mass. These equations lead to introduction of constitutive relationships like relative permeabilities (11).

Also discussed is the immiscible displacement when two phases flow simultaneously.

2.6.1 Piston-like displacement

Piston like displacedment is the ideal displacement mechanism. Oil is flowing in the precence of water, while behind th interface water alone is flowing in the presence of residual oil, k_{ro}. This favourable displacement only occur if the relative mobility ratio, M is less than 1 (18):

$$\frac{k_{rw}^{'}/\mu_w}{k_{ro}^{'}/\mu_o} = M \leq 1 \qquad \textbf{(2-29)}$$

When $M \leq 1$ the oil is capable of travelling with a velocity equal to, or greater than that of the water and the water cannot bypass the oil. The injection of water is the same as the production of oil.

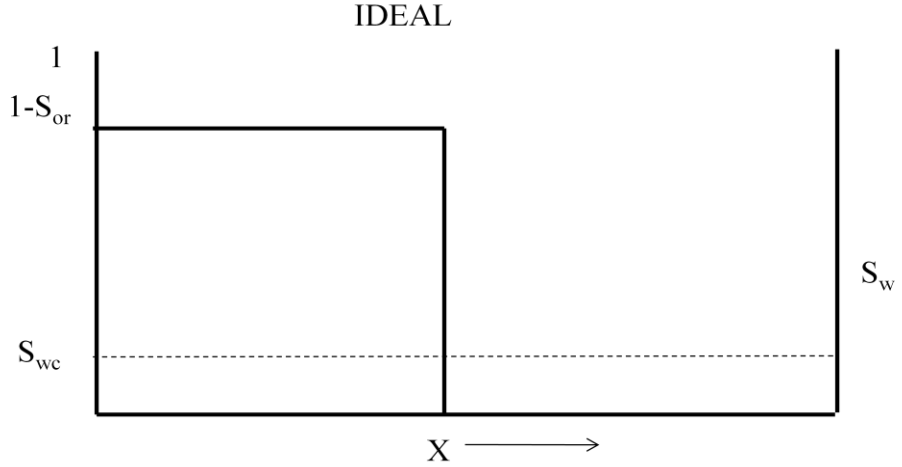

Plot 2-1 Ideal Displacement of Oil

2.6.2 Viscous fingering

In many cases a displacement is governed by what might be called viscous fingering (19). When the displaced fluid has a higher viscosity than the displacing fluid it can be associated with displacement processes where there are viscous instabilities (17). When the viscosity of the oil is higher it might happen that smaller fingers are formed (20). In immiscible displacement, will the behaviour of displacement be strongly dependent on capillary forces. Occurrence of perturbations which is fingering through the system is obtained when the less viscous displacing fluid flows more easily than the more viscous displaced fluid. The balance between the heterogeneity and the capillary forces of the porous medium affects the initiation of viscous fingers. When there is a balance, the viscous fingering can increase with the viscosity ratio, between the displaced and the displacing fluid. Unstable displacement process

is also together with viscous fingering also associated with early breakthrough of the displacing fluid (21). Figure 2-6 shows the behaviour of viscous fingering.

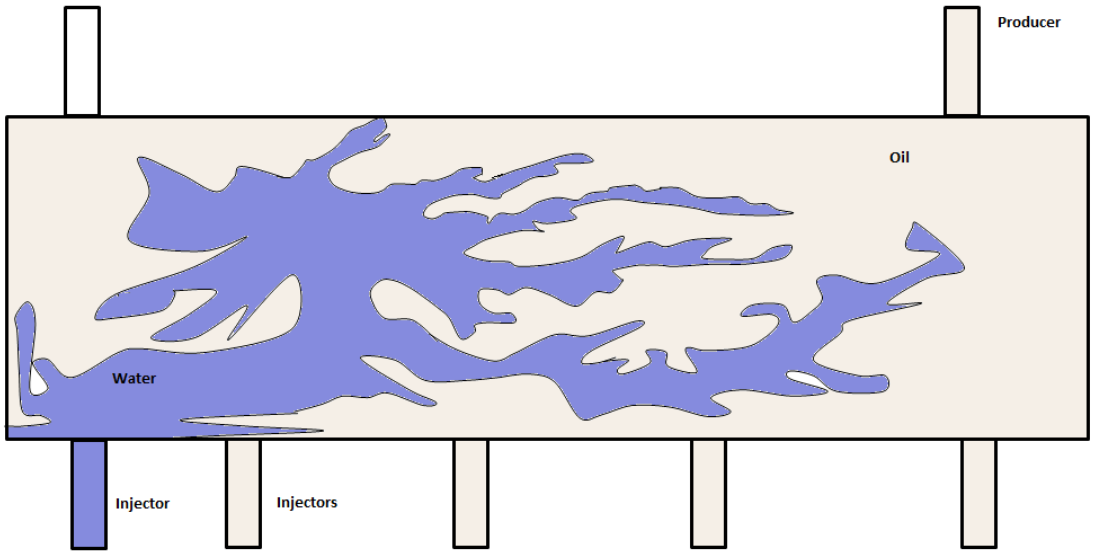

Figure 2-6 Viscous fingering

The breakthrough will of water might come before then expected, when there is viscous fingering. The porous medium is initially filled with oil. Longitudinal dispersion is assumed negligible in this case. Another consideration is if there are heterogeneities, because if heterogeneities are absent the displacement front should remain a plane surface during the displacement. And if there is a small region of higher permeability, the front entering this part of the region will travel much faster than the rest of the front (22). Differences in permeability heterogeneities can be the reason for the viscous fingers, and small scale permeability heterogeneities can also cause finger initiation (23). A place where the finger initiation occurs is at a mobility ratio greater than one.

Fingers can occur for the presence of permeability heterogeneities. For the porous media is the finger initiation easily visualized as a microscopically random pore structure and even for a pack of glass beads that appear macroscopically homogeneous.

According to Hill(14), the finger will remain stable if just across the interface of the finger the pressure in the displaced phase (oil) is greater than the displacing phase (water), i e(14):

$$P_w - P_o \leq 0 \tag{2-30}$$

The pressures can be obtained from(14):

Oil
$$P_o = p_0 + \rho_o g \Delta L \rho \sin\theta - \frac{\mu_o u \Delta L_p}{k_o} \tag{2-31}$$

Water
$$P_w = p_0 + \rho_w g \Delta L \rho \sin\theta - \frac{\mu_w u \Delta L_p}{k_w} \tag{2-32}$$

Onset of viscous fingering and the position of the front can be found by equation (2-33)(14).

$$\frac{dx_f}{dt} = \frac{-k\Delta P}{\varphi\mu_s(ML + (1-M)x_f)} \quad \textbf{(2-33)}$$

2.7 Darcy's law

2.7.1 Background

The first important experiments of fluid flow through porous media were reported by Dupuit in 1854, using water-filters. The results he gained showed that the pressure drop across a filter is proportional to the water filtration velocity.

2.7.2 Definition

Henry Darcy noted that the flow rate through sand filters obeys the following relationship (2):

$$q = k \times A\frac{h}{\Delta l} \quad \textbf{(2-34)}$$

q = fluid flow rate
h = difference in manometer levels (i.e. the hydrostatic pressure gradient across the filter)
A = the cross sectional area of the filter in flow transverse
Δl = the length of the filter medium in flow-parallel direction
k = proportionality coefficient (defined as permeability)

In this equation the viscosity, μ, was not included. The reason was that only water was used and the effect of its density and viscosity was negligible. The Darcy Law for linear horizontal flow of an incompressible fluid can be written as:

$$q = -A\frac{k}{\mu}\frac{dP}{dx} \quad \textbf{(2-35)}$$

The negative sign in front of the equation serves mainly to denote a decrease in flow in the direction of the flow, which means a negative pressure gradient in the x-direction. This physical formality is most commenly disregarded in order to obtain a non-negative value for the flow rate.

$$q = A\times\frac{k}{\mu}\frac{\Delta P}{\Delta L} \quad \textbf{(2-36)}$$

2.7.3 Units

When calculating the permeability, the Darcy law shows that the permeability has the dimension of surface area, L^2. This is not a convenient unit in order to express and perceive the fluid-transmission capacity of a porous medium. Permeability's unit is called *Darcy*, and the definition is as follows (2):

"The permeability of a porous medium is 1 Darcy if a fluid with viscosity of 1 cP and a pressure difference of 1atm/cm is flowing through the medium's cross-section of 1cm^2 at a rate of 1cm^3/s."

Below the units are converted to the SI unit system.

q = 10^{-6} m^3/s
μ = Pa×s = kg/ms
A = m^2
ΔP = Pa =kg/(ms^2)
L = m
1 D = 0,987 μm^2 = 9,87*10^{-13} m^2

Permeability is a tensor, which means that it may have different values in different directions. Vertical permeability, normal to the bedding, might be lower than the horizontal permeability, parallel to the bedding (2).

2.7.4 Limitations

The Darcy's law is only valid for slow, viscous flow.

At high flow rates the Darcy's law breaks down as the high velocity imposes a pressure drop which is no longer linear with the flow rate. At low flow velocities the difference between the actual pressure drop and that calculated by Darcy's law is negligible.

The Darcy Law only holds for viscous flow and as described in chapter 2.1.2, the medium must be 100% saturated with the flowing oil when the determination of the absolute permeability is made.

2.7.5 Applications

Darcy's law is applicable to the great majority of reservoirs producing oil. Application of Darcy's law to reservoir flow requires definition of the inner and outer reservoir boundaries. Several flow geometries that might be expected are (24):

- Cylindrical/radial flow
- Converged flow
- Linear flow
- Elliptical flow
- Pseudoradial flow
- Spherical flow
- Hemispherical flow

Cylindrical/radial flow geometry is probably the most representative for the majority of oil wells (24).

2.7.6 True fluid velocity

The velocity of a fluid through a porous medium's across cross-sectional area, *A*, called superficial or bulk velocity, can for a linear flow be written as:

$$u = \frac{q}{A} = \frac{k}{\mu}\frac{dP}{dX} \qquad \textbf{(2-37)}$$

The true velocity of the fluid flow through the pores is called interstitial fluid. The interstitial fluid velocity is higher than the bulk velocity, as the actual cross-sectional area is in average Φ times smaller than the bulk samples cross sectional area, *A* (2).

2.8 Displacement Efficiency

The displacement efficiency, E_D, for oil is defined as the ratio of mobile oil to original oil in place at reservoir conditions (25). Since an immiscible displacement always will leave behind some amount of residual oil, E_D will always be less than 1 (26).

The displacement efficiency is expressed as:

$$E_D = \frac{V_p S_{oi} - V_p S_{or}}{V_p S_{oi}} = \frac{S_{oi} - S_{or}}{S_{oi}} \quad \textbf{(2-38)}$$

If oil saturation is calculated to zero, E_D can reach 100%. Therefore it is of interest to reduce the residual oil saturation, thus increasing the displacement efficiency.

Assuming no gas present, S_{oi} and S_{wi} is given by:

$$S_{oi} = 1 - S_{wi} \quad \textbf{(2-39)}$$

E_D says something about how effective oil can be recovered, or how the behaviour of the water is during displacement of oil.

It can be assumed that the displacement efficiency is kept constant at the start of the displacement, and then $\overline{S}_w$ is also set to be constant. When $\overline{S}_w$ starts to increase E_D will continuously increase during the displacement.

The displacement efficiency can also be expressed as a function of the cumulative oil production, N_{pBt}:

$$E_D = \frac{N_{p\,Bt}}{1 - S_{wi}} \quad \textbf{(2-40)}$$

2.8.1 Mobility Ratio

The mobility ratio is a useful concept of the displacing and the displaced fluid phases. *M* is dimensionless and important in the displacement profile. It affects both vertical and horizontal displacement. The displacement decreases when *M* increases for a given volume of fluid injected. When *M > 1.0* the displacement becomes unstable, and is called viscous fingering. The larger value is referred to as unfavorable mobility ratio.

Mobility ratio for immiscible piston like displacement:

$$M = \left(\frac{k_{rw}}{\mu_w}\right)_{Sor} \left(\frac{\mu_o}{k_{ro}}\right)_{Siw} \quad \textbf{(2-41)}$$

k_{rw} and k_{ro} are measured at residual oil saturation and interstitial water saturation.
The mobility ratio for two or more flowing phases may change in position and time as the phase saturation changes:

$$M_{\bar{S}} = \left(\frac{k_{rD}}{\mu_D}\right)_{\bar{S}D} \left(\frac{\mu_d}{k_{rd}}\right)_{\bar{S}d} = \frac{(\lambda_D)_{\bar{S}D}}{(\lambda_d)_{\bar{S}d}} \quad \textbf{(2-42)}$$

Viscosity ratio (14)

$$\gamma = \frac{\mu_o}{\mu_w} \quad \textbf{(2-43)}$$

2.8.2 Volumetric Displacement Efficiency

The volumetric displacement efficiency is a measure of how effective the displacing fluid is moving out of the gravel pack. The result from the volumetric displacement indicates how much oil that will remain in the gravel pack.

As the volumetric efficiency will be <100%, some areas will be untouched by the displacement. It is therefore reasonable to assume that some of the displaced oil will migrate to these regions, thus imposing a local increase of oil saturation, S_{or}.

The residual oil will be located both where oil has been displaced by water and in those areas not affected by the displacement.

The volumetric displacement efficiency can be considered as the product of the area and vertical sweep efficiencies. E_V can therefore be described as (27):

$$E_V = E_A E_I \quad \textbf{(2-44)}$$

The area efficiency E_A and vertical efficiency E_I are defined by (26):

$$E_A = \frac{A_{swept}}{A_{total}} \quad \textbf{(2-45)}$$

$$E_I = \frac{SweptThickness}{TotalThickness} \quad \textbf{(2-46)}$$

In overall the total hydrocarbon recovery efficiency, RF, in a displacement process can be expressed as:

$$RF = E_D E_V \quad \textbf{(2-47)}$$

$$RF = E_D E_A E_I \quad \textbf{(2-48)}$$

2.8.3 Areal Displacement Efficiency

General

Areal displacement efficiency is controlled by the following main factors (14):

- Number of injection points to the gravel pack model
- Number of production perforations
- Reservoir permeability heterogeneity
- Mobility ratio

- Viscous forces
- Gravity

Before breakthrough is the areal displacement efficiency directly proportional to the volume of water injected in the gravel pack(14).

$$E_A = \frac{V_i}{PV(S_{oi} - S_{or})} \quad \textbf{(2-49)}$$

Areal displacement efficiency at breakthrough can be determined from empirical correlations based on the mobility ratio (28) (29): The displacing phase is completed when multiplying with *M* (14).

$$E_{ABt} = 0.54602036 + \frac{0.03170817}{M} + \frac{0.30222997}{e^M} - 0.00509693 \cdot M \quad \textbf{(2-50)}$$

Prediction Based on Piston-Like Displacement

For piston-like displacement the displacing phase will only flow in the swept region and the displaced fluid will flow in the unswept region. The production of the displacement phase is assumed to come entirely from the unswept region of the pattern. Equation (2-50)is only applicable where the displaced phase is the only phase flowing and if the mobility ratio is unity. It is applicable when there is a total flow out, but with the displaced phase properties replaced by the properties of the displacing phase.

Prediction Based on Mobile Displaced Phase behind the Displacement Front

For the displacement of two immiscible fluids such as water –oil displacement, there is typically two phase flow and a saturation gradient behind the front. For a piston-like displacement there will only be produced water after the breakthrough. But for water under-riding and viscous fingering the oil will be produced also after breakthrough of water. Some of that production will come from the unswept region and some from the swept region (14).

2.8.4 Vertical Displacement Efficiency

General

Vertical displacement efficiency is controlled by four factors:

- Gravity segregation caused by differences in density
- Mobility ratio
- Vertical to horizontal permeability variation
- Capillary forces

The Vertical Displacement Efficiency can be described by the following relationship (14)

$$E_I = \frac{N_{p,bt}}{M \cdot V_t} \quad \textbf{(2-51)}$$

Effect on Gravity Segregation and Mobility Ratio on Vertical Displacement Efficiency

Gravity segregation will happen when density differences between injected and displaced fluids are large enough to induce a significant component of fluid flow in the vertical direction when the principal direction of fluid flow is in the horizontal plane. When the displaced fluid is denser than the displacing fluid, the displacing fluid will under-ride the displaced fluid. For this, also gravity segregation will happen. Gravity segregation leads to an early breakthrough of the injected fluid and reduced vertical displacement efficiency.

Gravity Segregation for Horizontal Reservoir and Gravel Pack

An experimentally model has been used to define if gravity forces become important and to describe its effect on displacement efficiency. The experimentally laboratory model is both homogeneous and isotropic. Other information might be based on calculations made with numerical computer simulators. Craig et al. and Spivak (14) indicate the following effects of various parameters on gravity segregation:

1. Gravity Segregation increases with increasing horizontal and vertical permeability.
2. Gravity segregation increases with increasing density difference between the displacing and displaced fluids.
3. Gravity segregation increases with increasing mobility ratio.
4. Gravity segregation increases with decreasing rate. This effect can be reduced with viscous fingering.
5. Gravity segregation decreases with increasing level of viscosity for a fixed viscosity ratio.

If M > 1, the viscous fingering can occur along with gravity segregation. At conditions where gravity effects are important and the mobility ratio is unfavourable, vertical displacement can be affected by both the tendency of the displacing fluid to flow into the gravity tongue (14).

Effect of Vertical Heterogeneity and Mobility Ratio on Vertical Displacement Efficiency

Variation in vertical permeability in reservoirs is relatively common. The vertical variation might lead to reduction in vertical displacement efficiency at breakthrough in a displacement process owing to uneven flow in the different layers. This would occur at idealized conditions of unit mobility and in the absence of gravity segregation (14).

Displacement at Nonunit Mobility Ratio

Assuming piston-like displacement in a layered gravel pack (no crossflow), singelphase flow exists both ahead and in front of the displacement. If the mobility ratio, M, $\neq 1$ the total resistance across the system varies as a function of the volume injected, thus the flow varies at constant pressure drop. An expressions describing the displacement is found below(14):

$$\frac{dX_f}{dt} = \frac{-\lambda_{rD} k \Delta p}{\left[ML + (1-M)X_f\right]\phi(1-S_{dr}-S_{Dr})} \qquad \textbf{(2-52)}$$

This is a differential equation that by integration, separation of variables results in;

$$t = \frac{-\phi(1-S_{dr}-S_{Dr})}{\lambda_{rD} k \Delta p}\left[MLX_f + (1-M)\frac{X_f^2}{2}\right] \qquad \textbf{(2-53)}$$

Dykstra-Parsons Model for Vertical Heterogeneity

The effects of reservoir heterogeneity on vertical displacement efficiency can be estimated with simple models by assuming that the reservoir is represented by non-communicating layers and by neglecting gravity segregation. This model was developed by Dykstra-Parsons for piston like displacement in a linear reservoir flooded at constant pressure drop. The model is based on dividing the reservoir into n layers of equal thickness that have different permeabilities. When the displacement is piston-like, the vertical displacement efficiency given by (14):

$$E_I = \frac{n_j + \sum_{k=j+1}^{n} \frac{k}{k_j}}{n} \tag{2-54}$$

The vertical displacement efficiency for a non-unity mobility ratio, M, is given by:

$$E_I = \frac{n_j + \frac{(n-n_j)M}{M-1} - \frac{1}{M-1}\sum_{k=j+1}^{n}\left[M^2 + \frac{k}{k_j}\left(1-M^2\right)\right]^{1/2}}{n} \tag{2-55}$$

At piston-like displacement, described in chapter 2.6.1, only displaced fluid is produced before breakthrough and no displaced fluid is produced at breakthrough in a particular layer. The ratio of displacing fluid to displaced fluid at the producing well can be determined from the Dykstra-Parsons-Model and is given by the equations below (14):

$$F_{wo} = \frac{\sum_{k=1}^{j} k}{\sum_{k=1+j}^{n} k} \tag{2-56}$$

For M> or <1

$$F_{wo} = \frac{\sum_{k=1}^{j} k}{\sum_{k=j+1}^{n} \frac{k}{\left[M^2 + \frac{k}{k_j}\left(1-M^2\right)\right]^{1/2}}} \tag{2-57}$$

2.9 Frontal Advance Equations

The frontal advanced theory is predicted for water flooding performance in a linear system. Frontal advanced theory is applied to viscous water flooding. Finally dispersion or mixing when one fluid displaces the other miscible fluid is described, as are viscous fingering and its effect on displacement (14). The gravel pack medium is considered homogeneous with porosity, Φ, permeability, k, length L, and cross-sectional A.

Frontal advance:

Buckley Leverett Equation

$$\frac{dx_{S_w}}{dt} = \frac{q_t}{A\phi}\left(\frac{\delta f_w}{\delta S_w}\right)_{S=S_w} \quad \textbf{(2-58)}$$

For the Bucley Leverett equation the water in the rock is at interstitial saturation, S_{iw}. Interstitial water saturation is defined as the *"saturation at which the water is immobile which means that the permeability to water, k_{rw} is zero"* (14). There is also no gas saturation. When water is injected into the linear system at a sufficient rate for the frontal advance assumptions to apply, each water saturation, S_w, travels at a constant velocity through the system given by Equation (2-58) (14).

The Buckley Leverett theory assumes a so called diffuse flow condition, which means that fluid saturations at any point in the linear displacement path are uniformly distributed with respect to the reservori thickness. The main reason for making this assumption is that it permits the displacement to be described, mathematically, in one dimension and this provides the most basic possible model of the displacment process (2).

From the given equation above it is possible to calculate the fractional flow of water, when the system is horizontally and capillary and gravity forces are neglected. The formula is shown below.

The sum of the flow rate, q_t, is defined as the sum of the water and oil rate, if no gas is present:

$$q_t = q_w + q_o \quad \textbf{(2-59)}$$

Darcy's law for linear, steady state and simultaneous one dimensional, 1D, flow for oil and water, without influx of the gravity force is defined as:

For water

$$q_w = -\frac{k_w A}{\mu_w}\frac{\partial p_w}{\partial x} \quad \textbf{(2-60)}$$

For oil

$$q_o = -\frac{k_o A}{\mu_o}\frac{\partial p_o}{\partial x} \quad \textbf{(2-61)}$$

The derivative form of capillary pressure is:

$$\frac{\partial p_c}{\partial x} = \frac{\partial p_o}{\partial x} - \frac{\partial p_o}{\partial x} \quad \textbf{(2-62)}$$

The mobility ratio, *M*, is given by the mobility ratio for oil and water which means the displacing fluid λ_w divided by the displaced fluid λ_o:

$$M = \frac{\lambda_w}{\lambda_o} = \frac{\frac{k_w}{\mu_w}}{\frac{k_o}{\mu_o}} = \frac{k_w \cdot \mu_o}{k_o \cdot \mu_w} \quad \textbf{(2-63)}$$

By combining equations (2-60), (2-61), (2-62) and (2-63) the flow rate for oil and water can be expressed as:

Water
$$q_w = \frac{q_t - \frac{k_o}{\mu_o} \cdot \frac{\partial p_c}{\partial x}}{1+M} \quad \textbf{(2-64)}$$

Oil
$$q_o = \frac{M \cdot q_t - \frac{k_w}{\mu_w} \cdot \frac{\partial p_c}{\partial x}}{1+M} \quad \textbf{(2-65)}$$

Inserting equations (2-64) and (2-65) into equations **Error! Reference source not found.** and **Error! Reference source not found.** respectively gives:

Water
$$f_w = \frac{1+\frac{k_o}{q_t \cdot \mu_o} \cdot \frac{\partial p_c}{\partial S_w}\frac{\partial S_w}{\partial x}}{1+M^{-1}} \quad \textbf{(2-66)}$$

Oil
$$f_o = \frac{1+\frac{k_w}{q_t \cdot \mu_w} \cdot \frac{\partial p_c}{\partial S_w}\frac{\partial S_w}{\partial x}}{1+M} \quad \textbf{(2-67)}$$

If neglection of capillary pressure together with water saturation, S_w, the fractional flow can be simplified:

Water
$$f_w = \frac{1}{1+M^{-1}} \quad \textbf{(2-68)}$$

Oil
$$f_o = \frac{1}{1+M} \quad \textbf{(2-69)}$$

This assumption is valid only if the permeability is high. A large plateau of the capillary pressure function implies a homogeneous distribution of the pore throats and therefore high permeability.

If the oil displacement process is performed under isothermal conditions, the viscosity is constant and the fractional flow is only a function of the water saturation, as related through the relative permeabilities.

2.10 Buckley Lewerett-Theory

Buckley and Leverett made a theory about end effects and immiscible displacement fronts, with a dimensional analysis of displacement process and on a basis of relative permeability. They made a number of model experiments on the displacement. The formation they used consisted of sand layers of different grain sizes and contained both oil and a phase simulating connate water (19).

The Buckley Leverett Theory is known as a linear and one dimensional "leaking piston" displacement process. In the theory it is assumed that:

1. The fluids are non-compressible and immiscible
2. Homogeneous and isotropic porous medium
3. One dimensional (1D) and stable displacement
4. The multiphase Darcy Law can describe the filtration theory

The correct water saturation profile will be, with the use of Buckley Leverett technique, and requirement of a vertical line, will be:

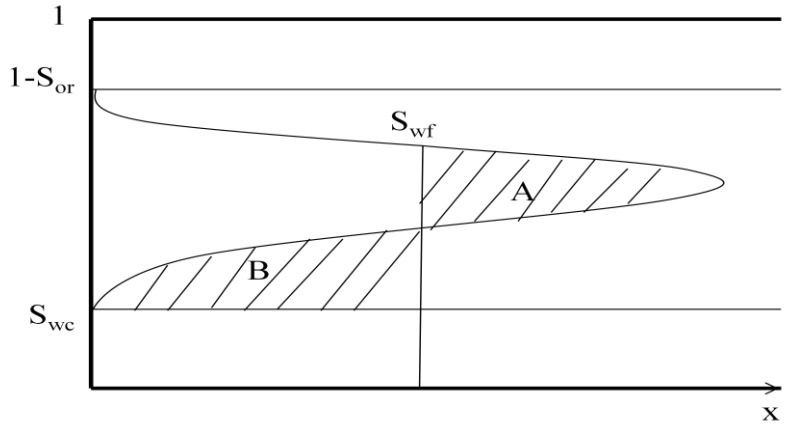

Figure 2-7 Water saturation distribution profile (29)

By integrating the saturation distribution over the distance from the injection point to the front will give a more accurate result (29).

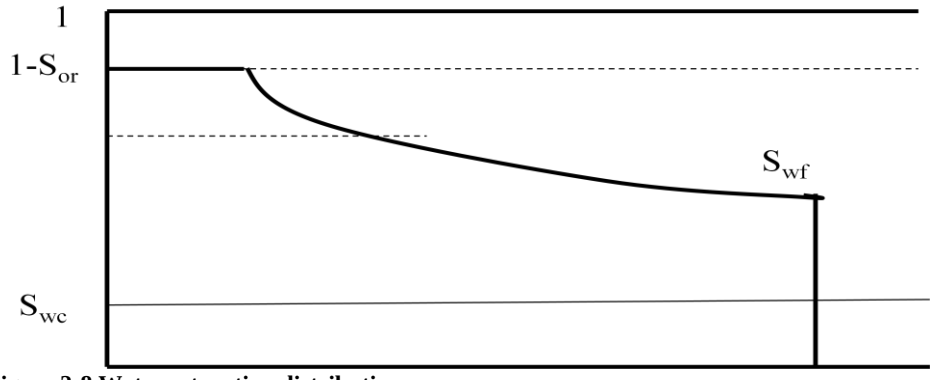

Figure 2-8 Water saturation distribution,
a function of distance prior to breakthrough(29)

Figure 2-8 shows the water distribution profile. Swf is the saturation at the shock front. A is the displaced area and B is the area left behind, both with the same volume. Swc is the water connate saturation.Figure 2-8 shows the water saturation distribution during a displacement. This can be seen as a function of distance prior to breakthrough.

2.11 Viscous Forces

When a fluid is flowing through a porous medium a pressure drop occur. The viscous forces are a reflection of the pressure drop that occurs when the fluid is flowing through the medium. A simple approximation used is to consider that the porous medium is flowing through a horizontally or a vertically tube. With this assumption it is possible to calculate the pressure drop with help terms of Darcy's equation:

$$\Delta p = -(0.158)\left(\frac{\bar{v}\mu L\phi}{k}\right) \qquad \textbf{(2-70)}$$

The typical values for the bulk of the reservoir volume 0.1 to > 1.0 psi/ft, 2280.1 to > 22801 Pa/m.

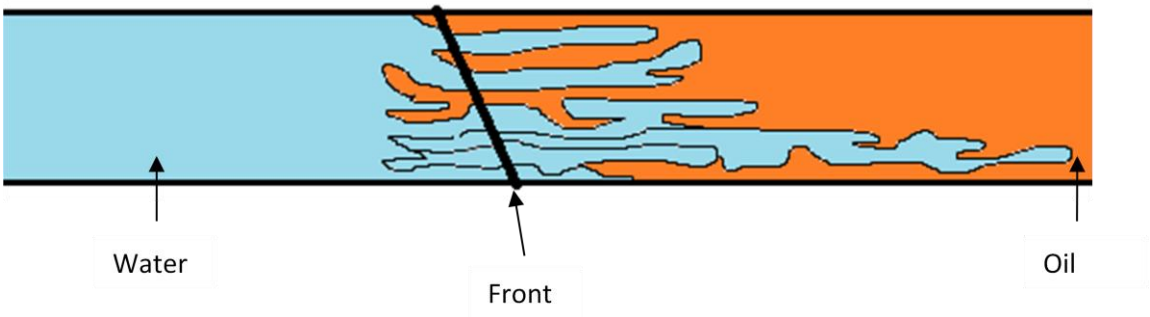

Figure 2-9 Viscous fingering due to capillary and gravity forces(29)

2.12 Immiscible Displacement

For an immiscible displacement the capillary pressure and interfacial tension have an effect on the displacement efficiency. Some residual fluid will be left after an immiscible displacement. For unstable immiscible flow the interfacial tension may have a dampening and promoting effect on viscous fingers. The interfacial tension will prevent the development of small perturbations on the finger surface. This results in all the fluid flowing into the already developed finger, promoting its growth. Large capillary numbers will result in a chaotic system where the finger dynamics is very complex. Few or single fingers is dominated by low capillary numbers. These fingers can be described by shielding, spreading and splitting (23). A finger lying ahead runs faster than the one lying behind. This is due to instability processes. The finger will then spread until it reaches its dominant width. If they still grew after finding its width, the finger will spread at the tip of the finger. The interfacial force should be as large as the finger tip starts to be unstable and low enough to cause spreading.

3 GRAVEL PACK DESIGN

3.1 Introduction

A physical model of a gravel pack can describe the process which is taking place when a fluid is flowing through it and give an understanding of the different flow behaviors described in chapter HOLD. From laboratory experiments and measurements a small part of the reservoir or the well as the gravel pack can be performed.

Two different experiments where performed:

1. A vertical test cell, described in chapter 3.2.
   The following data was obtained from this experiment; the permeably of the porous medium, the relative permeability of oil and water, the residual and interstitual saturation of oil and water. These results was used as input values in the main experiment.

2. Main experiment with horisontal gravel pack
   A horizontal model was designed in order to study the flow behavior of oil and water through a gravel pack

3.2 Test Cell Setup

In Figure 3-1 the schematic figure is shown. Oil is injected from bottom of test cell. Then the oil is flowing from bottom to top. The actual flow rate, q_{real}, and production of oil, is measured from the burette. The logging tool gives differential pressure between two end points. Table 3-1 shows the dimensions and distance between the different equipment. The flow here is in the y-direction.

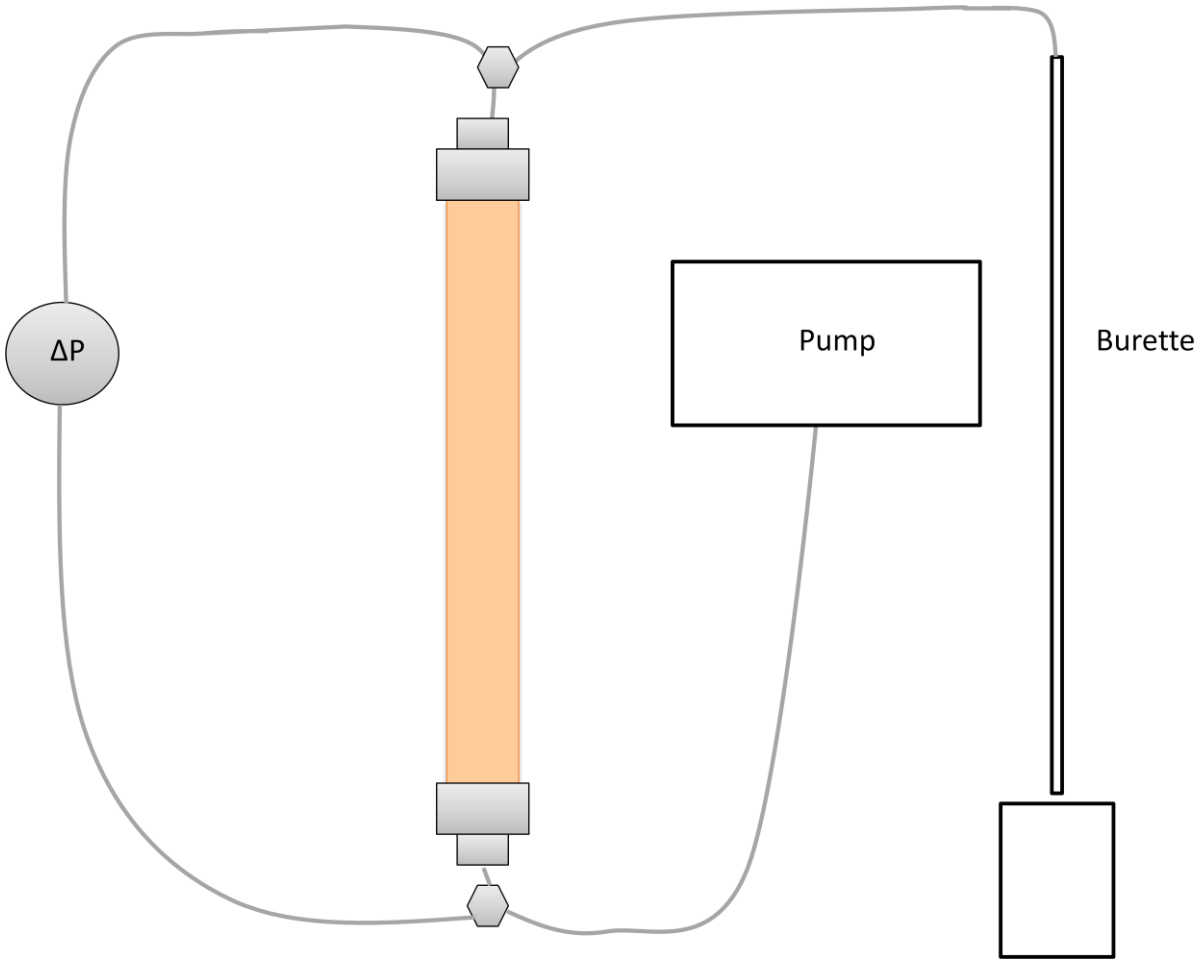

Figure 3-1 Schematic setup of Test Cell

Table 3-1 Dimensions of tubes and distance between equipment

Volume of burette [ml]	50
Height of burette [cm]	70
Height from pump to inlet valve manifold [cm]	45
Height from pump to outlet valve manifold [cm]	15
Height outlet to burette [cm]	14
Height outlet to manifold [cm]	6
Length of tube between outlet and burette [cm]	79
Length of tube from outlet to dP logger [cm]	119
Length from valve manifold to inlet [cm]	5,5
Length of tube from pump to valve manifold [cm]	100

3.3 Test Cell Specifications

When displacing flow in the vertical direction a cylindrical test cell is used.

Design of test cell is described in Table 3-2 below.

Table 3-2 Cylindrical test cell model

Length, L [m]	0.500
Inner Length, L [m]	0.468
Inner Diameter, ID [m]	0.0238
Area, A [m^2]	$4.4488*10^{-4}$
Volume, V_b [cm^3]	208.2646

Figure 3-2 Cylindrical test cell

3.4 Original Model

3.4.1 Description of Original Model

The overall purpose of the thesis was injecting water into the oil column in order to find out which effect water coning, from the reservoir, gave in a gravel pack.

In order to study the effect of water coning a relative large model, capable of withstanding a relative large pressure has to be built. Proposed dimensions are shown below.

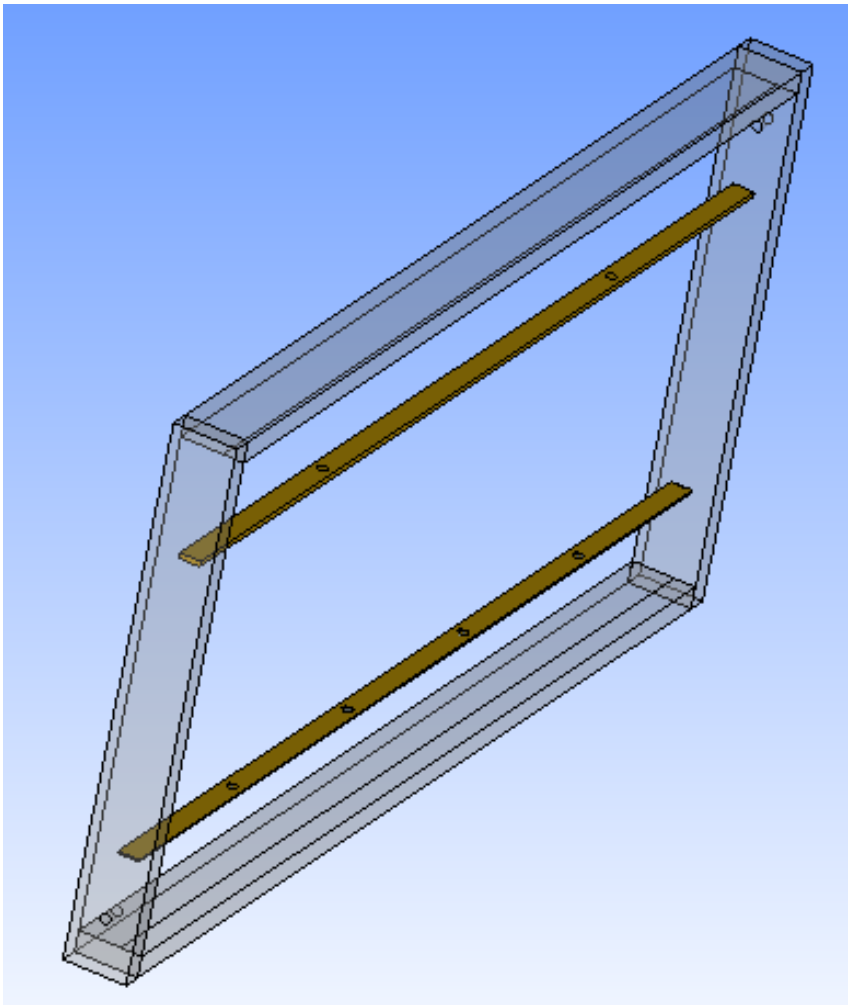

Figure 3-3 Illustration of original model

Height:	0.3m
Thickness of glass:	0.03m
Length:	1m
Width of formation and gravel pack:	2cm
Height of formation:	49cm
Height of gravel pack:	1cm

3.4.2 Glass Strength Calculation

Measurement of required glass strength needed to be calculated, for thickness, t = 3cm, The cross sectional area was calculated, where h=30cm. The cross sectional area (A_{glass}) of the glass is then calculated(30): At the top and bottom of the model it was planned to have aluminum u-profile to withstand the pressure from the porous medium and the flow through it. The internal pressure was approximated to be 5bar.

$$A_{glass} = t_{glass} \times h_{glass} = 0.03m \times 0.3m = 0.009m^2 \quad \textbf{(3-1)}$$

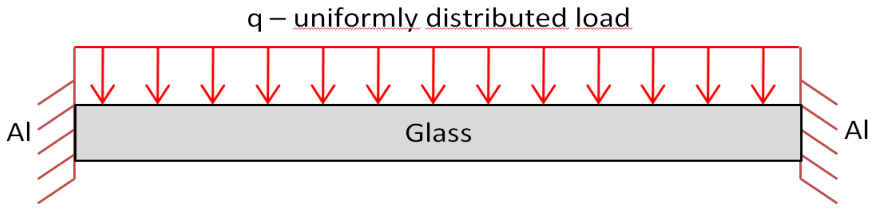

Figure 3-4 Uniformly distributed load on the glass, with aluminum u-profile in the upper and lower ends.

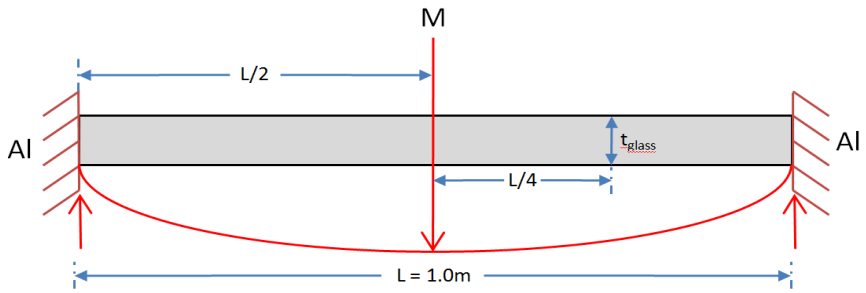

Figure 3-5 Momentum caused by the load

It is assumed that the internal pressure yields a uniformly distributed load across the glass plate. The load (*q - force per length*) can therefore be expressed as the internal pressure (*P*) multiplied with the height (H_{glass}) of the model.(30)

$$q = P \times h_{glass} = 0.3m \times 0.5MPa = 150000N/m \quad \textbf{(3-2)}$$

Further on, the momentum ($M_{average}$) caused by the load is calculated according to equation (3-3) below.(31)(32)

$$M_{average} = \frac{q \times L}{2} \times \frac{L}{2} - \frac{q \times L}{2} \times \frac{L}{4} = \frac{q \times L^2}{4} - \frac{q \times L^2}{8} \quad \textbf{(3-3)}$$

Moment balance, $M_{average}$

$$M_{average} = \frac{150000N/m \times (1m)^2}{4} - \frac{150000N/m \times (1m)^2}{8} = 18750Nm \quad \textbf{(3-4)}$$

$$\omega_b = \frac{t_{glass} \times h_{glass}^2}{6} = \frac{0.03m \times (0.3m)^2}{6} = 0.0045m^3 \quad \textbf{(3-5)}$$

The required yield strength of the glass plate can then be calculated according to equation (3-6) (31)(32)

$$\sigma_b = \frac{M_{average}}{\omega_b} = \frac{18750Nm}{0.00045m^3} = \underline{41.6MPa} \quad \textbf{(3-6)}$$

3.4.3 Conclusion

The required yield strength calculated above, is above the capacity of the glass plates available. And the internal pressure of 5bar was high for the glass plates. It was therefore decided to build a revised model of the test cell with a lower utilization of the material.

The revised model will not be able to demonstrate the effect from water coning in a gravel pack.

3.5 Revised Model

3.5.1 Design of Model

One model with transparent plates has been designed, with an injected porous medium (glass beads). The dimension of the model is discussed in the below. The model has been made of acrylic glass.

The glass beads used were carefully sieved for obtaining the proper size for gravel pack. Before experiment started they were properly saturated with silicon oil.

Oil of density ρ_o and viscosity μ_o fills the pores completely. Water is forced in from one side at an average pressure and flow rate (m3/sec). The density and viscosity of water are ρ_w and μ_w. The interfacial tension and wetting is noted with α and with contact angle θ of the system oil-water-solid material.

3.5.2 The Model's Input Data

For building a model a huge amount of data is needed. Petro-physical data like permeability and porosity is one of the most important ones and usually exhibits strong heterogeneities. Different grids of the gravel pack are also needed for the numerical calculations.

Permeability

The data for absolute permeability is critical for the modelling of most reservoir processes, and also the gravel pack. The absolute permeability exhibits strong heterogeneities. Absolute permeability is normally considered to be time independent so there is not supposed to vary with pressure, but if there is a strong influence on flow performance, the pressure drop will vary and also the permeability.

The absolute permeability has been obtained from analysis from test cell, with different flow rates and variation in pressure drop. This analysis is performed in chapter 4.10.

Porosity

Between the particles in the gravel pack there is space for fluid. The fluid occupies some part of the fraction of the reservoir volume. The occupied part of the volume is called porosity and is denoted with the sign, Φ.

The porosity is also strongly heterogeneous, like the permeability. The porosity of the medium (glass beads) used in the experiment is calculated in chapter 5.5.1.

Fluid Data Assumptions

Basic assumptions for the model are:

- Two phases; water and oil
- Two components; water and oil
- The water component only exists in water phase
- The oil component only exists in oil phase
- No phase transfer between water and hydrocarbons. This means that there is no dissolved oil in water and vice versa. And the water is still in water phase and consists of water component only.

Saturation Conditions

The model that is considered consist of two phases, water and oil, which are flowing simultaneously. The saturation of phase l, Sl, which is the fraction of the pore volume, occupied by a phase, and l can be both water and oil. If both oil and water phase are flowing simultaneously, the effective permeability of each phase depends on the saturation distribution. So if the saturations vary, the effective permeability also changes.

Another set of saturation dependent parameters is the capillary pressures. As described in chapter 2.1.7. This parameter can influence all different parts of the simulations, like initial fluid distribution, flow characteristics and the ultimate recovery.

The permeability in the model is assumed to be constant, thus capillary pressures and changes in saturation are neglected.

Finite differences and dimensions

Figure 3-6 shows the different blocks where the different boundaries have been placed in the middle of the inlet tubes.

The horizontal x-axis is divided into smaller segments, where the boundaries are with the horizontal perforations, and injection "holes" for water and oil.

The pressure drop was calculated between one grid block to the other one. The total pressure drop was found, when multiplying the darcy pressure drop (in x-direction) with the vertical friction pressure drop from inlet tubes (y-direction). An also important factor is the flow rate given from the inlet tubes. Calculation of flow rate was done in comparison with the pressure drop. Total flow rate was calculated and measured.

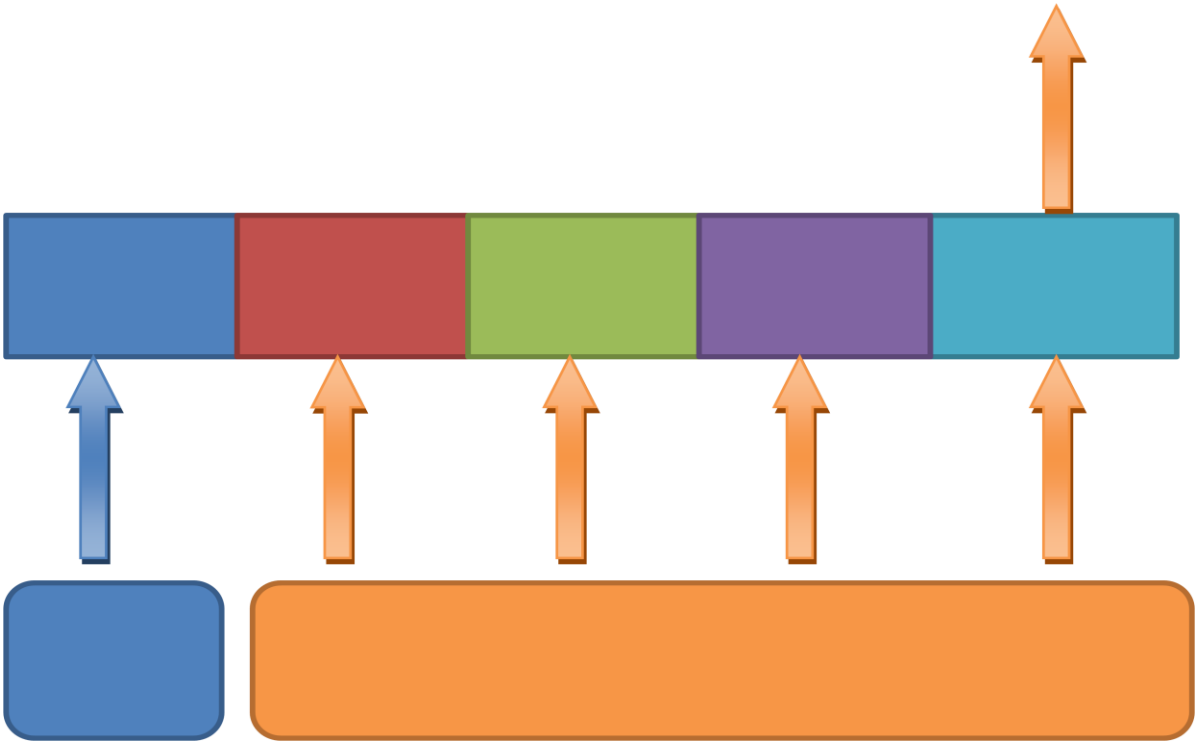

Figure 3-6 Gravel Pack divided into different blocks.
Water is injected from rightmost block toward leftmost block. Outlet is placed at the outlet block. Oil is injected from the other inlet, towards the outlet. Pressure drop is calculated for both vertical pipes and horizontal gravel pack. The arrows shows the flow direction of oil and water, injected in to the gravel pack. There are supposed to be two perforations here, but since one of them are decided to be closed, only one with the flow direction is drawn.

The flow from one block to another is determined with the pressure drop and the composition of the fluids in the upstream tanks (if it is water or oil). The fluid properties do not vary within the blocks. The total number of blocks does have an influence on the calculation when it comes to precision of describing the gravel pack model numerically.

To reduce the numerical error, the number of grid blocks can be increased, Figure 3-7 and Figure 3-8. Then the flow rate and the pressure drop calculations can be more accurate. But the time of modelling will frequently impose the limits on the size of the model.

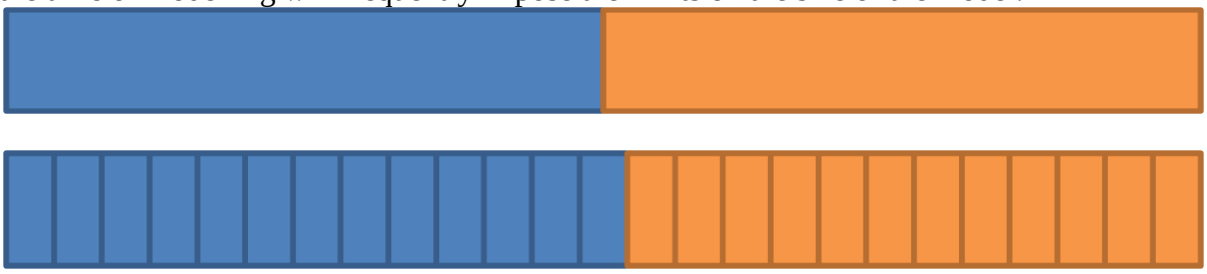

Figure 3-7 Number of blocks can be increased to reduce the numerical dispersion.
This picure is based on piston like displacement

Figure 3-8 Water is injected and "underride" the oil.

3.5.3 Properties and Dimensions

The model visualized under in different drawings is the drawing of the new revised model. This model has been used for the laboratory experiment for displacement of oil in gravel pack.

Spacer

The first drawing is visualizing the model from profile. In the middle of the whole block is an open space where the gravel is displaced into correct placing for optimum flow through gravel pack. This block is transparent, which means that it is possible to see how the flow is displacing from every possible angle. As seen there are some red and blue dots riddled. The leftmost and rightmost red hole is one of two perforations, perforated from gravel pack to well. The rightmost blue dotted riddle is the water inlet. Inlet for oil tubes are the four other blue dotted riddles. Gravel was displaced into the open space, from an open hole at the right side (purple dots). Flow direction was set to be from left to right. The spacer is shown in Figure 3-9 below. A design specification is given below.

Side Profiles

In Figure 3-10 the side profiles are drawn. The side profiles have been placed on the right side and the left side of the spacer, also ment as behind the spacer and in front of the spacer. The black dashed line is a milled area where there should be room for an o-ring, used to keep the model stiff, and to prevent leakage of oil. Specifications of the side profiles are given in Table 3-4.

End Profile

The end profile shown is from the right side of the model,Figure 3-12. In-between two Side Profiles is the spacer. Dotted black lines visualize placing of gravel pack. The purple circle is the injection of gravel pack.

Top

Figure 3-11 visualize the model seen from above. The spacer is placed in the middle with two longitudinal plates on both sides. The perforations, water and oil injections and opening to inject gravel is pointed out in the figure.

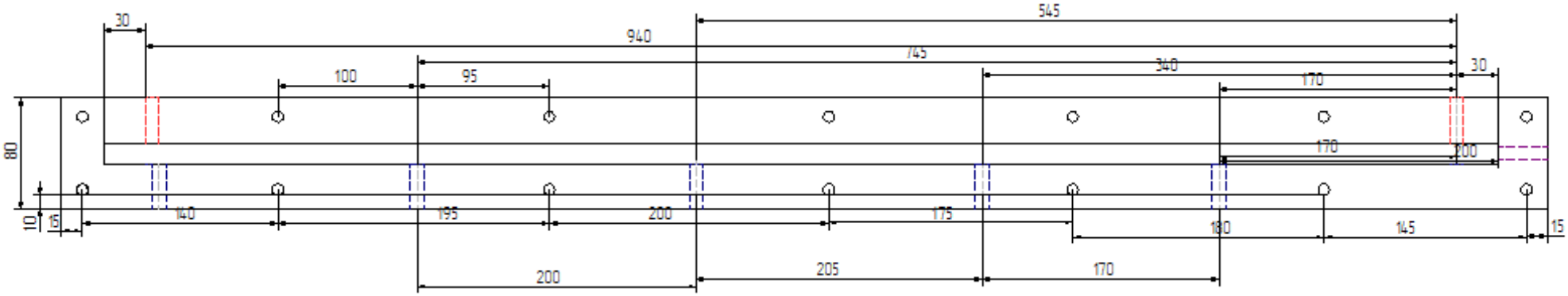

Figure 3-9 Design of spacer

Table 3-3 Design specifications

Total length of model [mm]	1060
Inside length *L*, [mm]	1000
Thickness bottom and top (above and under gravel pack) [mm]	32.5
Total height of model [mm]	80
Thickness of side walls [mm]	30
Thickness of end walls [mm]	30
Height of gravel pack, h_{gp} [mm]	15
Depth of gravel pack , D_{gp} [mm]	15
Length of gravel pack , L_{gp} [mm]	1000
Area of gravel pack, *A* [cm^2]	150
Cross sectional area, *A* [cm^2]	2.25
Volume of gravel pack, V_{gp} [cm^2]	225
Diameter of perforations (red dots) [mm]	approx 10
Diameter of inlet of water and oil tubes (blue dots) [mm]	approx 10
Diameter of packing hole (purple dots) [mm]	10
Number of bolts	14
Diameter of bolts [mm]	8

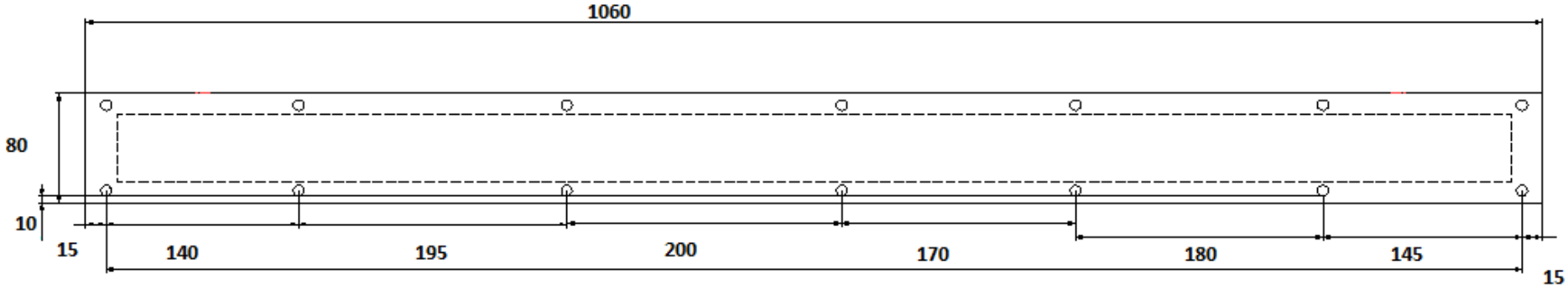

Figure 3-10 Side Profiles with bolts, length specification between bolts.
The dotted line is a milled trace for o-ring used to put the model stiff and to prevent leakage

Table 3-4 Side Profile specification for two units

Thickness of plates [mm]	30
Depth of plates [mm]	30
Length of plates [mm]	1060
Diameter of bolts [mm]	8
Number of bolts [units]	14
Distance from bottom edge to centre of bolt holes [mm]	14
Distance from upper edge to centre of bolt holes [mm]	14
Distance from end edge (left + right) to centre of bolt holes [mm]	19
Length between bolt holes parallel upper holes and bottom holes [mm]	140,195, 200, 170, 180, 145

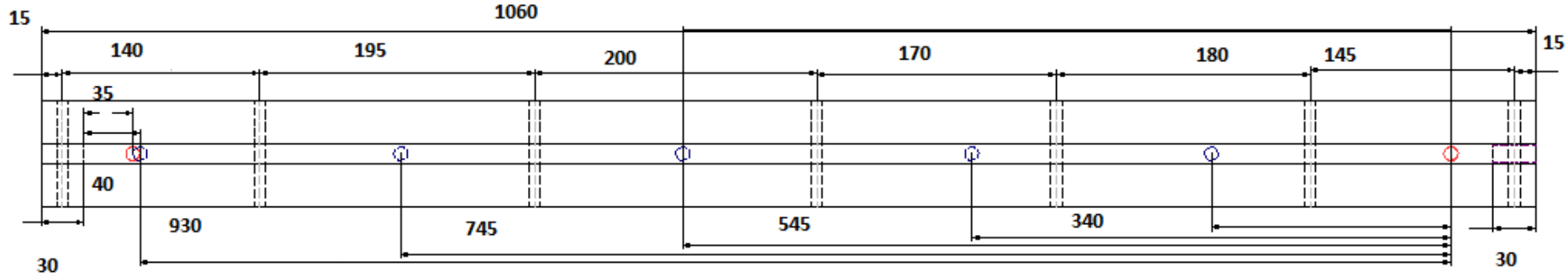

Figure 3-11 Model seen from above

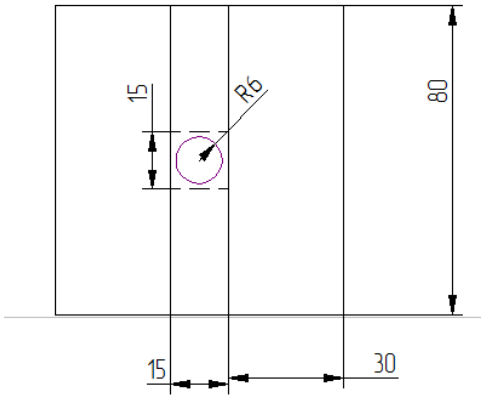

Figure 3-12 End Profile with spacer in the middle with two side profiles

Table 3-5 Specification of End Profile

Width of spacer [mm]	15
Thickness of side profiles [mm]	30
Radius of hole [mm]	5
Height of model [mm]	80

3.5.4 Mathematical model

A mathematical model of the gravel pack descibes the process which is taking place when a fluid is flowing through it. For the mathematical modelling of flow through a gravel pack, the physical system modelling is expressed in terms of equations. The model of flow is often called numerical models, using numerical terms. The following model used in this thesis is made for single phase, 1D flow, with the two components oil and water.

The accuracy of the performance predictions will depend on the characteristics of the model and the accuracy and completeness of the input description:

- The numerical equations will give only an approximated description of the physical process
- For the modelling of reservoir fluid in the gravel pack, approximations for the different units are used. So when using approximations the values from calculated data will be different from experimental data.
- The values of all variables, like porosity, permeability, viscosity of the medium and fluid, and the values for length of gravel pack, depth and height of gravel pack, need to be determined and clarified.

As described in chapter 3.5.3 the gravel pack model consist of one water filled tube and four tubes filled with oil, all connected to a rectangular model packed with glass beads. The glass beads are saturated with oil prior to the initiation of the experiment. A schematic illustration of the model is depicted below. Each inlet tube is assigned a letter, from A to E, while the outlet perforation is marked P. These letters corresponds to the subscripts used in the equations below. The flow direction is from inlet A to P and the pressure drop is measured between the high side, inlet A and the low side, perforation P.

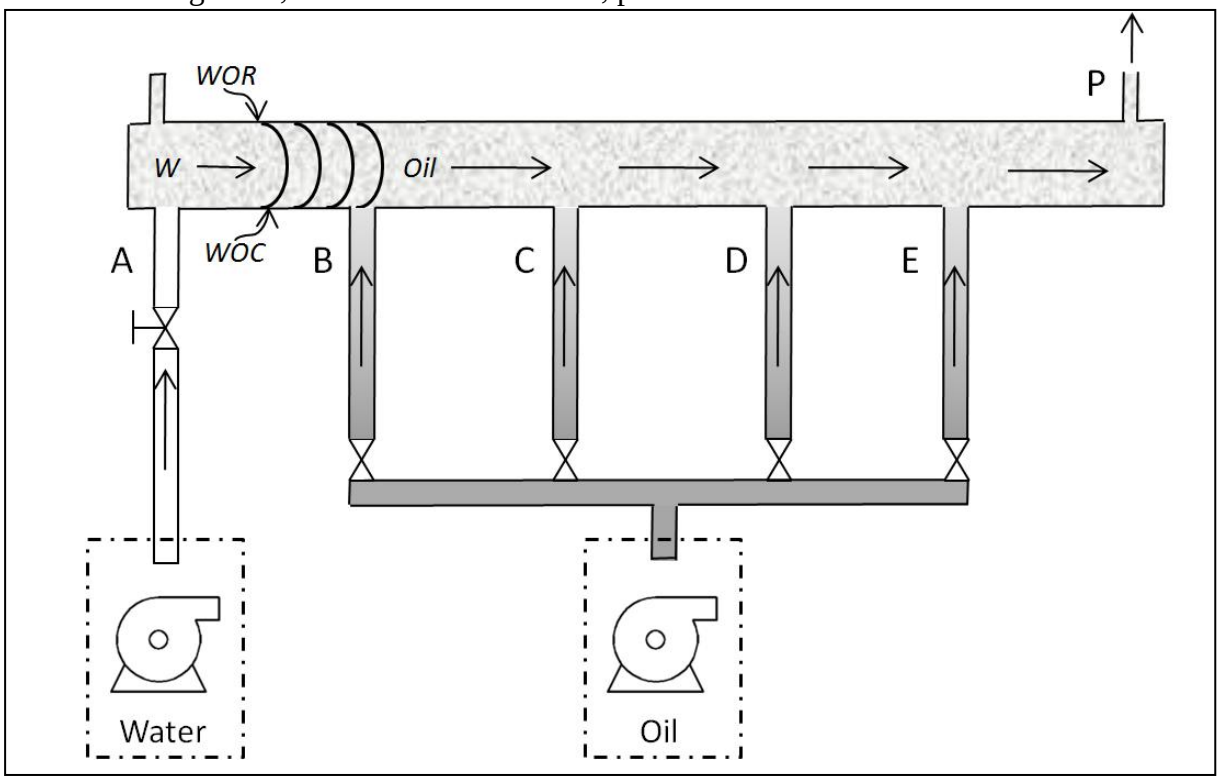

Figure 3-13 New revised model. One injection inlet for water and four injection inlets for oil.

Calculation basis

An analytic approach is used to estimate a value for the flow rate through the model. The flow rate is dependent of the available pressure provided by the pumps and limited by the hydrostatic head difference, the friction induced pressure drop through the tubes and by the pressure drop through the porous medium.

As the pressure at each inlet is known, as well as the ambient pressure at the perforation, *P*, it is possible to calculate the flow rate which corresponds to the known differential pressure.

Key assumptions

In order to simplify the calculation some assumptions are performed.

- It is assumed that the permeability of the porous medium is constant.
- It is assumed that the flow through each tube is independent of each other.

Calculations

As described above, the flow through the model is dependent on the available pressure difference between the pumps (P_a – pressure at tube A) and the pressure at the perforation (P_{atm}). The differential pressure (dP_{tot}) can therefore be expressed as:

$$dP_{tot_{a-p}} = P_a - P_{atm} \quad \textbf{(3-7)}$$

The differential pressure can also be described by the pressure drop through the model. The pressure drop consists of three elements; the hydrostatic head (dP_h), the friction induced pressure drop (dP_f) and the pressure drop through the porous medium (dP_D).

$$dP_{tot_{a-p}} = dP_{h_a} + dP_{f_a} + dP_{D_{a-p}} \quad \textbf{(3-8)}$$

As described by Bernoulli (33) the hydrostatic head is a function of the fluid density (ρ), the gravity (g), and the height difference (h) from pump discharge to the perforation.

$$dP_{h_a} = \rho_{water} \times g \times h_a \quad \textbf{(3-9)}$$

The pressure drop through the porous medium is described by Darcy's law (14)which consists of the following elements; the flow rate (q), the length of the model (L), the viscosity of the flowing medium (μ), the permeability of the porous medium (κ) and the cross sectional area of the model (A_{gravel}).

Note that the oil viscosity is used to calculate the pressure drop through the porous medium (including the pressure drop originating from A) as the model is saturated with oil and water will not flow until the oil is displaced.

$$dP_{D_{a-p}} = \frac{q_a \times L_{ap} \times \mu_{oil}}{\kappa \times A_{gravel}} \quad \textbf{(3-10)}$$

The frictional pressure drop can be expressed using a function for single phase pressure drop for laminar flow. (34) Laminar flow is valid for Reynolds number below 2300. The function consists of the following elements; diameter of the tube (D), the Fanning friction factor (f) (34) the density of the medium (ρ) and the velocity (U).

$$dP_{f_a} = \frac{4}{D_a} \times f_a \times \frac{1}{2} \times \rho_{water} \times U_a^2 \quad \textbf{(3-11)}$$

The velocity U can be expressed using the flow rate (q) and the area of the tube (A):

$$U_a = \frac{q_a}{A_a} \quad \textbf{(3-12)}$$

The Fanning friction factor is a function of the Reynolds number:

$$f_a = \frac{16}{Re} \quad \textbf{(3-13)}$$

The Reynolds number is a function of the density of the flowing medium (ρ), the velocity (U), the diameter of the tube (D) and the viscosity of the medium (μ).

$$Re = \frac{\rho_{water} \times U_a \times D_a}{\mu_{water}} \quad \textbf{(3-14)}$$

Combining equations (3-13)and (3-14):

$$f_a = \frac{16}{\frac{\rho_{water} \times U_a \times D_a}{\mu_{water}}} \quad \textbf{(3-15)}$$

The frictional pressure drop can therefore be expressed as:

$$dP_{f_a} = \frac{4}{D_a} \times \frac{16}{\frac{\rho_{water} \times U_a \times D_a}{\mu_{water}}} \times \frac{1}{2} \times \rho_{water} \times U_a^2$$

$$= \frac{4}{D_a} \times \frac{16}{\frac{\rho_{water} \times \frac{q_a}{A_a} \times D_a}{\mu_{water}}} \times \frac{1}{2} \times \rho_{water} \times \left(\frac{q_a}{A_a}\right)^2 = \frac{32 \times \mu_{water} \times q_a}{D_a^2 \times A_a} \quad \textbf{(3-16)}$$

Combining equations (3-9),(3-10),(3-11)and (3-13):

$$dP_{tot_{a-p}} = \rho_{water} \times g \times h_a + \frac{32 \times \mu_{water} \times q_a}{D_a^2 \times A_a} + \frac{q_a \times L_{ap} \times \mu_{oil}}{\kappa \times A_{gravel}} = P_a^w - P_{atm} \quad \textbf{(3-17)}$$

Solving for flow rate:

$$q_a = \frac{\left(P_a^w - P_{atm} - \left(\rho_{water} \times g \times h_a\right)\right)}{\left(\frac{32 \times \mu_{water}}{D_a^2 \times A_a} + \frac{L_{ap} \times \mu_{oil}}{\kappa \times A_{gravel}}\right)} \quad \textbf{(3-18)}$$

Assuming that the flow through each tube is independent of each other, the total flow rate can be expressed as:

$$q_{total} = q_a + q_b + q_c + q_d + q_e \quad \textbf{(3-19)}$$

Combining equation (3-18)and (3-19), using the notations indicated in Figure 3-13 the total flow rate can be expressed as:

$$q_{total} = \frac{\left(P_a^w - P_{atm} - \left(\rho_{water} \times g \times h_a\right)\right)}{\left(\frac{32 \times \mu_{water}}{D_a^2 \times A_a} + \frac{L_{ap} \times \mu_{oil}}{\kappa \times A_{gravel}}\right)} + \frac{\left(P_b^{oil} - P_{atm} - \left(\rho_{oil} \times g \times h_b\right)\right)}{\left(\frac{32 \times \mu_{oil}}{D_b^2 \times A_b} + \frac{L_{bp} \times \mu_{oil}}{\kappa \times A_{gravel}}\right)} + \frac{\left(P_c^{oil} - P_{atm} - \left(\rho_{oil} \times g \times h_c\right)\right)}{\left(\frac{32 \times \mu_{oil}}{D_c^2 \times A_c} + \frac{L_{cp} \times \mu_{oil}}{\kappa \times A_{gravel}}\right)} \ldots$$
$$\ldots \frac{\left(P_d^{oil} - P_{atm} - \left(\rho_{oil} \times g \times h_d\right)\right)}{\left(\frac{32 \times \mu_{oil}}{D_d^2 \times A_d} + \frac{L_{dp} \times \mu_{oil}}{\kappa \times A_{gravel}}\right)} + \frac{\left(P_e^{oil} - P_{atm} - \left(\rho_{oil} \times g \times h_e\right)\right)}{\left(\frac{32 \times \mu_{oil}}{D_e^2 \times A_e} + \frac{L_{ep} \times \mu_{oil}}{\kappa \times A_{gravel}}\right)} \quad \textbf{(3-20)}$$

<u>Calculation of flow rate and pressure drop using Goal Seek</u>

- First the input data was decided. The length from the different inlet holes to the perforation was decided. The height of the water and oil pipe was also set, the same with the inner diameter. The width and depth of the gravel pack was decided and calculated in advance. Permeability was set to be constant. The absolute inlet pressure was set to be constant. The density and viscosity of water was assumed, and the same for the density of oil.
- After deciding the input data, area of pipe and gravel pack was calculated, with using some of the input data.
- For the flow rate an initial calculation was assumed.
- For finding the frictional pressure drop, $\left(\frac{dP}{dy}\right)_{friction}$, calculation of Reynolds number, Re, friction drop, f, for both oil and water is needed, ref equation (3-15)
- The hydrostatic pressure drop, $\left(\frac{dP}{dy}\right)_{hydrostatic}$ ref equation (3-9)

- The Darcy Equation was used to calculate the pressure drop in the gravel pack with use of permeability and Darcy flow. From the hydrostatic pressure drop, frictional pressure drop and Darcy pressure drop, the calculation of total pressure drop, $dP_{calculated,}$ have been performed.
- If $P_{calculated} \neq dP_{real}$, then the initial assumed flow rate is incorrect. To find the correct flow rate Excel function *"Goal Seek"* is used. This function increases/decreases the flow rate until the $dP_{calculated} = dP_{real}$.
- The Goal Seek function is found on the Data tab in Excel, in the Data Tools, under the What-If Analysis, and then click on Goal Seek. In the Set Cell box, enter the reference for the cell that contains the formula that is supposed to be solved. To the value box, the wanted value has to be typed. In the By Changing cell box, the reference for the cell that contains the value that wanted to be adjusted. The Goal Seek changes must be referenced by the formula in the cell that is specified in the Set Cell box. When Run is clicked, the Goal Seek runs and produces a result. (35)

4 DETERMINATION OF TEST INPUT PROPERTIES

4.1 Equipment

4.1.1 Gilson Pump 305 Piston Pump

The 305 Master pump is designed as a system controller. It can operate as a stand-alone pump or as a system controller. The pump controls, as a system controller, a complete pumping system, elution pumps and injection pump. The pump can operate in three different modes (36):

1. Flow
   The pump provides a constant flow rate. It starts and stops with the Run and Stop key. The flow mode is for isocratic use only
2. Dispense
   The pump dispenses a specified volume. The pump starts when the start button is pressed and stops when the specified volume has been dispensed. The dispense mode is for isocratic use only.
3. Program
   The pump controls a multi pump system with up to two slave elution mumps and 1 slave injection pump. In this mode the pump can create gradients of flow rate and composition, open and close outputs to control other instruments and wait for signals from other instruments.

In flow mode, the pump provides a constant flow rate. Input is activated from the run key and stopped when pushing the stop key. The flow rate can be set between 0.01% and 100% of the pump head size. A flow rate will not be accepted if it is larger than the pump head size. The flow rate can be modified at any time during a run by keying a new value. It is possible to review and change the pump and I/O setup parameters except the pump head size during the run (36).

In the dispense mode the pump can be used to deliver a specified volume beginning when the run button or start input is activated, and finishing when the specified volume of liquid has been delivered. The parameters to be delivered are dispense volume and dispense flow rate or time of dispense. The maximum dispense flow rate depends on the refill time and compressibility. If the dispense flow rate or volume is not compatible with the head size, the software will not accept the value and a new value must be keyed in (36).

In the program mode the pump can create both flow rate and composition gradients, program timed events, and control an injection pump. The program can also simulate the flow and dispense modes, with the advantage of safety error files and the ability to program timed events (36).

4.1.2 Physica – Viscosity meter

Physica was used to measure viscosity of the different oils and water used. It was done to have a precise value of viscosity. The measuring system used was MK24 cone plate. (37)

Specifications of Physica:

Accurate readings	
Shear rate factor [s^{-1}]	6.05
Shear rate range [s^{-1}]	0-4.840
Shear stress range [Pa]	0-453
Viscosity range [Pa*s]	0.001-748

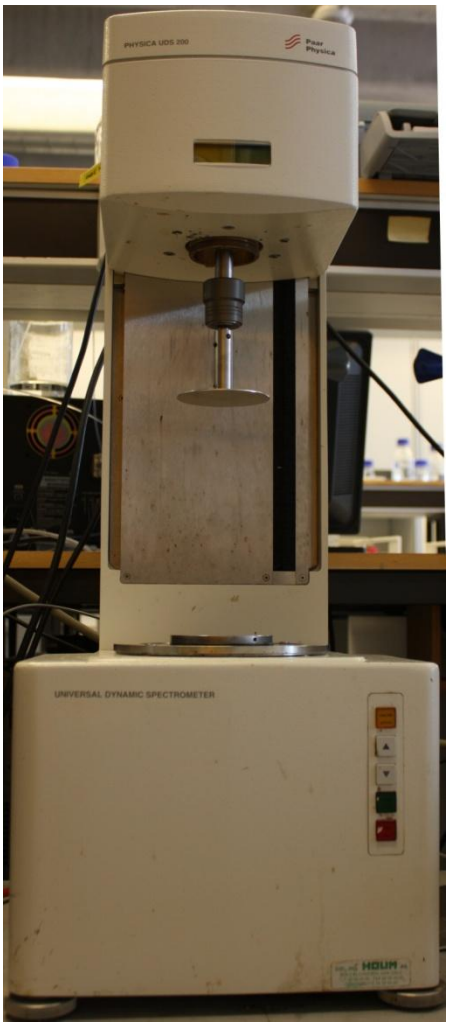

Figure 4-1 Physica -Viscosimeter

4.1.3 Anton Paar - DMA 4500/5000 Density/Specific Gravity/Concentration Meter

The DMA 4500/5000 is an oscillation U-tube density meter measuring with high accuracy in wide viscosity and temperature ranges. It provides stability and makes adjustments at temperatures other than 20ºC. (38)

To perform measurements, one out of 10 individual measurement methods is selected. And the sample is filled to the measuring cell. An acoustic signal informs when the measurement is finished, and results are automatically converted (including temperature compensation where necessary) into concentration, specific gravity or other density-related units using the built-in conversion tables and functions. The accuracy of the DMA 4500 is $5x10^{-5}$ g/cm^3. (38)

Measurements

There are different measurement methods and among them is density measurement. Measurement of density and specific gravity including viscosity correction for liquids of viscosity below 700mPa*s. This method is suitable for highly accurate measurements of the true density of liquids.

The sample used has to be homogeneous and free of gas bubbles. Suspensions or emulsions may tend to separate in the measuring cell, giving incorrect results. And a sample temperature similar to the measuring temperature of 20ºC reduces the measuring time. A waste bottle is placed at the outlet of the measuring cell and the samples need to be used together with the nozzles. This is in order to avoid glass breakage of the measuring cell. The syringe is attached slowly and continuously until a drop emerges from the other nozzle. The syringe is left in the filling position to prevent leakage.

Table 4-1 Technical Data

Measuring range	0-3 g/cm^3
Repeatability	
Density	1 x 10^{-5}
Temperature	0.01 ºC
Measuring temperature	0ºC-90ºC
Pressure range	0-10 bars
Amount of sample in the measuring cell	Approx. 1ml
Measuring time per sample	Approx. 30 sec.

4.1.4 Rosemount dP logger

The differential pressure is measued with a standard Rosemount dP logger. The differential pressure is measured between the two perforations on the horizonthal gravel pack model as described in chapter 3.5.3.

4.1.5 AccuPyc 1340 Pycnometer

The AccuPyc 1340 Pycnometer is a fully automatic gas displacement pycnometer. Analyses are started, data collected, calculations performed and results displayed without further operatior intervention. Autopyknometer is used for laboratory work to find the density of a substance with an unknown volume. The technique for the instrument is to compress identically two quantities of dry gas at the same temperature and pressure, but initially of equal volume because of the space occupied by a sample. Even at the same temperature the compression of unequal volume results in unequal pressure. Then an adjustment has to be made in the volume of the lower gas while under-compression to bring it to the higher. The compression of two gasses has then been removed and the gas pressures are equalized.

Compression of gases is applied with unequal pressure testing. The pressures must be more equal than before, because of the volume adjustment. In the following, further volume adjustments have been made and the decompression, equalization and recompression repeated until pressure equality is established. The sum of the volume adjustments is equal to the sample volume. This volume is then electronically divided by the sample weight to give the sample volume (39).

Table 4-2 Environment and physical specifications

Height [cm]	17.9
Width [cm]	27.3
Depth [cm]	36.2
Weight [kg]	9.3

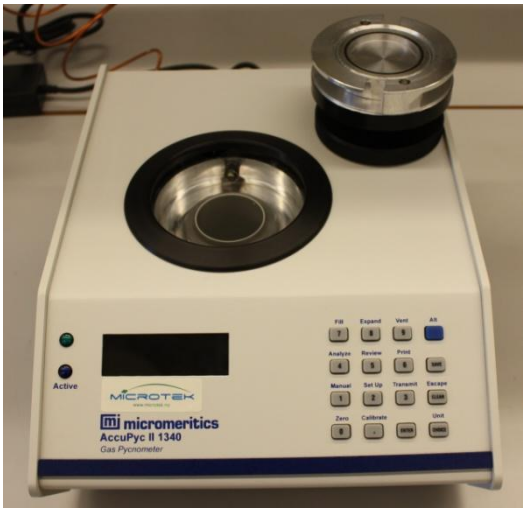

Figure 4-2 Autopycnometer

4.1.6 Du Noüy Ring Method

Du Noüy ring method is used to measure surface tension of fluids. The method involves lifting a platinum ring on the surface of a fluid or at the interface between two immiscible fluids. The force that is required to lift the ring from the liquid's surface is measured and is called the interfacial or surface tension (40). The interfacial tension is measured between Bayol35 and ionized water, and Marcol82 and ionized water.

4.1.7 Pressure testing of revised model

After compiling the three plates together, the model was pressure tested. Unfortunately it was discovered that the model started to leak severly at a pressure of 2.0barg. Therefore, the experiments had to be performed with a lower dP than anticipated.

4.2 Determination of Permeability

4.2.1 Permeability of Test Cell

The absolute permeability has been measured in a vertical circular test cell. The porous medium was a cell composed of unconsolidated glass beads saturated with oil. The oil fills the sample pores completely and shows little or no connection between interactions with the glass beads. The oil's molecules are able to penetrate even the smallest pore throats. This means that the pore channels will be involved in the fluid transmission and hence the permeability measured will be a good estimation of the pore network's bulk transmissibility (2).

4.2.2 Conditions for Permeability Measurements

The permeability of the oil saturated glass beads is measured for a horizontal flow and the basic conditions have to be satisfied (2):

- Incompressible fluid
- 100% fluid saturation in the sample
- Stationary flow (constant transverse cross-section)
- Laminar fluid flow
- No chemical reactions or ion exchange between the fluid and the glass beads

The permeability is measured by Equation (2-35):

$$q = -\frac{Ak}{\mu \Delta L}\Delta P$$

Where q and ΔP and the other remaining data are measured and calculated. Value of k is determined by plotting the measured the measured data in a two-axial diagram and finding a trend line for the projected points. The permeability, k, is then calculated from the line slope's equation, $y = ax + b$. By plotting the data in a graph it is also possible to determine the quality of the measurements. A non linear trend of the projection points or if the data points are relatively wide spread will indicate a bad correlation between the measured variables, or that some of the measurements conditions have not been satisfied (2).

$$q = \frac{Ak}{\mu \Delta L}\Delta P = a \times \Delta P \quad \textbf{(4-1)}$$

$$a = \frac{Ak}{\mu \Delta L} \quad \textbf{(4-2)}$$

$$k = \frac{q\mu \Delta L}{A \Delta P} \quad \textbf{(4-3)}$$

R^2 in the graph is the regression and it says something about the linearity of the plot. The closer to 1.000 the value of R^2, the more linear is the plot, and the more confidence of the measurements.

4.3 Determination of fluid properties

4.3.1 Chemicals

Bayol 35

Bayol is a highly refined white mineral oil and lubricant (41).
Benefits for this oil are;

- Whater white colour
- Non-staining
- Odour free
- Non-reactive
- Low aromatic contents

The colour and degree of refining are adequate for certain processing applications (41).

Table 4-3 Typical properties (41) (42)

Bayol 35	
Density [kg/m^3]	791
Colour, Saybolt	+ 30
Kinematic Viscosity, [cSt]	2,3 (from manufacturer)
Flash Point, COC,[°C]	
Flash Point, TCC Closed Cup, [°C]	96
Appearance and odor	Clear colorless oil with a neutral odor
Density, [g/ml]	0,79
Boiling point	N/A
Viscosity [mm^2/S] [40°C]	2
Viscosity [Pa*s]	0,00099088
Vapour Pressure [kPa] [20°C]	Very low
Evaporation Rate	Very low
Solubility in water [20°C]	Insignificant
pH	Non-relevant
Flash Point Method	>75°C PMCC ASTM D-93

Marcol 82

Marcol is a highly refined white mineral oil and lubricant (43)
Benefits for this oil are;

- Clean colourless
- Non-staining
- Odour free
- Non-reactive
- Low aromatic contents

Table 4-4 Typical properties (43)

Density [kg/m^3]	850
Colour,	No colour
Kinematic Viscosity, [cSt]	2,3 (from manufacturer)
Flash Point, COC,[°C]	
Flash Point, TCC Closed Cup, [°C]	96
Appearance and odor	Clear colorless oil with a neutral odor
Density, [g/ml]	0,85
Viscosity [mm^2/S] [40°C]	14.5
Vapour Pressure [kPa] [20°C]	<0.013
Solubility in water [20°C]	Insignificant
pH	Non-relevant

Lissamine Red 6 B

Lissamine Red 6B is a dye used to colour water.
The following will give the reader an understanding of Lissamine Red 6 B

Table 4-5 Physical and Chemical Properties

Molar mass	$566.48\,g/cm^3$
Formula	$C_{20}H_{19}N_2NaO_9S_2$
Form	Solid
Colour	Dark red
Odour	Not available (N/A)
pH value	N/A
Melting point	N/A
Boiling point	N/A
Ignition temperature	N/A
Flash point	N/A
Explosion limits	N/A
Density	N/A
Solubility in water (20°C)	N/A

4.3.2 Density measurements

The different fluids used were Bayol35, Marcol82 and ionized water. The densities of the oil were measured with Anton Paar DMA 4500 density meter. Density of Bayol35 was not used for calculation, only for visualization purposes and informational uses. The density of ionized water and Marcol82 was used for calculation of pressure drop and total flow in the modelling of the horizontal and vertical displacement in the gravel pack. The data used for density of the different oil is shown in Table 4-6

4.3.3 Viscosity

The viscosity of the different types of oil and ionized water was measured with Paar Physica US 200 Viscosity meter. The measuring system used was MK 24, with different shear rates. The viscosity was used in calculation of absolute permeability in Equation (2-34). The viscosity used for calculation is shown in Table 4-6. The information and procedure for Physica can be found in chapter 4.1.2.

4.3.4 Surface and Interfacial Tension

Surface tension of water and the different oil was measured with Du Noüy ring method. The interfacial tension between Bayol35 and ionized water and Marcol82 and ionized water has been measured. Du Noüy ring method is introduced in chapter 4.1.6

Table 4-6 Specifications of oil and water used for displacing fluid

	Bayol35	Marcol82	Ionized Water	Bayol35 + Ionized Water	Marcol82 + Ionized Water
Density ρ [$^{g}/_{cm3}$]	0.78955		0.99141		
Specific gravity [s.g.]	0.7910		0.9932		
Viscosity [Pa*s]	0,00245	27.2	0.00126		
Temperature [^{0}C]	20	20	20		
Surface tension [$^{mN}/_{m}$]		26.4	70.4		
Interfacial tension between Bayol35 and ionized water is 27.4 $^{mN}/_{m}$					
Interfacial tension between Ionized water and Marcol82 is 42.1 $^{mN}/_{m}$					

4.4 Preparation of Porous Medium

4.4.1 Glass beads drying

The gravel pack is made by glass beads of silica in the size of 250 to 355µm, and is assumed to be homogeneous and isotropic.
In order to get sufficient separation of glass beads they were dried at a sufficient temperature at 90° C for several hours. After drying process the glass beads were separated in different convenient sizes.

4.4.2 Glass Beads Separation

For correct gravel sizing the formation grain size and range must be determined accurately. A representative formation sand sample is extracted, dried, weighted, separated and passed through sieves of different openings.
The grain size separation was done with Haver EML digital T Test Sieve Shaker to separate the different particle sizes. The instrument can be seen in Figure 4-3. Different sieves with different mesh size were used for the separation.

The particles size for the gravel pack was decided to be around 255-355µm. The permeability for this size was measured to be 52.23 D for the viscosity
The sieves' mesh sizes for finding the correct reservoir particles was, 100µm, 125µm, 180µm, 250µm, 355µm, 400µm, and 500µm. The majority of particle size was between 250-355µm. This was done first to find the correct particle size for the gravel pack.

The mesh size is related to the standard openings of sieves and the definition of mesh is:

"Mesh = number of openings per inch, counting from the center of any wire in the sieve to a point exactly 1-in. distant. Mesh sizes are read as follows; 20/40mesh commercial gravel passes through a 20mesh sieve and is retained by a 40mesh sieve."

Figure 4-3 Haver EML 200 digital T Test Sieve Shaker used for separation of glass beads

4.5 Density of Silica Glass Beads

The density of glass beads was measured with Autopycknometer and is shown below.

$m_{beaker} = 35{,}60g$

$m_{beaker+particles} = 143{,}90g$

$m_{particles} = 108{,}30g$

$V_{avg} = 43{,}4635cm^3$

$Std.dev = \sigma = 0{,}0101cm^3$

$$\rho_{particles} = \frac{m_{particles}}{V_{avg}} = \underline{2{,}491746g/cm^3} \approx \underline{2{,}49g/cm^3}$$

From the equation above it is possible to see that the standard deviation, σ, is relatively high. The density of the particles is distributed between 2.48g/cm^3 and 2,50g/cm^3.

4.5.1 Density of Glass Beads with Le Chatelier method

Le Chatelier Method is used to dobble check the density of glass beads.

The Le Chatelier bottle (Figure 4-4) was filled up with water at room temperature. This is done to provide an accurate result of the density. Then the initial volume, V_i, and weight of the bottle, m_i, are found. A certain amount of the glass beads are carefully added into the bottle. Care must be taken so that the bottle neck is not sealed.

Thereafter the Le Chatelier bottle is filled with glass beads up to the next reading level, 20ml. The specific density of the glass beads can then be calculated from the volume, V_t and the weight of the bottle, m_t.

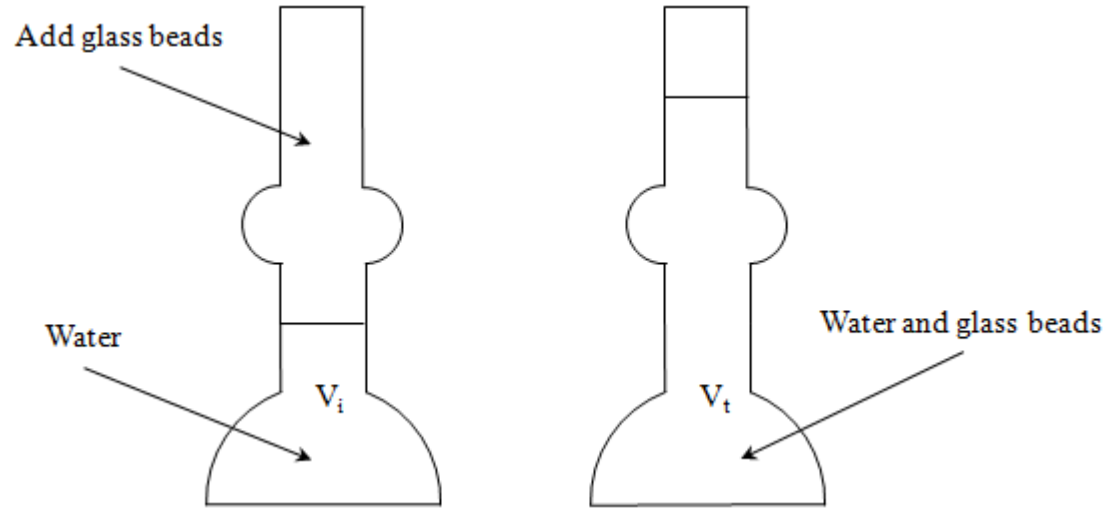

Figure 4-4 Le Chatelier Method

$$m_{cylinder+water} = 383.6g$$

$$m_{total} = 432.9g$$

$$V_p = 20cm^3$$

$$\rho_{glassbeads} = \frac{m_{total} - m_{cylinder+water}}{V_p} = \underline{2.48\,g/cm^3}$$

4.6 Porosity Measurement of Silica glass beads

Porosity was measured in order to calculate the theoretical fluid flow through the gravel pack. The porosity is calculated to Φ=0.41, ref chapter 5.5.1

4.7 Saturation of Porous Medium

Glass beads were saturated with oil approximately 24hours before packing started. A large amount of oil was used to saturate the amount of needed glass beads.

4.8 Packing of Porous Medium in Test Cell

As mentioned in chapter 2.3.4 packing of the porous medium is of high importance. To get the best condition for a good packing of glass beads, a shake machine used. A shake machine is used so that the glass beads are placed in the best manner. The cross-section area of the test cell is narrow and it is easy for particles to adhere to the wall. The test cell was placed on the top of the shake machine. Shaking from the machine, along with gravity, makes glass beads

fall easily into place. In between packing it is important to check the test cell for air. Since the air can cause erroneous permeability and porosity measurements, it is important to clear the air as soon as air is seen in the cell. The air was removed by stirring gently so that the air bubbles ascended to the surface. In some cases it was difficult to remove the air, therefore a part of the glass beads had to be removed and packed again.

4.9 Packing of Porous Medium in Gravel Pack model

Packing of porous medium into the gravel pack model was challenging. Since the size of the gavel pack is thin and long care had to be taken during packing. Particles had to be brought down gently in order to make them sit properly. Oil had to be drained out continuously. The model was set at an angle such that particles slid down the wall and oil flowed upwards along the other wall. This procedure was performed until the glass beads were packed to the top. At this stage great care and accuracy had to be taken in order to avoid that the glass beads got stuck in the threads where the plug was fixed.

4.10 Measurement of Absolute Permeability with specified size of particles

It has been demonstrated that a good packing has a major influence on the permeability. Nevertheless, the influx of air had its contribution on the permeability and it was decided to use another pump for the measurements. Pharmacia pump gives a flow rate from 0-1000ml/h, which is much lower than the previous pump, but still able to use for flow measurements and the most important; it did not give any influx of air.

Seave analysis was performed in order to have a specific grain size for the formation in the cell. This analyisis is described in chapter 2.3. Grain size between 250 and 355µm on the glass beads was used. The permeability, *k*, was found by rearranging the Darcy equation as described in 4.2.2. The flow rate, Q_{inn}, and the pressure drop ΔP was measured. All the measured data was plotted and the permeability determined where a best fit regression line for the data points was found.

From the tables in Appendix A the permeability can be calculated for both the measurements. The permeability value is determined by plotting the measured data in a two axial diagram. A best fit regression line was found between the plots of flow rate, q vs. pressure drop, ΔP.

Plot 5-2and Plot 5-3 below describes the flow rates and the pressure drop for determination of absolute permeability. The fluid and cell specifications are given in Table 4-6 and chapter 3.3 respectivly.

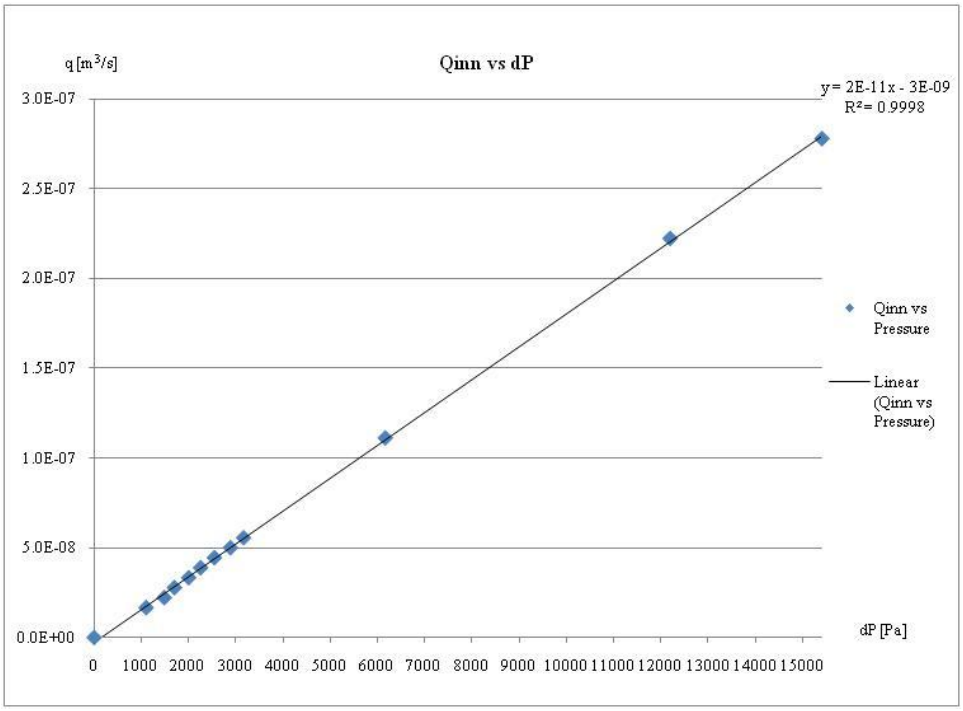

Plot 4-1 The plot gives the flow rate, Qinn for pump, vs. pressure drop, dp/dx This is used for finding the permeability value

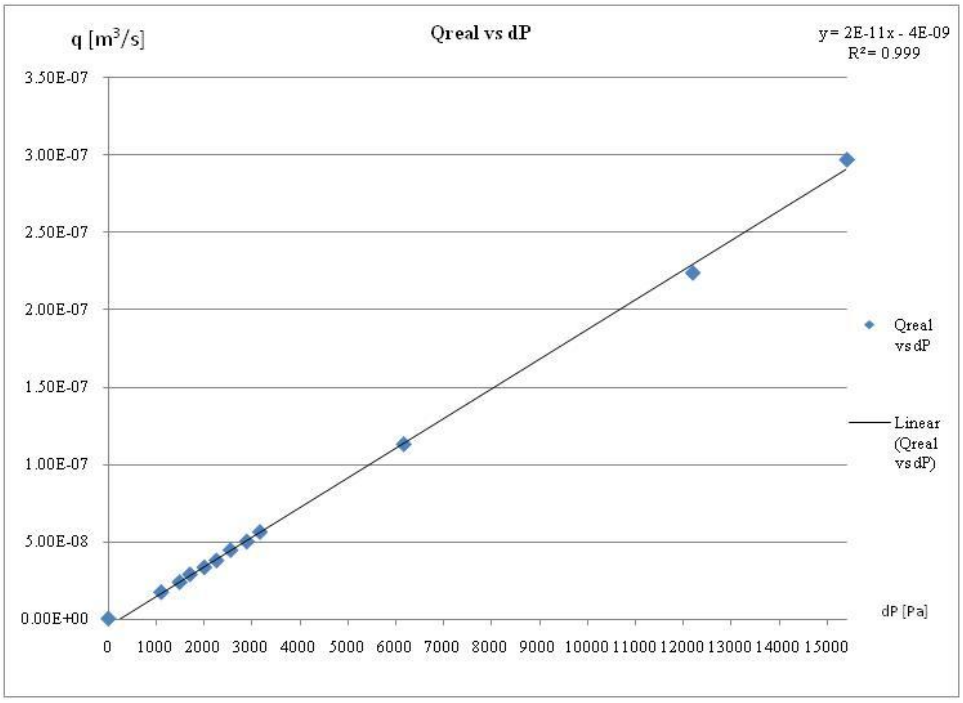

Plot 4-2 The plot gives flow rate, Qreal, vs. Pressure Drop, for measured flow rate

As can be seen from Plot 4-1 and Plot 4-2, the regression values are close to 1, and the absolute permeability can be calculated accuratly with equation (4-3).

Absolute permeability: $$k = \frac{\mu L q}{A \Delta P} = \underline{\underline{52.23D}}$$

5 DISPLACEMENT OF OIL IN POROUS MEDIUM

5.1 Experiments Performed

Experiments were performed for horizontal, vertical upward and vertical downward flow. Different flow rates, from 40ml/h to 20ml/min, were used for the experiments. The displacement was performed both in horizontal and vertical upward flow. The vertical downward flow was performed, due to have a better packing of the porous medium. Vertical upward flow was also performed to find the absolute permeability. For comparison purposes, identical experiments were performed. For the immiscible displacement experiments, water was used to displace first light oil (Bayol35), for upward flow, and heavy oil (Marcol82), for horizontal displacement.

5.2 1D displacement of Oil in Porous Vertical Medium

The displacement of oil by water from the porous gravel pack has been studied for the simple case of packs of unconsolidated material made up of grains of nearly uniform size. The experiment is related to water-drive processes in oil reservoirs. Bayol35 was the wetting and flowing oil, with a viscosity of 2.45cP. Bayol35 represented the oil phase. Ionized water dyed with lissamine red represented the water phase.

Water is injected at the lower. Flow direction was vertical upwards. The pressure drop between the outlet and the inlet was measured. Water and oil were collected in receivers. One of them can be seen in picture below.

The ultimate recovery was determined and calculated. And the same with breakthrough recoveries.

5.2.1 Visualization of Displacement

Production point

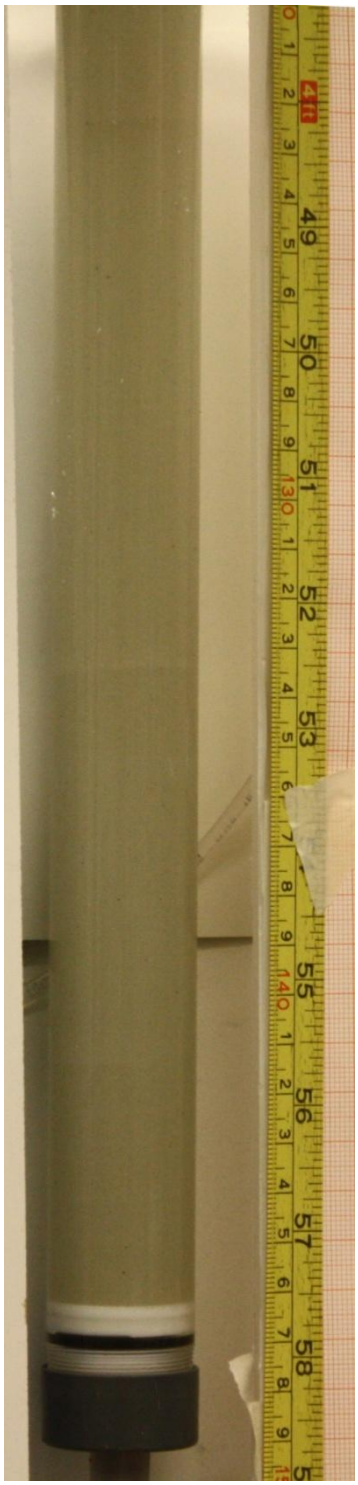

Start test, 16.03.2010 14:39

16.03.2010 15:28
Injection of water. White area is probably viscous fingers. The arrow shows the displacement distance.

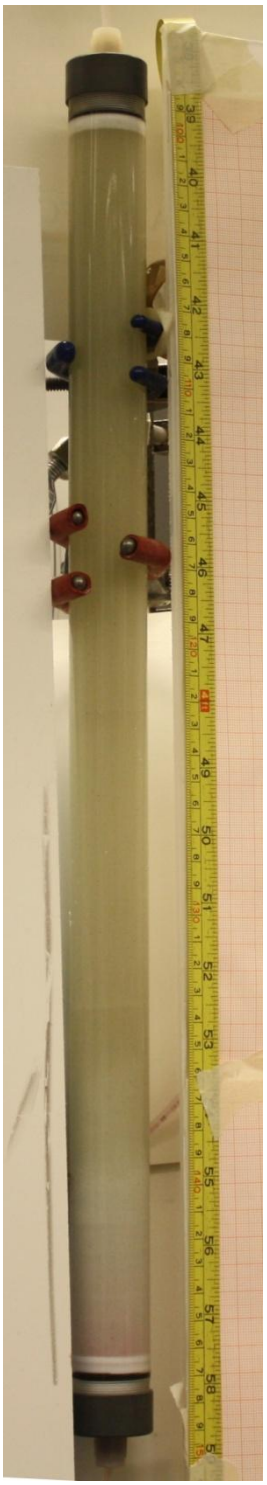

16.03.2010 15:29
Three minutes after injection. Can see some red water injected.

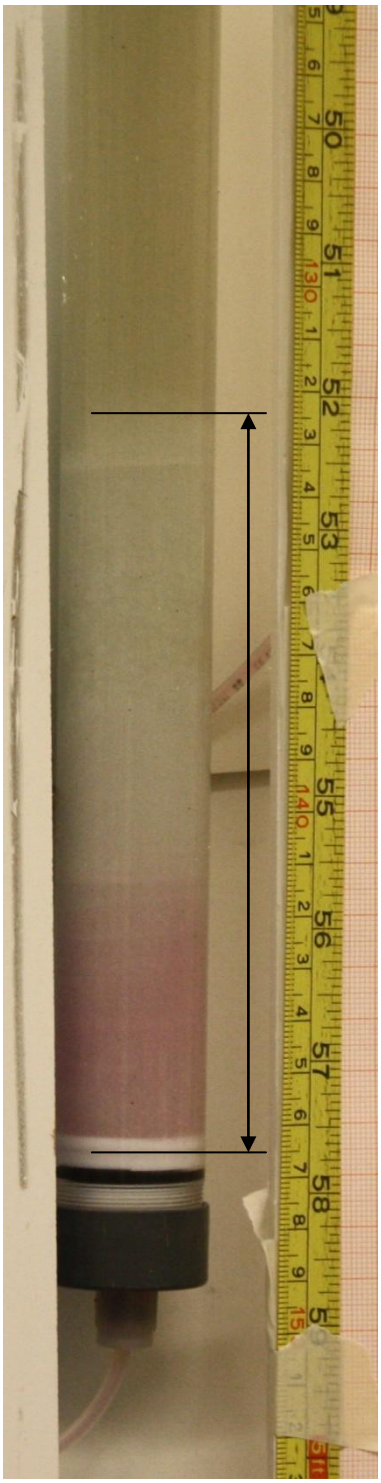

16.03.2010 15:32
Six minutes after injection. Oil displaced 14.2cm in six minutes.

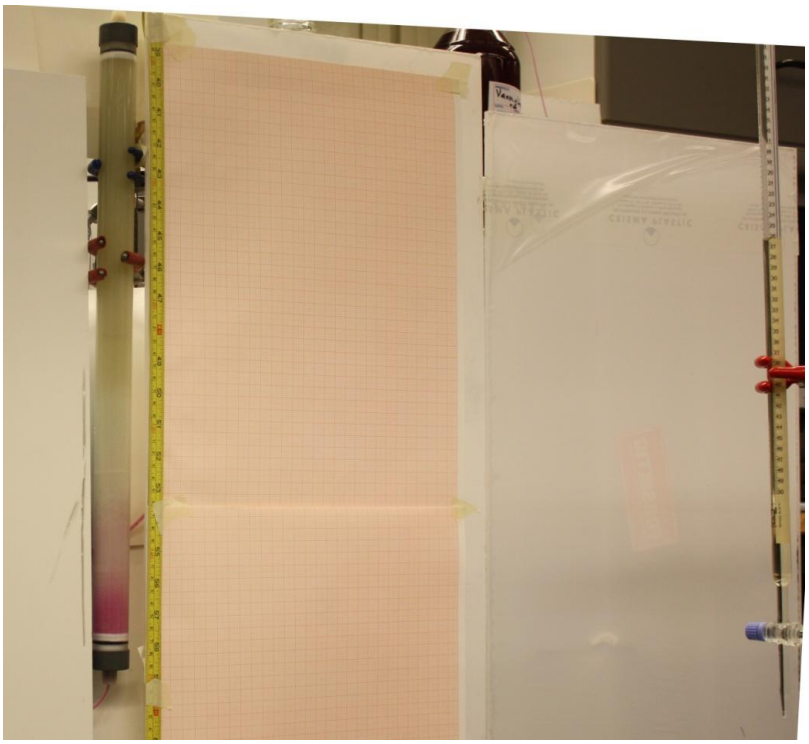

16.03.2010 15:35 Displaced oil and produced oil after 9 min. Can see strong red water in the bottom of the model.

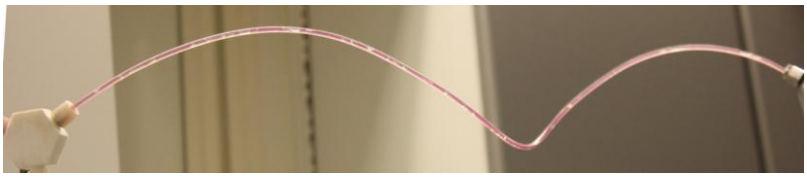

16.03.2010 16:20 Low capillary pressure in the tube

16.03.2010 15:37
11 min.

16.03.2010 15:42
16 min.

16.03.2010 15:44
18 min.

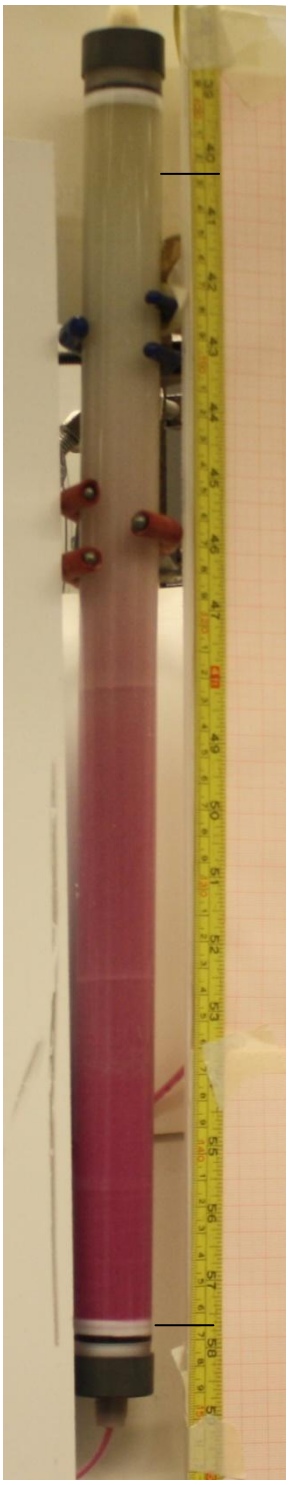

16.03.2010 15:45
19 min

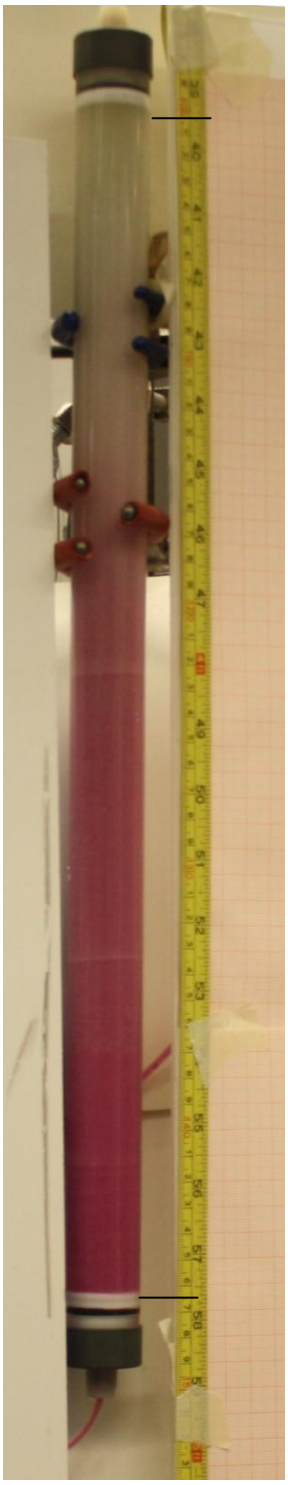

16.03.2010 15:47
21 min

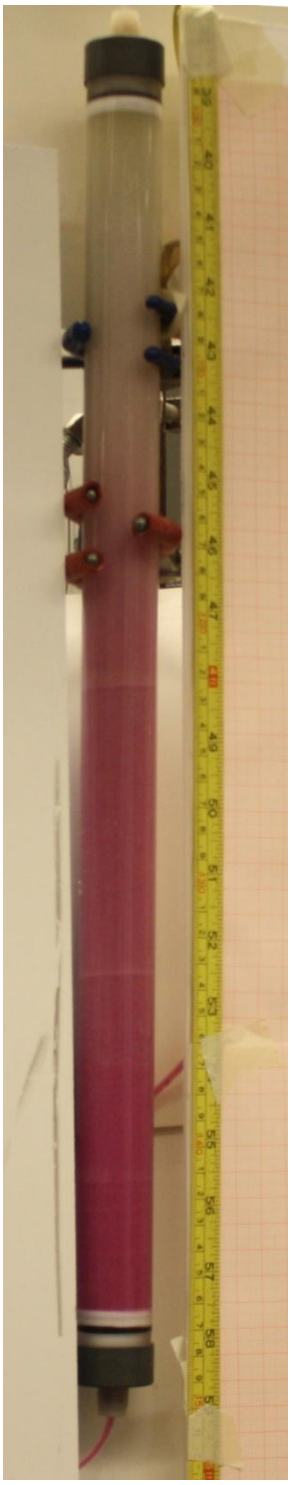

16.03.2010 15:48
Breakthrough after 22 min.

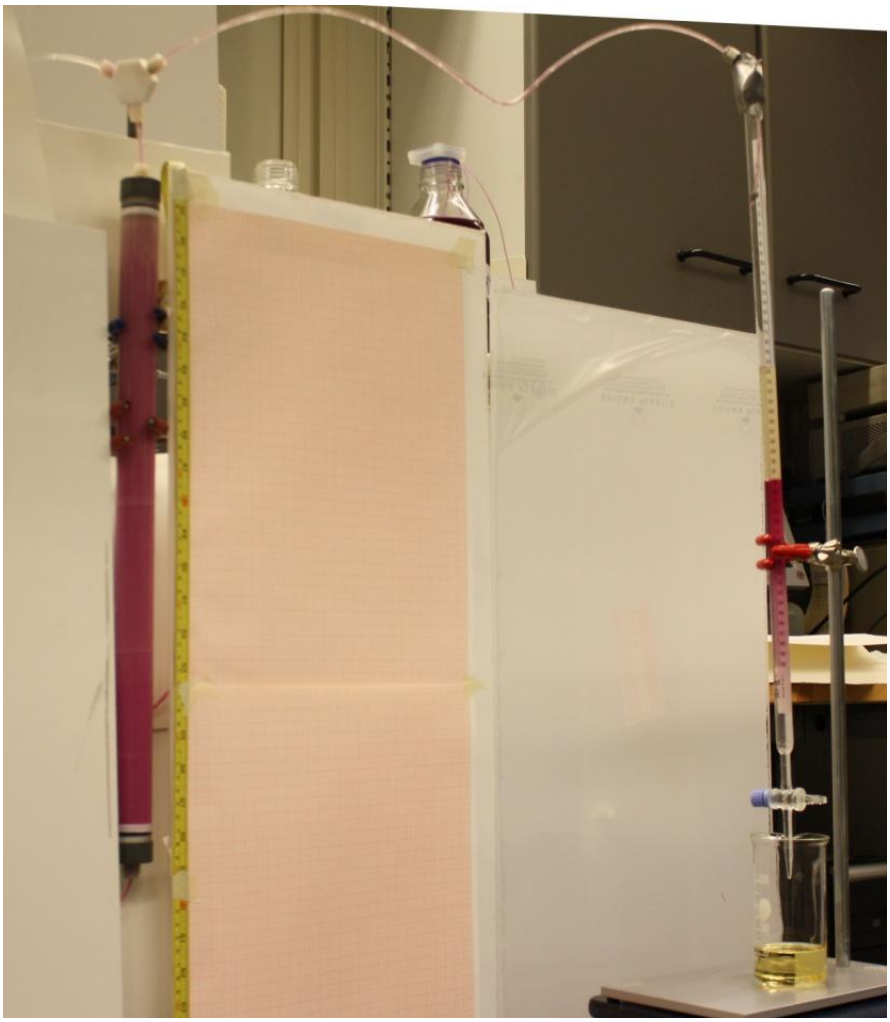

16.03.2010 15:57 production of oil and producing water

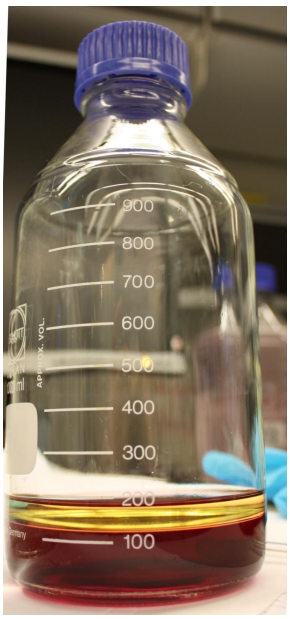

16.03.2010 17:03 Produced oil

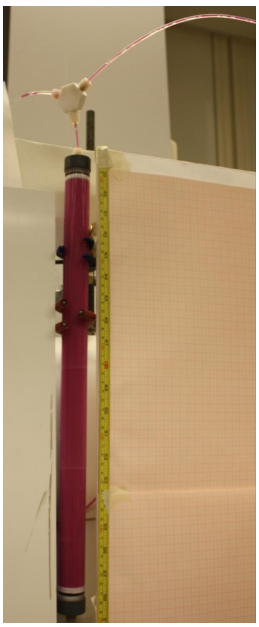

16.03.2010 19:20 Water saturated model with residual oil

5.3 1D displacement of Water in Porous Vertical Medium

The experiment was performed to determinde the relative permeability.

5.4 1D Displacement of Oil in Porous Horizontal Gravel Pack Model

The displacement of oil by water from the porous gravel pack has been studied for the simple case of packs of unconsolidated material made up of grains of nearly uniform size. The oil used for gravel pack saturation and flow is Marcol82, with a viscosity of 27.2 cP. The visualization is shown in Appendix G.

5.4.1 Visualization of displacement

Visualization of displacement in horizontal gravel pack

10. June 2010, 10:47:12 Injection has started to travel through the gravel pack. Already it can be seen that gravity segregation is affecting the displacement, due to denser water than oil. The water has segregated down in the first oil injection tube. This injection tube had to be closed.

The injection of water is appearing at a given distance from the gravel pack wall. This makes that the oil in at the end will not be displaced.

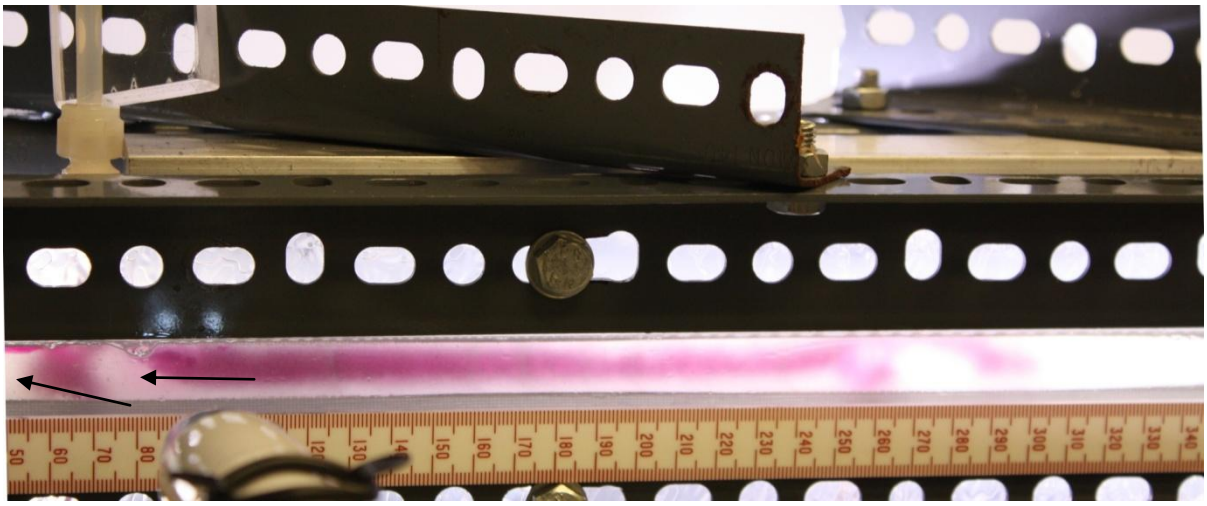

10. June 2010, 10:47:16 Ten minutes after water was injected into the porous medium. It was observed that the water front went up in the closed perforation just after water entering the gravel pack. It went down again and started to move through the gravel pack. On the left corner (arrows), there is a “dead zone” where the water will not displace the oil. This is oil entrapment, and the oil will probably not be recovered. When the water is flowing to the second oil inlet the water curves over an oil section. The reason for the curve is that the inlet is still injecting oil into the gravel pack. Since the oil is lighter than the water it will move upwards and the water will create a curve and try to segregate.

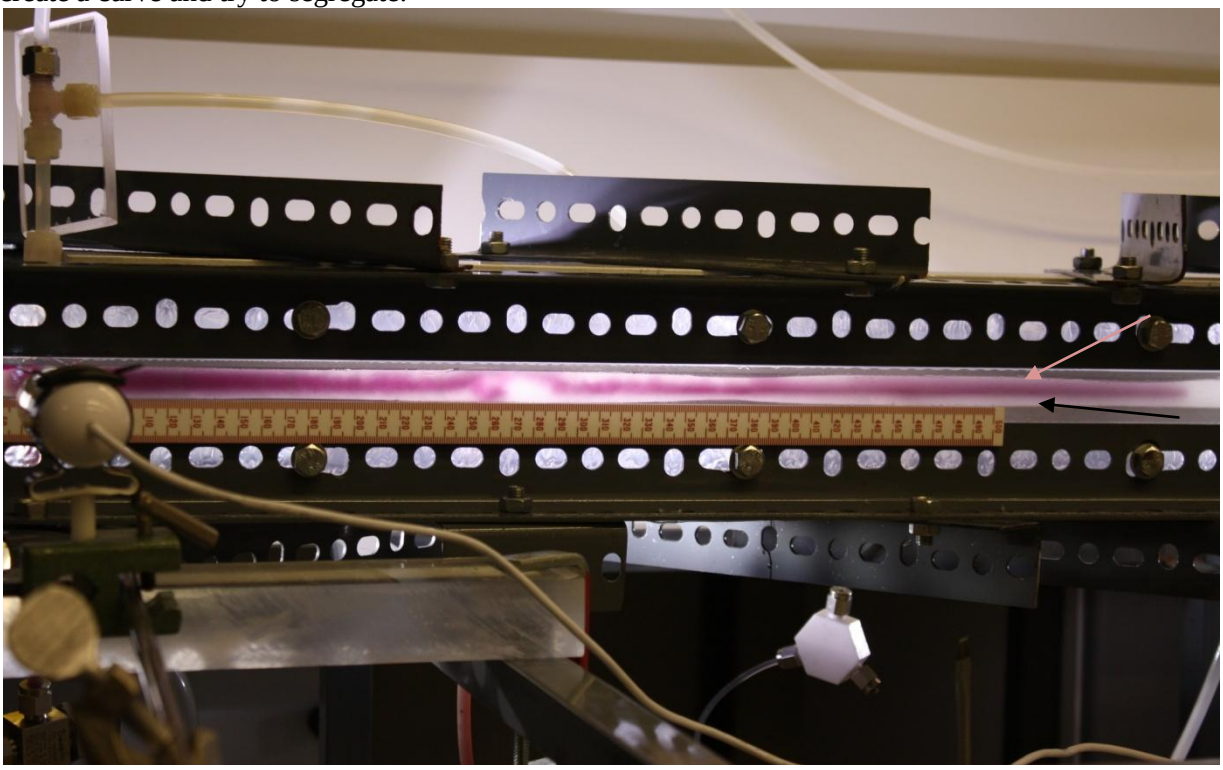

10. June 2010, 10:54:58

Water is fingering through the gravel pack and the oil tubes are still injecting. While the water is fingering, the oil will also still produce and it appears that the oil is making “a layer” under the water finger. This layer also appears above the water finger. The arrows on the figure visualize the different layers. For this particular experiment, it is special that the oil is creating a layer under the water. But it is probably due to the continuous injection of oil from the reservoir. The oil injection rate from the first inlet tube is very low (approximately 1.0ml/min) and the flow in the other injection tubes are increasing in flow rate the closer they are to the perforation. The water will flow by the part of least resistance. Therefore it is reasonable to assume that the pressure in the water phases is below the oil pressure. After the water reached the injection inlet the oil is continuously injecting into the gravel pack and the oil will under ride the water. The water will therefore not be able to displace this injected oil as it will flow continuously from the reservoir to the production perforation.

Two effects can be seen in the figure above. There are three layers in the gravel pack. One with initial oil, the viscous water finger and the continuous flow of oil. The water and oil is continuously injected with approximated same velocity. When the water is injected and starts to produce the oil, it tries to under ride the oil and a viscous finger will occur. But since there is continuous injection of oil and the oil in the gravel pack is continuously moving, there will not be gravity segregation of water at the bottom of the gravel pack which indicates that water does not under-ride the injected oil. The other effect is that the water under-ride the oil that is not injected from the formation. Then there will be water under-riding, and oil will be as a layer over the viscous water finger. The figure below shows the layering in more detail. The layers seem to be different, where the viscous finger is the largest one.

The viscous front is difficult to see on these figures. Normally it lies behind the viscous finger.

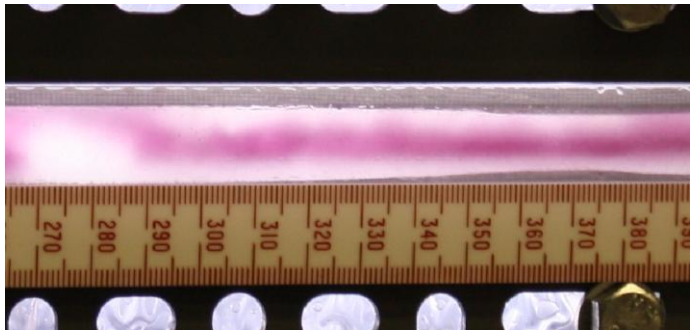

Fig... Layering of oil and viscous finger. The viscous front is lying behind the finger.

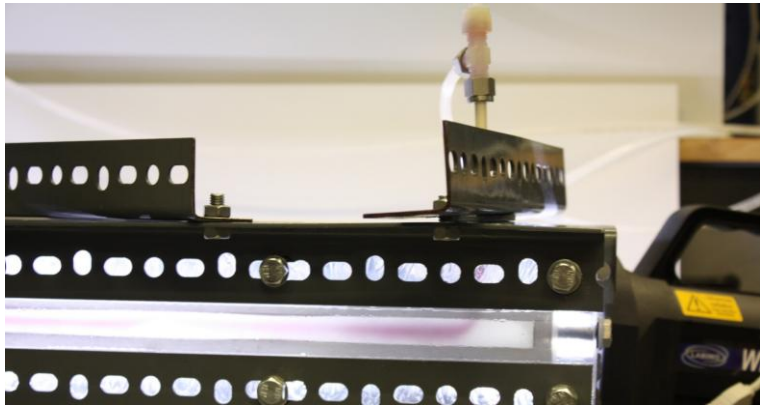

10. June 2010, 10:58:14 Breakthrough

The viscous finger reached the perforation and breakthrough occurred after 19min and 20sec. This is close to the calculated time at 21min 30sec. Here is also possible to see some oil entrapped in the reservoir. The oil in the right end of the model will probably not be displaced. The viscous finger is directly flowing through the production perforation and water will be produced together with the initial and injected volume of oil.

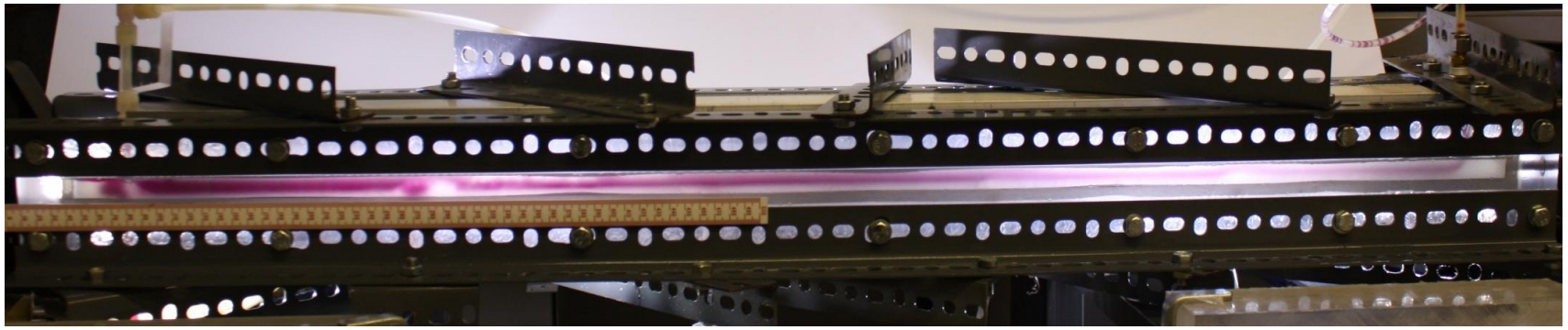

10. June 2010, 11:26:20 The viscous finger has reached the breakthrough and the water has been started to be produced.

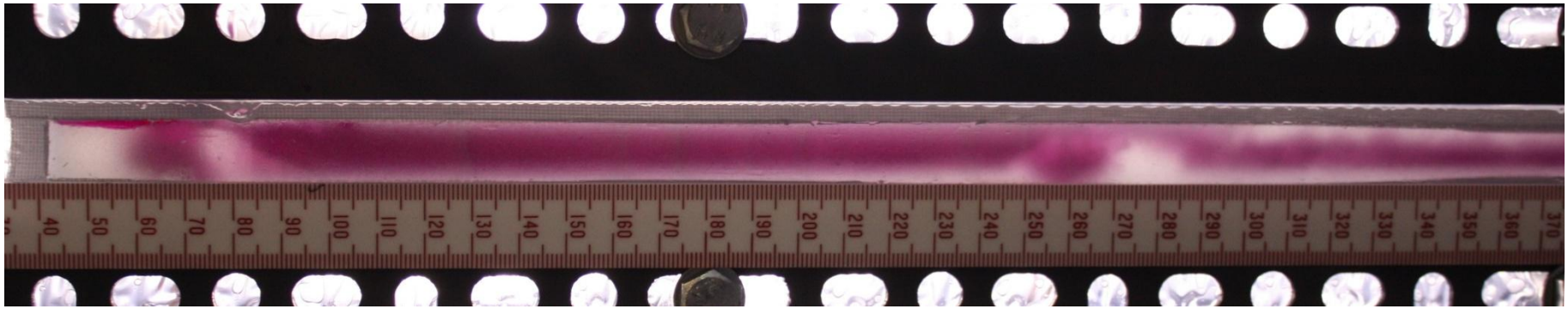

10. June 2010, 11:27:44 This is also at the water injection tube, where the water is injected into the oil column. There are some vertical lines across the gravel pack. Indicates vertical permeability. The permeability there can be higher than the absolute permeability. Vertical variation in permeability is relative common. When the permeability is higher, the flow will tend to move faster. It is difficult to predict since no prediction of permeability layering has been done. As mentioned in chapter…. If there is variation in permeability, it may lead to a reduction of vertical sweep efficiency at breakthrough.

Figures below are from the inlet tubes from water and oil (formation)

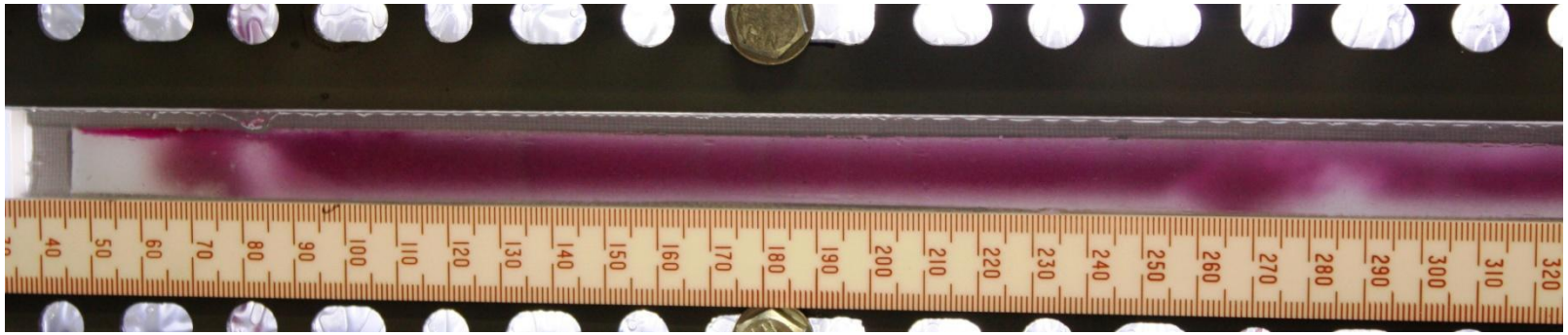

10. June 2010, 11:41:22 Water inlet tube, showing the entrapped oil and vertical layers.

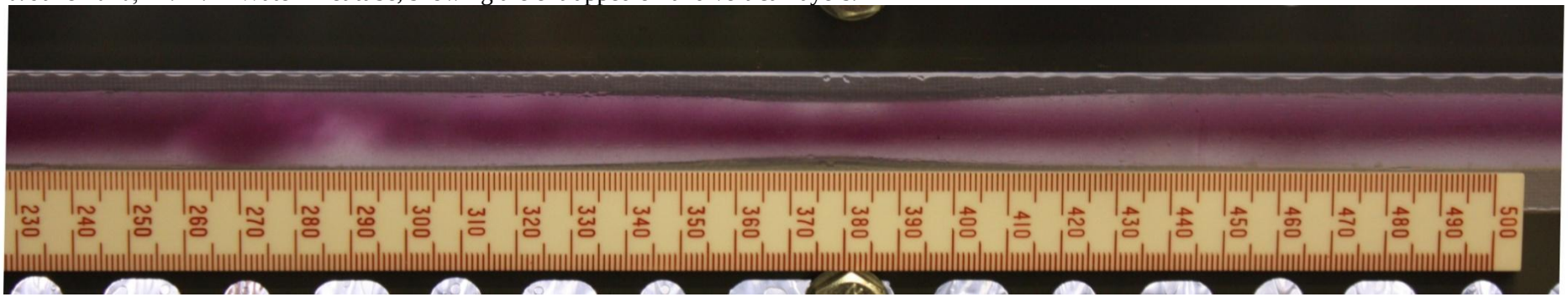

10. June 2010, 11:41:26 First inlet tube of oil.

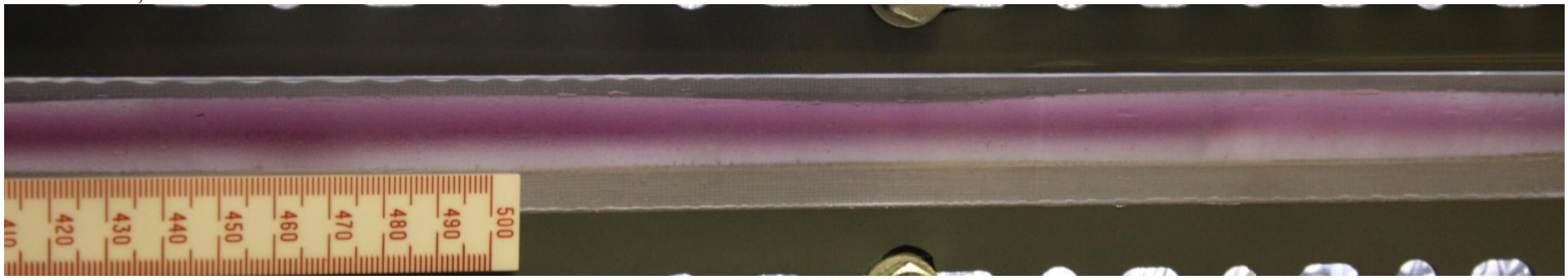

10. June 2010, 11:41:28 the middle of the model

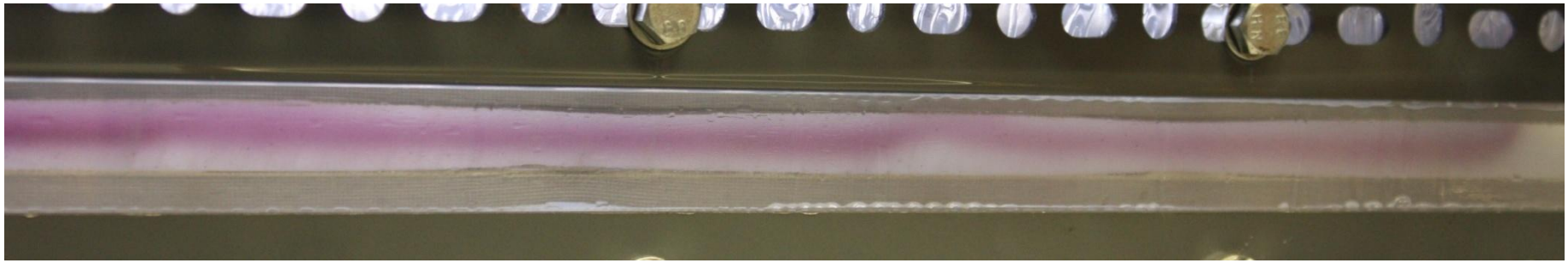

10. June 2010, 11:41:30 At the third and the fourth oil injectors. And the figure below shows the production outlet.

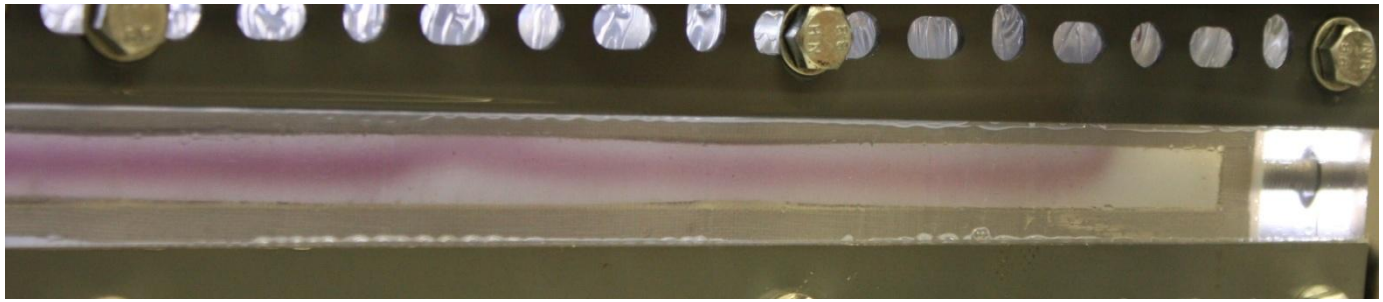

Saturation and Permeability Differences in different horizontal layers

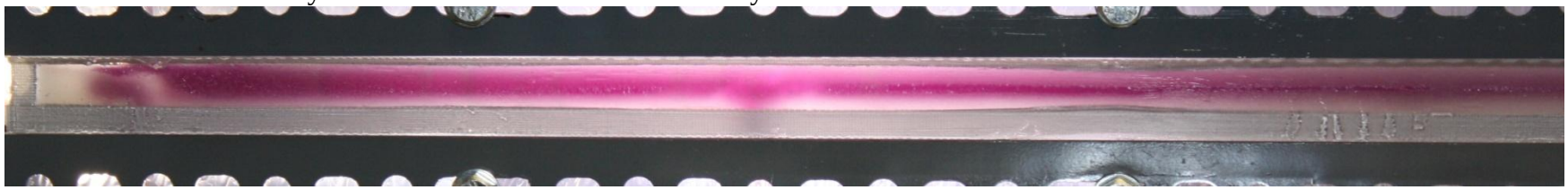

10. June 2010, 12:27:58 Even if saturation differences have not been included in this thesis it can be seen in the figures above and below. The water saturation is strong in the beginning with the water injection point. And it reduces after the length of the gravel pack.

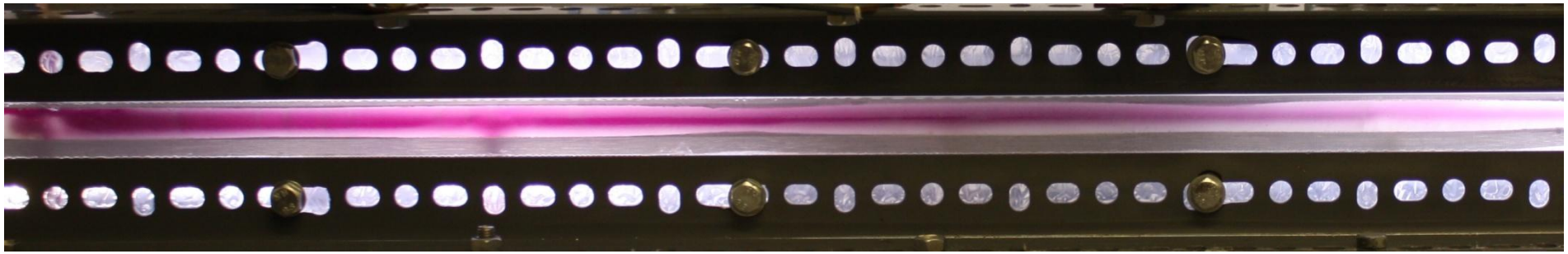

10. June 2010, 13:24:20

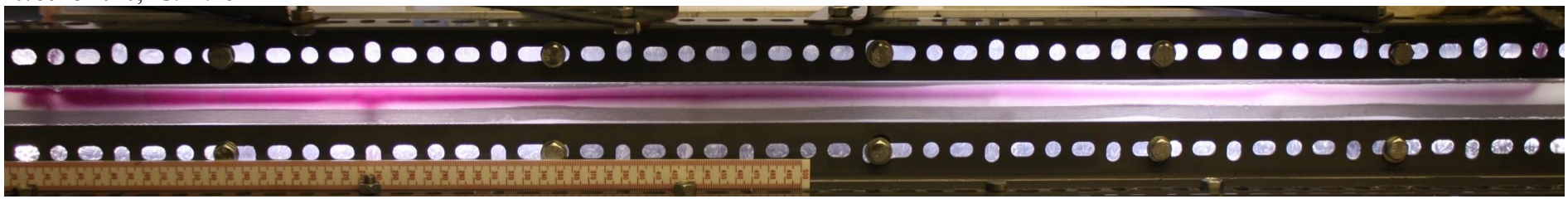

10. June 2010, 13:25:30

The figure visualize that there is water saturation differences. The saturation is stronger where the water is injected and is reducing after the displacement length.

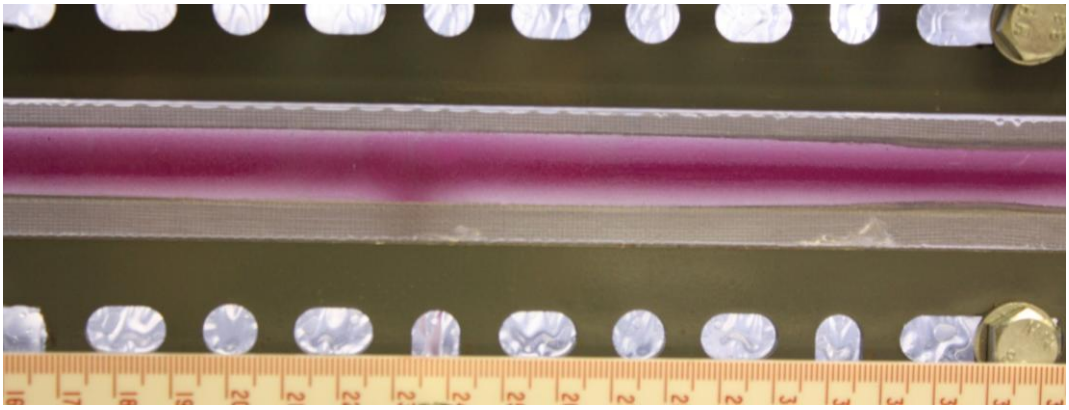

10. June 2010, 13:26:00 Different saturation distribution in the gravel pack. Viscous fingering.

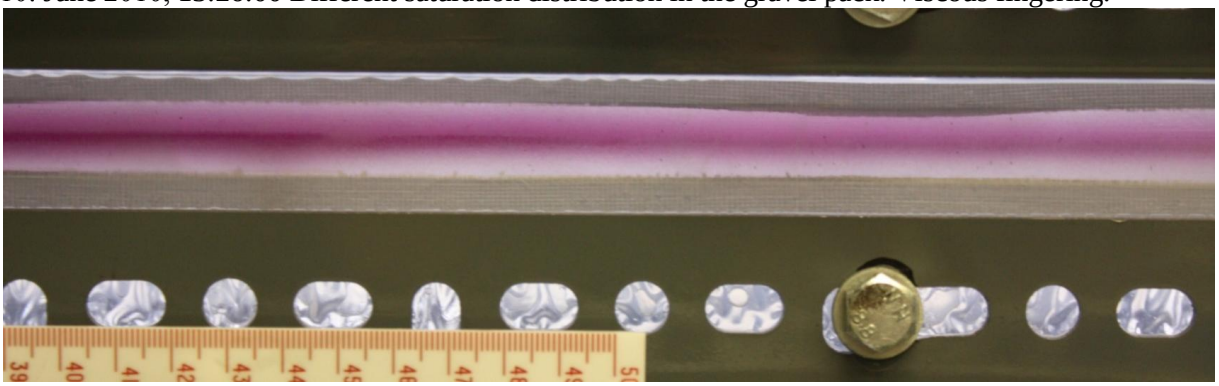

10. June 2010, 13:26:08

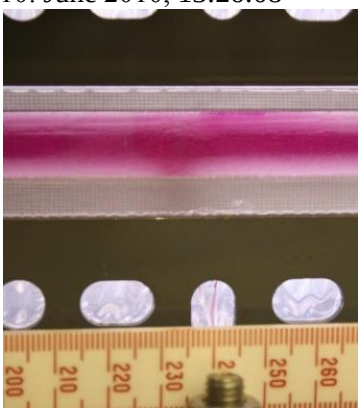

10. June 2010, 15:57:44

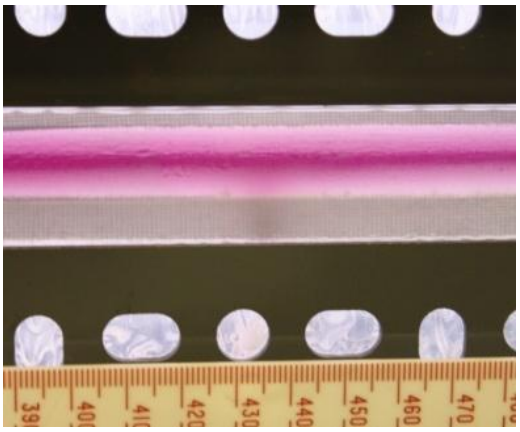

10. June 2010, 15:58:14

5.5 Results and discussion

The displacement experiments are conducted on one dimensional gravel pack with only one configuration to investigate the effectiveness of displacing water in a vertical well. Two runs were conducted, one where displacing oil with water, and the other where displacing water with oil.

Before the displacement by oil, the cell was flooded with oil. The oil flood experiments were conducted with two different gravel packs. The first one were for calibration of pump. The second experiment was reused twice, both for determination of absolute permeability.

5.5.1 1D displacement of Oil in porous vertical medium

Porosity

The porosity is the relation between injected oil in the cell, V_p, and the total volume in the cell, which can be occupied by fluids and porous medium, ref Equation (2-2).

$$\phi = \frac{V_p}{V_b} = \frac{86.28}{208.204} = \underline{0.41}$$

As described in chapter 2.3.4 the porosity for unconsolidated gravel varies between 0.25 and 0.48. The medium in the test cell is therefore considered to be relatively porous. This can mean that the glass beads are poorly consolidated to newly deposited (4).

Saturation

Saturation of oil and water after displacement of oil is found from Equation (2-15):

$S_o + S_w = 1$

Residual oil saturation, S_{or}, is found from Equation (2-17).

$$S_{or} = \frac{V_{oi} - V_o}{V_p} = 3.48 \cdot 10^{-3} ml/cm^3 = \underline{3.48 \cdot 10^{-3} ml/ml}$$

Initial water saturation, S_{wi}:is derived from Equation (2-15)

$S_{or} + S_{wi} = 1$

$S_{wi} = 1 - S_{or} = 1 - 3.4789 \cdot 10^{-3} = 0.9965 ml/cm^3 = \underline{0.997 ml/ml}$

Relative permeability and relative permeability curves

Relative permeability relates the absolute permeability of the porous system with the permeability of oil and water.

In the beginning was the medium 100% oil saturated. Then the permeability of oil is the same as the absolute permeability as calculated in chapter 4.10.

$k_o = k = \underline{52.23}$

Relative permeability, k_{ro}, of oil for 100% S_o is calculated from Equation (2-8)

$$k_{ro} = \frac{k_o}{k} = \frac{52.23}{52.23} = \underline{1.0}$$

Relative water permeability, $k_{rw}(S_w)$ after displacement by water is calculated from Equation (2-11).

$$k_{rw}(S_w = 1 - S_{or}) = \frac{k_w(S_w)}{k} = \frac{36.67D}{52.23D} = \underline{0.702}$$

Stable or unstable finger

As described in chapter 2.6.2, it is possible to evaluate the developement of the front displacement by comparing the oil and water pressure, ref Equation (2-30)

Assuming $p_0 = 0.036 bar$

Equation (2-31)gives:

$$P_o = 3600 Pa + 789.5 kg/m^3 \times 9.81 m/s^2 \times 0.0815 m \times \sin(90)...$$

$$... - \frac{0.00245 Pas \times 2.48 \times 10^{-4} m/s \times 0.0815 m}{52.23D \times 9.876 \times 10 - 13 m^3/D} = 0.123 bar$$

And from Equation (2-32)

$$P_w = 3600Pa + 991.41kg/m^3 \times 9.81m/s^2 \times 0.0815m \times \sin(90)...$$
$$...- \frac{0.00126Pas \times 2.48 \times 10^{-4} m/s \times 0.0815m}{36.67D \times 9.876 \times 10 - 13m^3/D} = 0.128bar$$

Comparing the results:

$$P_o - P_w = -0.00209bar \Rightarrow P_o - P_w \leq 0$$

Based on the above it is shown that the front will be unstable.

Viscous Forces in Vertical Displacement

Average velocity

$$\bar{v} = \frac{q}{A} = \frac{1.11 \cdot 10^{-7} \, m^3/s}{4.448 \cdot 10^{-4} m} = \underline{2.48 \cdot 10^{-4} \, m/s}$$

Viscous forces have been found by Darcy' equation
For the water flood

$$\Delta P = \frac{\bar{v} \cdot \mu \cdot L \cdot \phi}{k} = \frac{2.48 \cdot 10^{-4} \, m/s \cdot 0.00126Pa \cdot s \cdot 0.468m \cdot 0.399}{52.23 \cdot 9.876 \cdot 10^{-13} m^2} = \underline{1131.2Pa} = \underline{0.0113bar}$$

For the oil flood

$$\Delta P = \frac{\bar{v} \cdot \mu \cdot L \cdot \phi}{k} = \frac{2.48 \cdot 10^{-4} \, m/s \cdot 0.00246Pa \cdot s \cdot 0.468m \cdot 0.399}{52.23 \cdot 9.876 \cdot 10^{-13} m^2} = \underline{2209Pa} = \underline{0.0221bar}$$

Pressure drop in a pore throat by the use of Poiseuille's law

For water

$$\Delta P = \frac{8\mu Lq}{\pi r^4} = \frac{8 \cdot 0.00126Pa \cdot s \cdot 0.468m \cdot 1.11 \cdot 10^{-7} \, m^3/s}{\pi \cdot (0.0238m)^4} = \underline{1.678 \cdot 10^{-9} \, Pa}$$

For oil

$$\Delta P = \frac{8\mu Lq}{\pi r^4} = \frac{8 \cdot 0.00246Pa \cdot s \cdot 0.468m \cdot 1.11 \cdot 10^{-7} \, m^3/s}{\pi \cdot (0.0238m)^4} = \underline{0.00101Pa}$$

It is difficult to predict the pressure drop in a pore throat. The same is with the pressure required to force the liquid through a pore throat. During the displacement of the oil, the fluid has to flow through many different throats, and many different paths for the fluid flow exist. For predicting this, trapping forces in a single capillary needs to be calculated. The wetting angle between all the different pores needs to be estimated. And then estimate the pore velocity of the displacing fluid water to displace the isolated oil drop from the pore. The pore channels are also not straight and smooth, but irregularly shaped.

Production rate decline

Data points for the plot can be found in the Appendix E.

Plot 5-1 Production rate vs time

5.5.2 1D displacement of Water in porous vertical medium

Porosity

The porosity is equal to the porosity calculated in chapter 5.5.1

$\phi = \underline{0.41}$

Saturation

Saturation of oil and water after displacement of water is found from Equation (2-15):

$S_o + S_w = 1$

Irreducible water saturation, S_{wi} is calculated from Equation (2-18):

$$S_{wi} = \frac{V_{wi} - V_w}{V_p} = \frac{83.276 - 64.20}{208.204} ml/cm^3 = \underline{0.0916 ml/ml}$$

Oil saturation at irreducible water saturation is calculated from Equation (2-15).

$$S_{oi} = 1 - S_{iw} = 1 - 0.0916 = 0.9084 ml/cm^3 = \underline{0.908 ml/ml}$$

Relative Permeability

Relative permeability of oil with irreducible water saturation is calculated from Equation(2-11)

$$k_{ro}(S_w) = \frac{k_o(S_w)}{k} = \frac{43.37D}{52.23D} = \underline{0.83}$$

Maximum effective permeability to oil is found from Equation (2-4)

$k_o(S_w=S_{wc}) = k \times k_{ro}$'

The resulting curves are shown below:

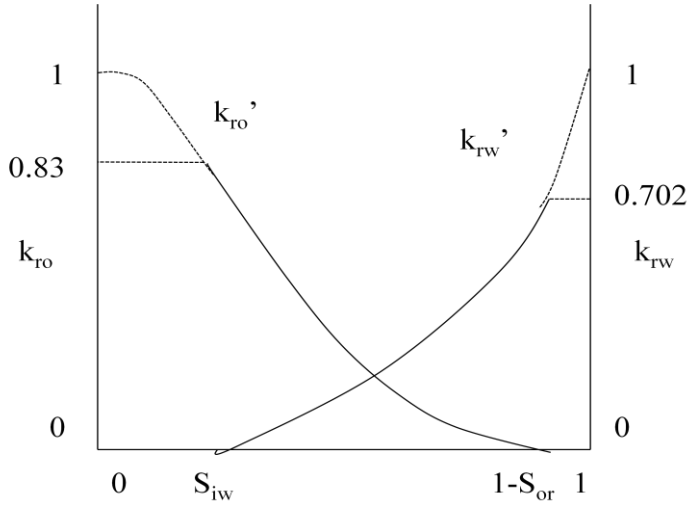

Plot 5-2 Relative permeability curves with values of kro, krw

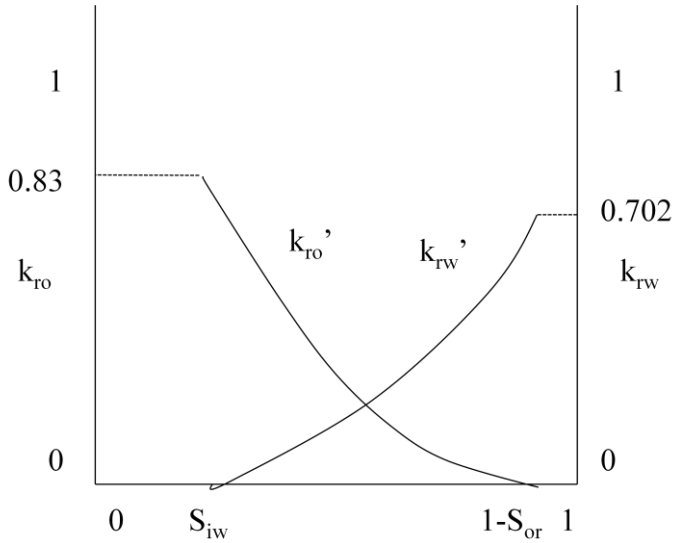

Plot 5-3 Normalizing relative permeability

Fractional Flow of 1D vertical displacement

$q_w = 400ml/h$ at t = 0 min

$q_o = 0ml/h$ at t = 0 min

$q_o = 400ml/h$ at t = 1min

$q_o = 400ml/h$ at t = 22min

$q_t = q_w + q_o = 400ml/h = 1.11*10^{-7}\, m^3/\underline{\min}$

Mobility Ratio

$$M = \frac{\lambda_w}{\lambda_o} = \left(\frac{k_{rw}}{\mu_w}\right)_{Sw}\left(\frac{\mu_o}{k_{ro}}\right)_{Siw} = \frac{0.702}{1.26}\frac{2.46}{0.83} = \underline{1.65}$$

The mobility ratio here can also be considered as a end point mobility ratio, since the calculated relative permeability ratio to water and oil that occur during displacement. The curves of the end point permeability ratio are shown in Plot 5-2and Plot 5-3

For stabilizing the displacement is the shock front mobility ratio, Ms, shown:

$$M_s = \frac{k_{ro}(S_{wf})/\mu_o + k_{rw}(S_{wf})/\mu_w}{k_{ro}^{'}/\mu_o} = \frac{0.83/2.46 + 0.702/1.26}{0.83/2.46} = \underline{2.65}$$

Since no measurements have been done on permeability and saturation of shock front the values will be the same as the end point mobility ratio. The Buckley-Leverett displacement is not stable and viscous channelling of water appeared.

The mobility ratio is higher than 1, M ≥ 1, which gives an unsatisfied condition and give the reason for viscous channelling of water through the oil. Because of gravity segregation and that water has a higher density than oil does the water underlay and displaces the oil. The channelling is viscous fingering of water and gave an earlier breakthrough than predicted.
This displacement is unstable due to the high mobility between the displaced and the dity between the displaced and the displacing fluid. Since the injected water is denser than the displaced oil, gravity segregation occurred and the displacing water under rides the displaced oil. The gravity can be used to advantage to improve displacement performance.

Oil/Water Viscosity Ratio

$$\gamma = \frac{\mu_o}{\mu_w} = \frac{2.46cP}{1.26cP} = \underline{1.95}$$

The oil/water viscosity ratio is high, together with the mobility ratios, which gives an unstable displacement.

Fractional flow of water

$$f_w = \frac{q_w}{q_w + q_o} = \frac{1}{1 + M^{-1}} = \frac{1}{1 + 1.65^{-1}} = \underline{0.622}$$

$$f_o = \frac{q_o}{q_w + q_o} = \frac{1}{1 + M} = \frac{1}{1 + 1.65} = \underline{0.377}$$

These equations are predictable for high permeabilities.

Vertical Displacement Efficiency in application of Darcy's equation

By using the Darcy equation to find the immiscible displacement, the displacement is considered as piston like displacement. Even if viscous fingering occurred and gravity segregation, the denser water will push the oil as a piston-like displacement.

$$\frac{k_{rD}k}{\mu_D}\frac{dp}{dy}\bigg|_D = \frac{k_{rd}k}{\mu_d}\frac{dp}{dy}\bigg|_d$$

$$M\frac{dp}{dy}\bigg|_D = \frac{dp}{dy}\bigg|_d$$

$$\Delta P = \Delta P_D + \Delta P_d$$

$$\Delta P = X_f\frac{dp}{dy}\bigg|_D + \left(L - X_f\right)\frac{dp}{dy}\bigg|_d$$

$$\Delta p = \left[X_f + \left(L - X_f\right)M\right]\frac{dp}{dy}\bigg|_D$$

$$\frac{dp}{dy}\bigg|_D = \frac{\Delta p}{\left[X_f + \left(L - X_f\right)M\right]}$$

From Darcy's equation:

$$v_D = \frac{dX_f}{dt} = \frac{-k_{rD}k}{\mu_D}\frac{dp}{dy}\bigg|_D\left(\frac{1}{\phi(1-S_{dr}-S_{Dr})}\right)$$

v_d = linear velocity of displacing phase front
S_{dr} = residual saturation of the displaced phase
S_{Dr} = residual saturation of the displacing phase

$$\frac{dX_f}{dt} = \frac{-\lambda_{rD}k\Delta p}{\left[ML+(1-M)X_f\right]\phi(1-S_{dr}-S_{Dr})}$$

This is a differential equation that by integration, separation of variables results in;

$$t = \frac{-\phi(1-S_{dr}-S_{Dr})}{\lambda_{rD}k\Delta p}\left[MLX_f + (1-M)\frac{X_f^2}{2}\right]$$

The location of displacing phase of water;

$$X_f = \frac{-ML \pm \left[(ML)^2 - \frac{2(1-M)\lambda_{rD}k\Delta pt}{\phi(1-S_{or}-S_{wr})}\right]^{1/2}}{(1-M)}$$

$$= \frac{-1.65\cdot 0.468m \pm \left[(1.65\cdot 0.468m)^2 - \frac{2(1-1.65)\frac{0.702}{0.00126Pa\cdot s}52.23\cdot 9.876E^{-13}\cdot 3610Pa\cdot 1320s}{0.399(1-3.48E^{-3}-0.0916)}\right]^{1/2}}{1-1.65}$$

$$= \frac{-0.7722}{-0.65}m \pm 0.643481943m$$

$$X_{f1} = 0.4158m = \underline{41.58cm}$$

$$X_{f2} = -1.96m$$

X_{f1} will be used since the location of the displacing phase fluid front cannot be negative.

Time, t, when the front reaches the position X_f,

$$t = \frac{-\phi(1-S_{or}-S_{iw})}{\lambda_{rw}k\Delta p}\left[MLX_f + (1-M)\frac{X_f^2}{2}\right]$$

$$= \frac{0.399\cdot(1-3.48E^{-3}-0.0916)}{\frac{0.702}{0.00126Pa\cdot s}\cdot 52.23\cdot 9.876E^{-13}m^2\cdot 3610\text{Pa}}\left[1.65\cdot 0.468m\cdot 0.4158m + (1-1.65)\frac{(0.4158m)^2}{2}\right]$$

$$= 15.37\,\text{min}$$

$$= \underline{15\,\text{min}\,22\,\text{sec}}$$

Volume of water injected before breakthrough

$$V_i = A(1-S_{or}-S_{wr})X_f = 0.00044488m^2(1-3.48E^{-3}-0.0916)0.4158m = \underline{0.000167m^3 = 167ml}$$

V_i = volume injected
A = cross-sectional area of the medium

Velocity of the displacing phase front

$$v_D = \frac{dX_f}{dt} = \frac{0.4158m}{922.2s} = \underline{4.51\cdot 10^{-4}\,m/s}$$

Average Pressure drop

$\Delta P = 0.0361bar = 3610Pa$

Time t, when position, X_f = *46.8cm*

$$t = \frac{-\phi(1-S_{or}-S_{iw})}{\lambda_{rw} k\Delta p}\left[MLX_f + (1-M)\frac{X_f^2}{2}\right]$$

$$= \frac{0.399\cdot(1-3.48\cdot10^{-3}-0.0916)}{\frac{0.702}{0.00126Pa\cdot s}\cdot 52.23\cdot 9.876E^{-13}m^2\cdot 3610\text{Pa}}\left[1.65\cdot 0.468m\cdot 0.468m + (1-1.65)\frac{(0.468m)^2}{2}\right]$$

$$= 1009.99s$$

$$= \underline{17\,\text{min}\,23\text{sec}}$$

Time t, when position, X_f = *50cm*

$$v_D = \frac{dX_f}{dt} = \frac{0.468m}{1009.99s} = \underline{4.63\cdot10^{-4}\ m/s}$$

$$t = \frac{-\phi(1-S_{or}-S_{iw})}{\lambda_{rw} k\Delta p}\left[MLX_f + (1-M)\frac{X_f^2}{2}\right]$$

$$= \frac{0.399\cdot(1-3.48E^{-3}-0.0916)}{\frac{0.702}{0.00126Pa\cdot s}\cdot 52.23\cdot 9.876E^{-13}m^2\cdot 3610\text{Pa}}\left[1.65\cdot 0.468m\cdot 0.50m + (1-1.65)\frac{(0.50m)^2}{2}\right]$$

$$= 1061s$$

$$= \underline{17\,\text{min}\,41\text{sec}}$$

$$v_D = \frac{dX_f}{dt} = \frac{0.50m}{1061s} = \underline{4.7\cdot10^{-4}\ m/s}$$

Volume water injected at X_f = *50cm*

$$V_{wi} = A(1-S_{or}-S_{wr})X_f = 0.00044488m^2(1-3.48E^{-3}-0.0916)0.50m = \underline{0.000201m^3 = 201ml}$$

Injection rate after breakthrough;

$$i_{abt} = \frac{k_{rw}kA}{\mu_w}\frac{\Delta p}{L} = \frac{0.702\cdot52.23\cdot9.876\times10^{-13}m^2\cdot0.00044488m^2}{0.00126Pa\cdot s}\cdot\frac{3610Pa}{0.468m} = \underline{0.99\,m^3/s}$$

Volume injected at any time after breakthrough

$$V_{iabt} = V_{ibt} + i_{abt}(t-t_{bt}) = 0.000167m^3 + 0.99m^3(1320s) = \underline{1.696\times10^{-4}\,m^3}$$

Displaceable PV after displacement by water and oil

$$V_{pd} = V_p(S_{oi}-S_{or}) = Ah\phi(S_{oi}-S_{or})$$

$$= 4.4488\cdot10^{-4}m^2\cdot0.468m\cdot.399(0.908-3.48\cdot10^{-3})ml/ml$$

$$= \underline{7.54\cdot10^{-5}m^3}$$

Dimensionless injection rate, the injected volume divided by placeable PV,

$$\gamma = \frac{V_{wi}}{V_{pd}} = \frac{2.01\cdot10^{-4}m^3}{7.54\cdot10^{-5}m^3} = \underline{2.67\,m^3/m^3}$$

Water injection rate at the same point

$$q = i_{abt}\cdot\gamma = 0.99\,m^3/s\cdot2.67\,m^3/m^3 = \underline{2.64\,m^3/s}$$

Viscous Fingering

The idealized piston like behaviour is not followed since the viscosity of water is less than the viscosity of oil.

$$\gamma = \frac{\mu_o}{\mu_w} = \underline{1.95}$$

The viscous ratio between the oil, bayol35 and water is 1.95. In this event, viscous fingering occurs during the displacement process. Flow in the fingers is mixed with bypassed oil and it is creating a much longer mixing zone.

Areal Displacement Efficiency

Areal displacement efficiency before breakthrough is equivalent to the volume of water injected.

$$E_A = \frac{V_i}{PV(S_{oi} - S_{or})} = \frac{0.000167m^3}{0.0002082m^3\left(0.908 - 3.43\cdot10^{-3}\right)} = \underline{0.887} = \underline{88.7\%}$$

Displacement efficiency at breakthrough

$$E_{Abt} = 0.54602036 + \frac{0.03170817}{M} + \frac{0.30222997}{e^M} - 0.00509693\cdot M$$

$$= 0.54602036 + \frac{0.03170817}{1.65} + \frac{0.30222997}{e^{1.65}} - 0.00509693\cdot 1.65$$

$$= 0.6149$$

$$= \underline{61.49\%}$$

Cumulative Oil Produced

$$N_p = V_p(S_{oi} - S_{or})E_{Abt} = 4.4488\cdot10^{-4}m^2\cdot 0.468m\cdot .399\cdot\left(0.908 - 3.43\cdot10^{-3}\right)\cdot 0.6149 = 0.000075m^3 = \underline{46.1ml}$$

The gravity force has been neglected here and principally have the other factors mentioned in 2.3 been focused on during the study. Five injection tubes have been used for flow. For the permeability heterogeneity it is difficult to develop correct correlations.

Gravity force has been neglected in the model, but densities of oil and water have been adjusted in the tubes and the inlet to the gravel pack, which means that gravity override, is minimized.

The fronts and interfaces between the displaced and displacing fluids were monitored by use of dyed water that was photographed.

Vertical Displacement Efficiency

Dykstra Parsons Model

$$E_I = \frac{n_j + \sum_{k=j+1}^{n}\frac{k_k}{k_j}}{n} = \frac{1 + \frac{52.23}{52.23}}{1} = \underline{1.0}$$

$$E_I = \frac{n_j + \frac{(n-n_j)M}{M-1} - \frac{1}{M-1}\sum_{k=j+1}^{n}\left[M^2 + \frac{k_k}{k_j}\left(1-M^2\right)\right]^{1/2}}{n} = \frac{\frac{1}{1.65-1}\left(1.65^2 + \frac{52.23}{52.23}\left(1-1.65^2\right)\right)^{1/2}}{1} = 1.53$$

$$F_{wo} = \frac{\sum_{k=1}^{j}k_k}{\sum_{k=j+1}^{n}\frac{k_k}{\left[M^2 + \frac{k_k}{k_j}\left(1-M^2\right)\right]^{1/2}}} = \frac{\frac{52.23}{52.23}}{1.65^2 + \frac{52.23}{52.23}\left(1-1.65^2\right)} = \underline{1.0}$$

Calculation of Vertical Displacement efficiency at breakthrough

From calculated N_p:

$$E_I = \frac{N_{p,calc}}{M\cdot V_t} = \frac{0.000045m^3}{1.65\cdot 0.00008672m^3} = \underline{0.31}$$

From measured N_p

$$E_I = \frac{N_p}{M \cdot V_t} = \frac{0.000083m^3}{1.65 \cdot 0.00008672m^3} = \underline{0.58}$$

Displacement efficiency

$$E_D = \frac{V_p S_{oi} - V_p S_{or}}{V_p S_{oi}} = \frac{S_{oi} - S_{or}}{S_{oi}} = \frac{0.908 - 3.48 \cdot 10^{-3}}{0.908} = \underline{0.996}$$

Displacement Efficiency Equation

$$E_D = \frac{N_{p\,Bt}}{1 - S_{wi}} = \frac{0.0000538}{1 - 0.997} = 0.0179 = \underline{1.79}$$

Volumetric Displacement Efficiency for measured N_p based on area efficiency on breakthrough

$E_V = E_A E_I = 0.887 \cdot 0.58 = \underline{0.514}$

Recovery Efficiency:

$RF = E_D E_V = 0.996 \cdot 0.514 = \underline{0.51\%}$

1D displacement of oil by water

The displacement experiments are conducted on one dimensional gravel pack with only one configuration to investigate the effectiveness of displacing water in a vertical well. After the displacement was the cumulative oil production at breakthrough and after breakthrough determined. The volume of oil produced at breakthrough, $V_{op,bt}$ = *83.28ml* over a time of 22min. Volume of oil produced after breakthrough was 3ml. $V_{op,t}$ = *86.28ml*. The oil and water saturation is different throughout the displacement. The flood front saturation will differ from some extent to the average saturation. The residual oil saturation is *3.43*10^{-3} ml/ml*, this gives a water saturation of *0.998ml/ml*. This low and high oil and water saturation means that almost all oil was displaced and produced. The residual oil is most probably left in the different pores. The recovery factor is 99.44%.

The displacement here is governed by what might be called viscous fingering. The displaced oil has a viscosity of 2.46 cP where the viscosity of the displacing water is 1.26cP. The viscosity relation will give a value larger than 1, which means that there are viscous instabilities in the displacement front. Since the viscosity of oil is higher than the viscosity of water, viscous fingers have been established. Perturbations, which is the white area on the pictures, has been established when the water is displacing the oil. The water here is moving faster than the oil, since the water is less viscous than the displaced oil. The small tiny horizontal lines in the porous medium can be small areas larger permeability and the front entering could travel much faster than the rest of the front. Probably there are more of them, just smaller than that are shown on the pictures. This can together with the unfavourable viscosity ratio and the mobility ratio be the reason for the viscous fingers. When there is difference in gravity between the displacing fluid and the displaced fluid it will have an effect on the displacement. $\lambda_o > \lambda_w$ and $\rho o < \rho w$, 0.78955g/cm3<0.99141g/cm3. When the gravel pack is vertical there will be vertical upward flow. When the water is denser than the oil it can be helpful for the displacement in vertical upward direction, in that way that the gravity will help to stabilize the front. Since the average displacement velocity is low, it can help to reduce the fingers at the interface.

5.5.3 1D displacement of oil in horizontal Gravel Pack model

Assumptions

- The model used is linear, horizontal and of constant thickness
- The flow is incompressible and obeys Darcy's law
- After the displacement there is high residual oil saturation
- The flow displacement is by viscous fingering
- There are injection of oil from the formation (4 oil tubes under the gravel pack model)

- Capillary and gravity forces are negligible
- The permeability and relative permeability are the same for the entire system.
- Use the same porosity as for the particles in vertical displacement
- The relative permeability will be assumed the same as the relative permeability in the vertical displacement.

Absolute permeability for flow in horizontal direction

$$k = \frac{\mu \cdot L \cdot q}{A \cdot \Delta P} = \left(\frac{0.0272Pa \cdot 1.0m \cdot 4.45 \cdot 10^{-8}\, m^3/s}{2.25 \cdot 10^{-4}\, m^2 \cdot 15000Pa} \right) \cdot 9.876 \cdot 10^{13} = \underline{363.13D}$$

Calculated permeability is higher than anticipated based on the previous calculation in chapter 4.10 with a permeability of 52.23D. This is maybe caused by high viscosity of the flowing oil. The main cause of high permeability is believed to be because of porous packing and the mentioned viscosity of the oil. Another reason might be the occurence of an oil pocked during packing of the gravel pack, because of a leakage in one of the perforations. The air pocket is located under the "non-producing" perforation on the left side of the gravel pack. The air pocket is illustrated in Figure 5-1 and Figure 5-2 below. This is one of the proofs of porous packing. This model is also a square, and the gravel is circular so the gravel will have problems with packing in the corners of the model. Thereby will the permeability be different from permeability in of packing in a cylindrical model.

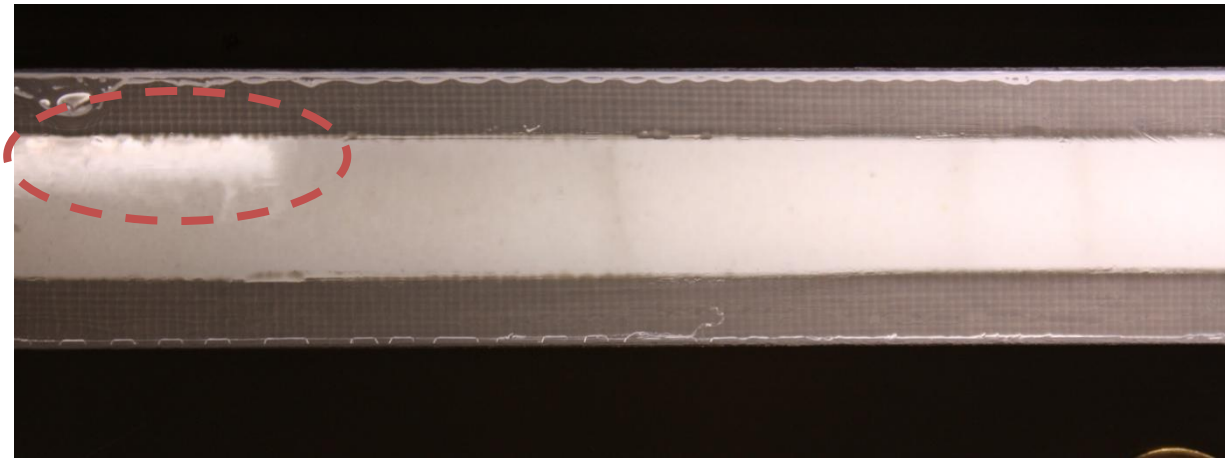

Figure 5-1 Air pocket at water injection tube

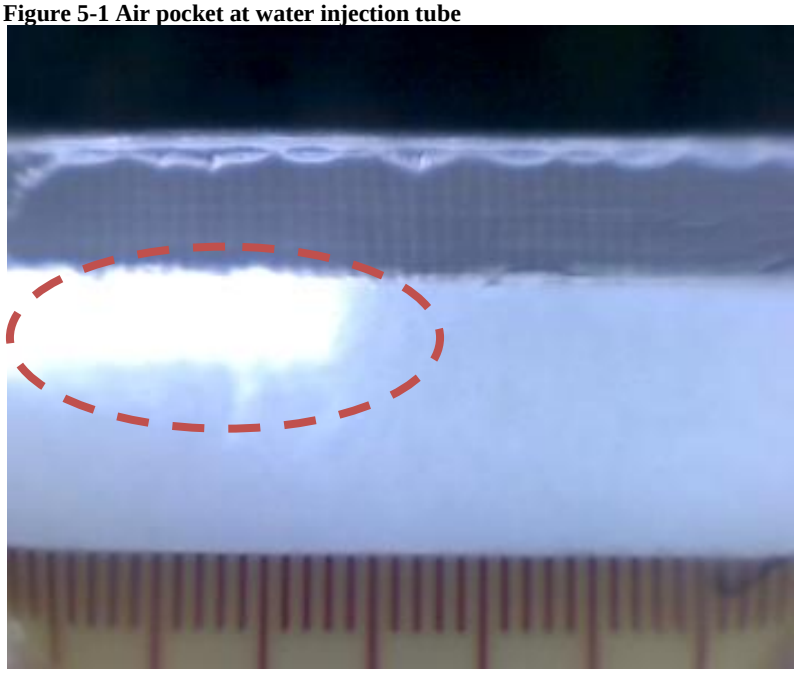

Figure 5-2 Air pocket at water injection tube

1 D displacement of in horizontal displacement of oil

V_{oi} [ml]	92,25
V_{op}[ml]	53,8

The initial oil injected was not measured and is calculated from the porosity and the bulk volume, V_b, of the gravel pack.

Saturation

Since there is no flow measurement from the formation, and that flow measurement on the pump does not give correct value a calculation of saturation was done based on

1. assuming no injection of oil (theoretical minimum and maximum value)
2. assuming injection of oil

By the assumption of no injection of oil the saturation will become

$$S_o + S_w = 1$$

$$S_{or} = \frac{V_{oi} - V_o}{V_p} =$$

S_o	0.171	Assuming no injection of oil (theoretical minimum value)
S_{wr}	0.829	Assuming no injection of oil (theoretical maximum value)

Oil pump flow meter indicates a flow of:	2	ml/min
Assuming 54% error due to leakage:	1,08	ml/min
Water pump gives correct flow rate	2	ml/min

The correct flow rate was measured by injection of oil into the column and measured the produced oil in a burette over a certain time.
Assume pore volume of water injected = V_{op}

Total oil injected:	20,6496	ml	$2.065*10^{-05}$ m^3

Then the saturation will give

S_{or}	0,263
S_w	0,737

This is the saturations that will be used in former calculations. The data for produced oil and water can be found in Appendix I.

Relative Permeability

Relative permeability relates the absolute permeability of the porous system with the permeability of oil and water.
In the beginning was the medium 100% oil saturated. Then the permeability of oil is the same as the absolute permeability.
$k_o = k =$ 363.13D
Relative permeability, k_{ro}, of oil for 100% S_o;

$$k_{ro} = \frac{k_o}{k} = 1$$

The Relative water permeabilities have been assumed to be the same as the one for displacement in vertical direction

Displacement by water

$$k_{rw}(S_w = 1 - S_{or}) = \frac{k_w(S_w)}{k} = \underline{0.702}$$

Displacement by oil

$$k_{ro}(S_w) = \frac{k_o(S_w)}{k} = \underline{0.83}$$

The irreducible water saturation and oil saturation at irreducible water saturation will also be assumed to be the same as in vertical displacement by oil,

$$S_{iw} = \frac{V_{wi} - V_w}{V_p} = \underline{0.106 ml/ml}$$

Oil saturation at irreducible water saturation

$$S_o = 1 - S_{iw} = 1 - 0.106 = 0.894 ml/cm^3 = \underline{0.894 ml/ml}$$

Maximum effective permeability to oil

$$k \cdot k_{rw}(S_w) = 363.13 \cdot 0.702 = \underline{254.92D}$$

$$k \cdot k_{ro}(S_w) = 363.13 \cdot 0.83 = \underline{301.39D}$$

Fractional Flow of 1D vertical displacement

$q_w = 2ml/\text{min}$ at *t = 0min*

$q_o = 0.7ml/\text{min}$ at *t = 0min*

$q_o = 0.7ml/\text{min}$ at *t = 19.2min*

$$q_t = q_w + q_o = 2ml/\text{min} + 0.7ml/\text{min} = \underline{2.7ml/\text{min}} = \underline{4.50 \cdot 10^{-8} m^3/s}$$

Mobility Ratio

$$M = \frac{k'_{rw}/\mu_w}{k'_{ro}/\mu_o} = \frac{0.702/1.26}{0.83/27.2} = \underline{18{,}26}$$

The mobility ratio is high, >> 1, which gives an unfavourable condition and give the reason for viscous fingering of water. The water will travel faster than the oil and create an early breakthrough of production of water into the well. The viscous fingering is due to the high viscosity ratio of the displaced oil and the displacing water.

Oil/Water Viscosity Ratio

$$\gamma = \frac{\mu_o}{\mu_w} = \frac{27.2cP}{1.26cP} = \underline{21.59}$$

The viscosity ratio is >> 1. This implies that together with the mobility ratio, the water will create a viscous finger.

Viscous fingering

The pictures have been used to calculate the velocity and position of the viscous finger. The points of the finger in the pictures taken during displacement have been used as a reference note, and the time the finger reached this point has been used to find the velocity. The table below shows the breakthrough time for the viscous finger, the position after a certain time and the velocity for the finger.

Table 5-1 Time, position and velocity and average velocity for the viscous finger

t [min]	10	16	19,200
t [sec]	600	960	1152,000
x_f [m]	0,294	0,594	0,988
u_{avg} [mm/s]	0,49	1,65	5,146
U [mm/s]	0,98	2,32	7,972

The values from the table have been plotted below.

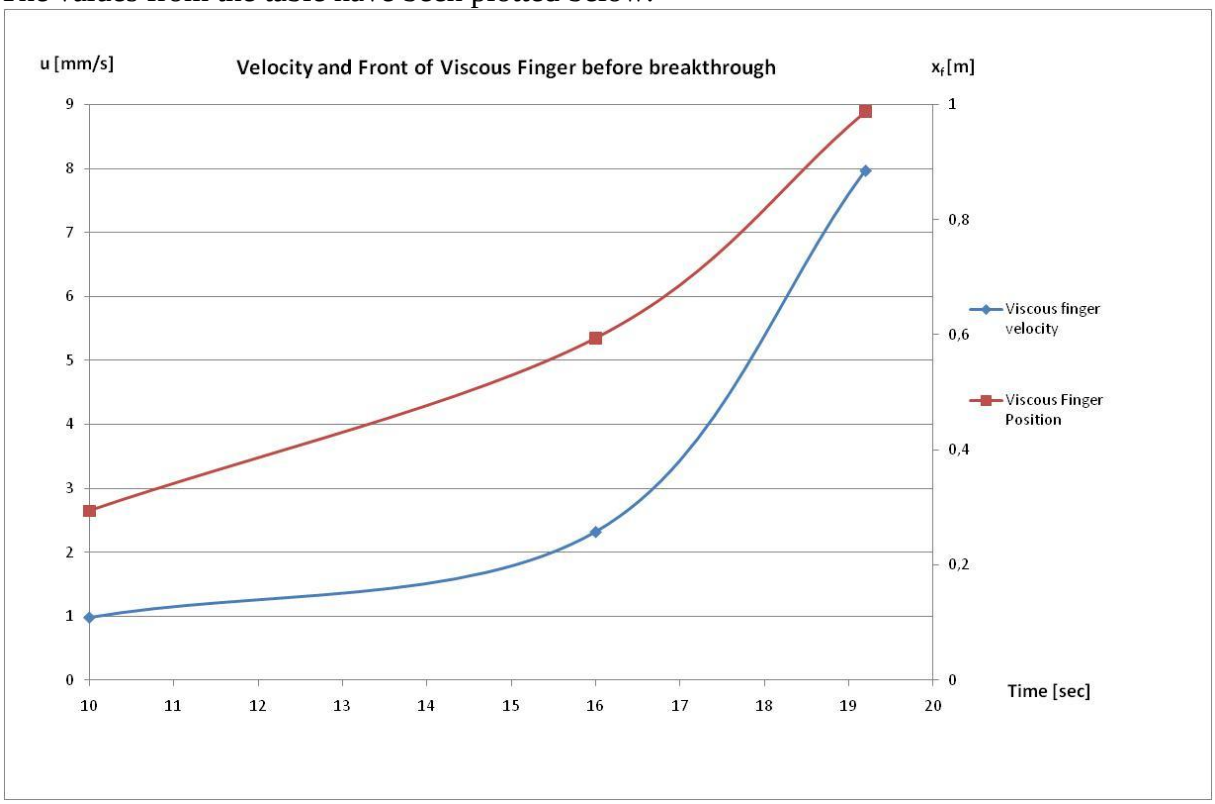

Plot 5-4 Velocity and front of the viscous finger before breakthrough

The plot shows how the viscous finger is moving through the gravel pack. U is the velocity and Xf is the position of the finger. Displacement is shown over time. The velocity is increasing the more the finger reaches the oulet perforations. This might be due to the continuous injection of oil from the formation.

Table 5-2Time and position of the front before and at breakthrough

t	100	200	300	400	500	600	700	800	900	1000	1100	1152
x_f [m]	0,017	0,034	0,052	0,070	0,090	0,110	0,131	0,154	0,178	0,204	0,232	0,248

The values from the Table 5-2 of time and position before and at breakthrough are plotted below, Plot 5-5 The viscous front. The time is on the x-axis and the position on the y-axis. The distance of the front have been found by Equation (2-33).

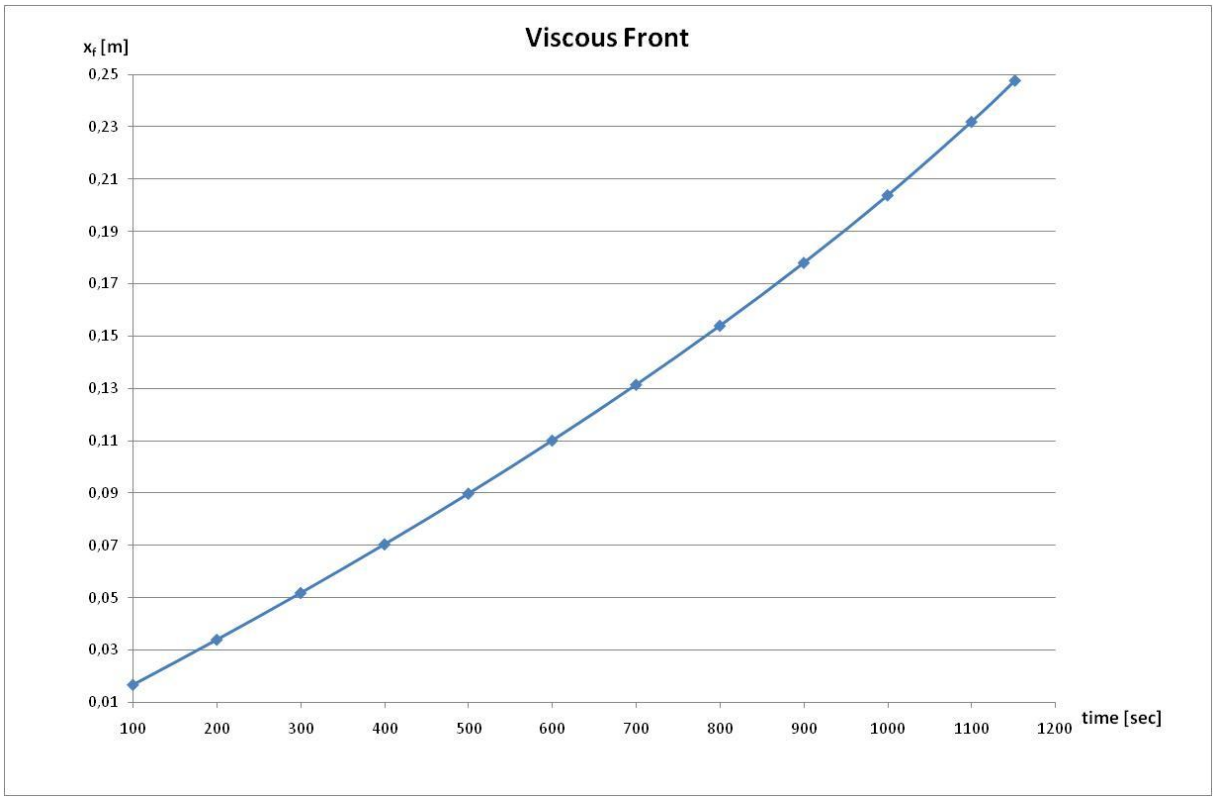

Plot 5-5 The viscous front during displacement over a time t.

The plot above shows the viscous front as the viscous finger is moving. This viscous front is moving very slowly compared to the viscous finger. At breakthrough (1152sec) has the front only moved 0.25m while the viscous finger has reached the perforation.

Viscous Forces in Horizontal Displacement

Average water rate before breakthrough

$$q_w = \frac{V_{op}}{t} = \underline{4.68968 \cdot 10^{-8}\ m^3/s}$$

Average water velocity

$$\bar{v} = \frac{q}{A} = \frac{4.68968 \cdot 10^{-8}\ m^3/s}{2.25 \cdot 10^{-4}\ m} = \underline{2.0843 \cdot 10^{-4}\ m/s}$$

Viscous forces have been found by Darcy' equation
For the water flood

$$\Delta P = \frac{\bar{v} \cdot \mu \cdot L \cdot \phi}{k} = \frac{2.0843 \cdot 10^{-4}\ m/s \cdot 0.0272 Pa \cdot s \cdot 1.0m \cdot 0.41}{363.13D \cdot 9.876 \cdot 10^{-13} m^2} = \underline{6481.414\text{Pa}} = \underline{0.648\text{bar}}$$

Pressure drop in a pore throat by the use of Poiseuille's law

For water flow
Assumption for this equation:

- Cylindrical pore throat

$$\Delta P = \frac{8\mu L q}{\pi r^4} = \frac{8 \cdot 0.0272 Pa \cdot s \cdot 1.0m \cdot 0.33 \cdot 10^{-7}\ m^3/s}{\pi \cdot (0.015m)^4} = \underline{0{,}04515 Pa}$$

Difficult to predict this value since the pore channels are not cylindrical, but irregular.

Production

Data points for plots below is found i the Appendix I.

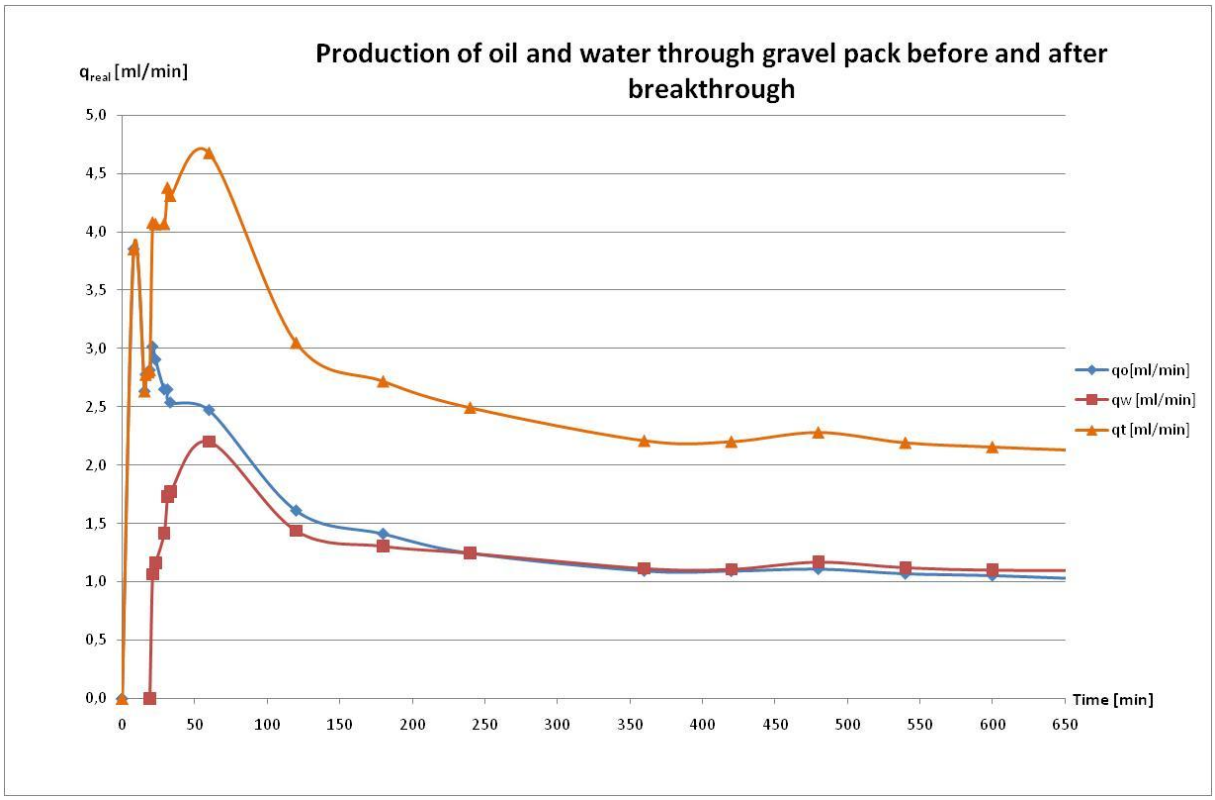

Plot 5-6 Production of oil and water through gravel pack

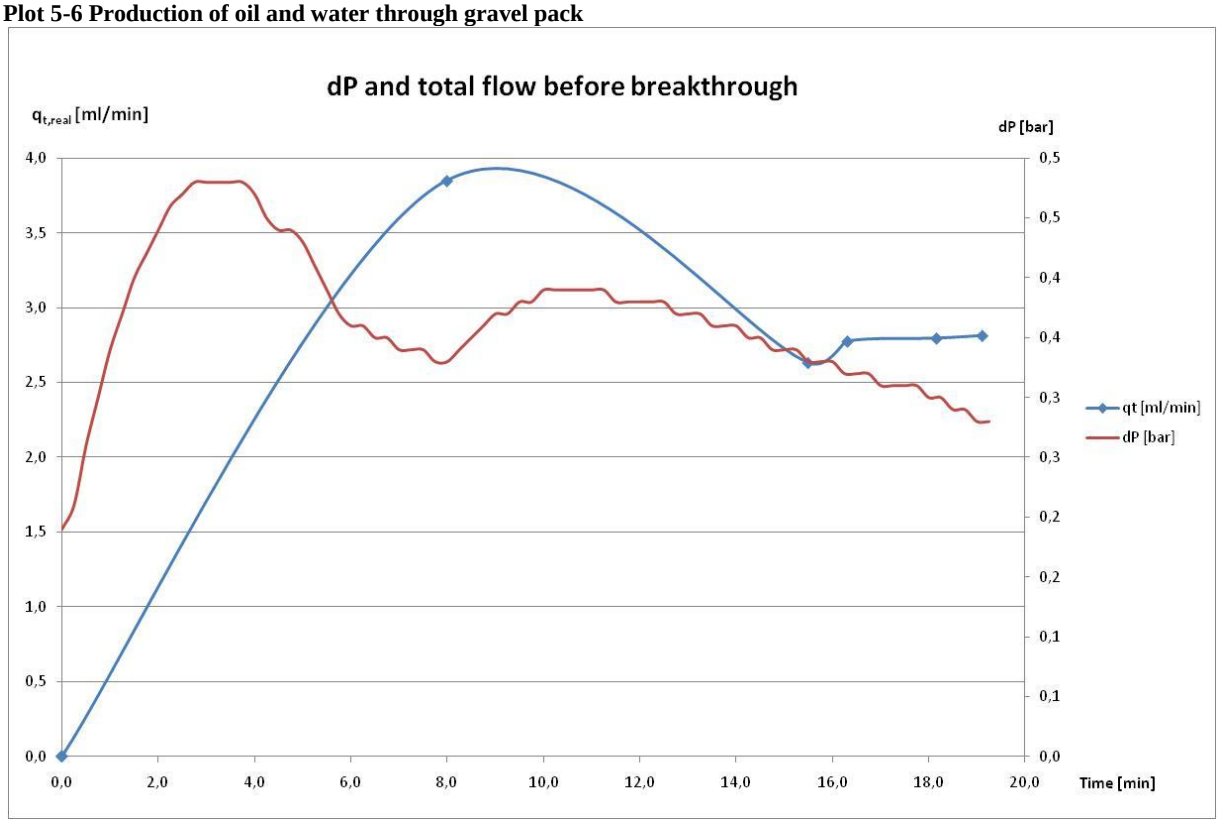

Plot 5-7 dP and total flow befor breakthrough

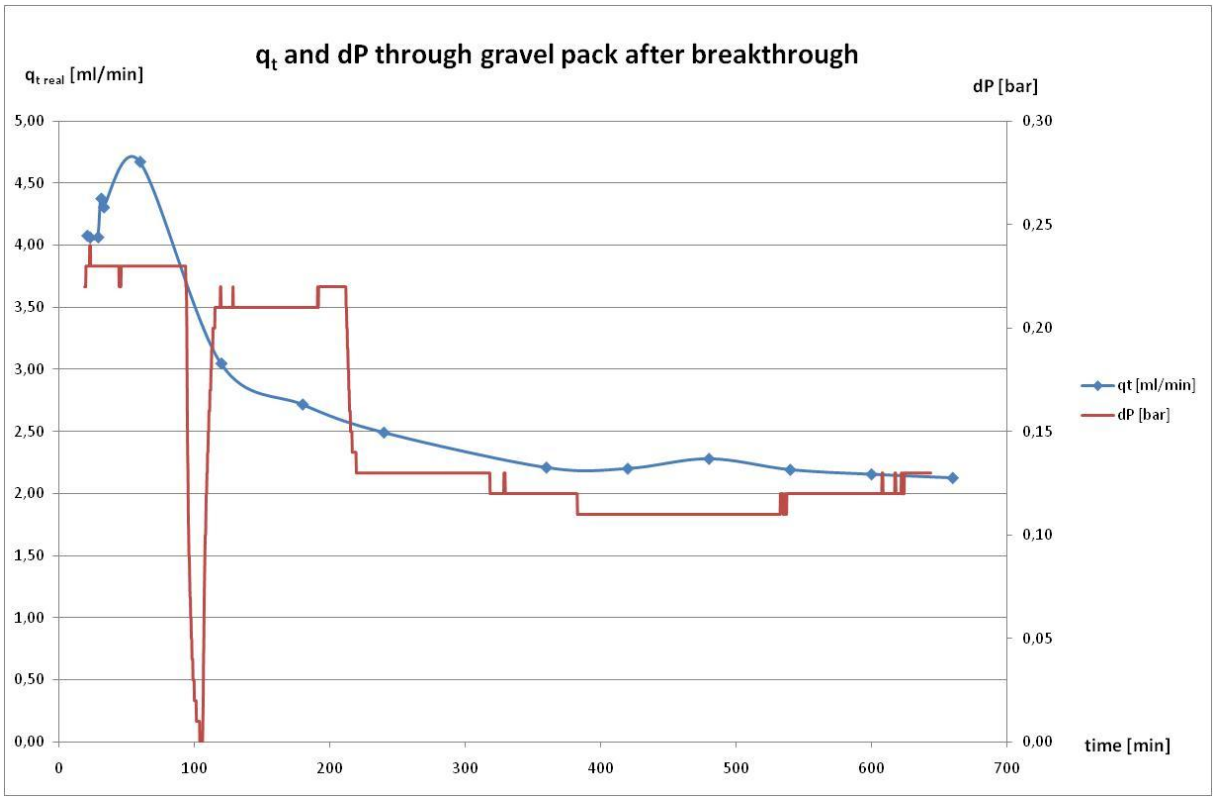

Plot 5-8 Flow and dP throgh gravel pack after breaktrough

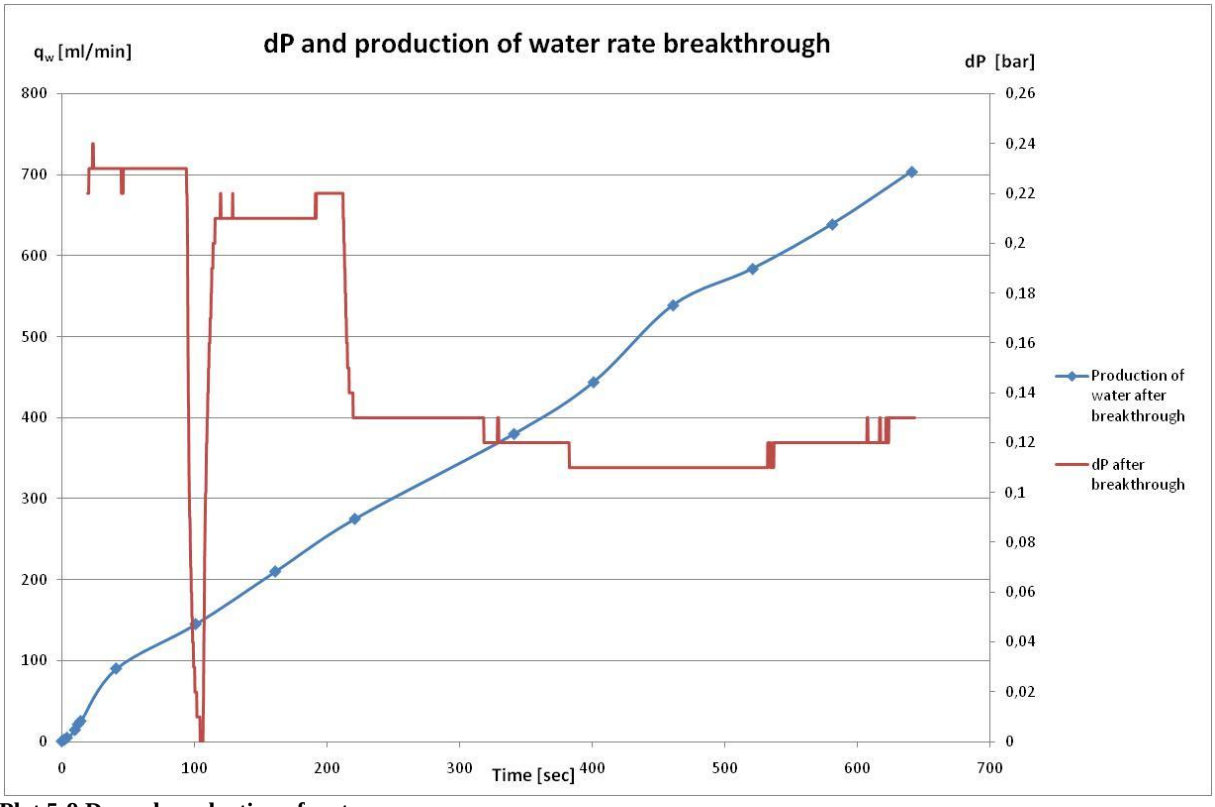

Plot 5-9 Dp and production of water

Average water rate, $q_{w,avg} = 4.246*10^{-6}\ m^3/s = 4.25ml/min$

Volume of water injected before breakthrough

$$V_i = A(1-S_{or}-S_{wr})X_f = 0.000224m^2 \cdot (1-3.48\cdot10^{-3}-0.737335)\cdot 1.0m = 0.0000583m^3 = \underline{58.3ml}$$

Volume injected at any time after breakthrough

$$V_{iabt} = V_{ibt} + i_{abt}(t-t_{bt}) = 0.0000583m^3 + 4.246*10^{-6}m^3/s\cdot(1152s) = \underline{4.95\times10^{-3}m^3}$$

Displaceable PV after displacement by water and oil

$$V_{pd} = V_p(S_{oi}-S_{or}) = Ah\phi(S_{oi}-S_{or})$$

$$= 2.25\cdot10^{-4}m^2\cdot1.0m\cdot.41(0.908-3.48\cdot10^{-3})ml/ml$$

$$= \underline{83.42ml}$$

Cumulative oil produced before breakthrough, N_{pd} at breakthrough;

$N_{pd,bt} = \underline{53.8ml}$

Cumulative oil produced after breakthrough

$N_{pd,after\ bt} = 678ml - 53.8ml = \underline{624.2ml}$

Measured pore volume injected

$PV = \underline{1390ml}$

Area Displacement Efficiency

Areal displacement efficiency before breakthrough is equivalent to the volume of water injected.

$$E_A = \frac{V_i}{PV(S_{oi}-S_{or})} = \frac{0.0000583m^3}{0.000225m^3(0.908-3.48\cdot10^{-3})} = \underline{0.286} = \underline{28.6\%}$$

Displacement efficiency at breakthrough

$$E_{Abt} = 0.54602036 + \frac{0.03170817}{M} + \frac{0.30222997}{e^M} - 0.00509693\cdot M$$

$$= 0.54602036 + \frac{0.03170817}{18.6} + \frac{0.30222997}{e^{18.6}} - 0.00509693\cdot18.6$$

$$= 0.4529$$

$$= \underline{45.3\%}$$

Cumulative Oil Produced Calculated

$$N_p = V_p(S_{oi}-S_{or})E_{Abt} = 2.25\cdot10^{-4}m^2\cdot1.0m\cdot.41\cdot(0.908-3.43\cdot10^{-3}) = 0.0000379m^3 = \underline{37.9ml}$$

Calculation of Vertical Displacement efficiency at breakthrough

From calculated Np:

$$E_I = \frac{N_{p,calc}}{M\cdot V_{t,bt}} = \frac{0.0000379m^3}{18.6\cdot0.0000583m^3} = \underline{0.0349 = 3.49\%}$$

From measured Np

$$E_I = \frac{N_p}{M\cdot V_t} = \frac{0.0000538m^3}{18.6\cdot0.0000538m^3} = \underline{0.0537 = 5.37\%}$$

Displacement Efficiency

$$E_D = \frac{N_{p\,Bt}}{1 - S_{wi}} = \frac{0.0000538}{1 - 0.997} = 0.0179 = \underline{1.79}\%$$

Volumetric Displacement Efficiency for measured N_p, based on area efficiency at break through

$$E_V = E_A E_I = 0.4529 \cdot 0.0537 = \underline{0.024}$$

Recovery Efficiency from equation 2.43

$$RF = E_D E_V = 0.044 = \underline{4.4\%}$$

Breakthrough time

$$t_{Bt} = \frac{V_{inj}}{q_{inj,water+oil}} = \frac{58.3ml}{2.71ml/\min} = 21.52\,\min = \underline{21\min 30\sec}$$

This is high compared to the pressure drop during the displacement. It might be of the high absolute permeability of 363.13D for this displacement.
The total amount of displaced oil in the horizontal gravel pack was 53.8ml. The total amount of injected oil is 92.25ml. This value is assumed to be correct, but may differ because of the high permeability. The total amount of oil injected before breakthrough was found by use of the bulk volume and the porosity. This assumption will also affect the displacement efficiencies, in areal, vertical and volumetric efficiencies. The overall recovery is low only 4.4%, the same is it for the displacement efficiency. The total amount of water injected is almost the same as the oil produced, 58.3 ml injected and 53.8ml produced. The low recovery efficiency is most probably because of the early breakthrough of water. The values differensiate from the measured values, can be a reason of the relative permeabilities and the assumptions made during the calculations.

5.6 Recommendations

T

REFERENCES

1. **Wiggins, Michael L.** *Petroleum Engineering Handbook.* [ed.] Larry W. Lake. NA. NA : NA, 2007. Vol. IV. NA.
2. **Zolotukhin, A. B. and Ursin, J. R.** *Introduction to Petroleum Reservoir Engineering.* Stavanger : HøyskoleForlaget AS - Norwegian Academic Press, 2000.
3. **Hiort, Aksel.** *Introduction to Reservoir Technology/Introducksjon til Reservoir Teknikk.* Stavanger : Universitetet i Stavanger, 2009.
4. **Nelson, Philip H. and Batzle, Michael L.** *Single Phase Permeability.* [ed.] John R. Fanchi. Colorado : Society of Petroleum Engineers, 2006. Vol. I.
5. **Christiansen, Richard L.** *Petroleum Engineering Handbook.* [ed.] Larry W. Lake and John R. Fanchi. Colorado : Society of Petroleum Engineers, 2006. Vol. I, Chapter 15. ISBN 978-1-55563-108-6.
6. **Kleppe, Hans.** *Reservoir Simulation.* Stavanger : University of Stavanger, Institute of Petroleum Technology, 2007.
7. **Christiansen, Richard L.** *Relative Permeability and Capillary Pressure.* [ed.] Larry W. Lake and John R. Fanchi. Colorado : Society of Petroleum Engineers, 2006. Vol. I, Chapter 14. ISBN 978-1-55563-108-6.
8. **Schlumberger.** Schlumberger Oilfield Glossary. *Oilfield Glossary, Irreducible Water.* [Online] Schlumberger. [Cited: 27 May 2010.] http://www.glossary.oilfield.slb.com/Display.cfm?Term=irreducible%20water.
9. **Selley, Richard C.** *Elements of Petroleum Geology.* 2nd Edition. San Diego : Academic Press, An Imprint of Elsevier, 1998. ISBN-10: 0-12-636370-6.
10. **Schlumberger.** *Schlumberger Oilfield Glossary.* [Online] Schlumberger, 25 May 2010. http://www.glossary.oilfield.slb.com/Display.cfm?Term=pore%20throat.
11. **Nordhaug, Hans Fredrik.** *Modeling of Multi Phase Flow in Porous Media: Operator Splitting, Front Tracking, Interfacial Area and Network Models.* Department of Mathematics, University of Bergen. Bergen : Department of Mathematics, University of Bergen, Oct. 2001.
12. **Porras, Juan Carlos, Barbato, Roberto and Salazar, Diomedes.** *Upscaling From Core Data to Production: Closing the Cycle. A Case Study in the Santa Barbara and Pirital Fields, Easten Venezuela Basin.* Various Countries : SPE, June 2-5, 2002.
13. **Beard, D. C. and Weyl, P. K.** *Influence of Texture on Porosity and Permeability of Unconsolidated Sand.* Midland, Texas, Stony Brook, New York : The American Associatwn of Petroleum Geologists Bultetin, 1973. pp. 349-369. Vols. V.57, nr.2.
14. **Green, Don W. and Willhite, G. Paul.** *Enhanced Oil Recovery.* Richardson, Texas : Henry L. Doherty Memorial Found of AIME, Society of Petroleum Engineers, 1998.
15. **Ahmed, Tarek H.** *Reservoir engineering handbook.* s.l. : Elsevier/Gulf Professional, 2006 .
16. **Smaoui, Nejib and Gharbi, B. Ridha.** *Using Karhunen-Loéve decomposition and artificial neural network to model miscible fluid displacement in porous media.* Department of Mathematics and Computer Science, Department of Petroleum Engineering, Kuwait University. Kuwait : Applied Mathematical Modelling, Elsevier, 1999. pp. 657-675.
17. **Hornof, V. and Morrow, N. R.** *Flow visualization of the Effects of Interfacial Tension on Displacement.* New Mexico Petroleum Recovery Research Center, University of Ottawa. Ottawa, New Mexico : SPE, 1988.
18. **Dake, L. P.** *Fundamentals of Reservoir Engineering.* Amsterdam, The Netherlands, Oxford, UK : Elsevier, 1978.
19. **Engelberts, W. F. and Klinkenberg, L. J.** *Laboratory Experiments on the Displacement of Oil by Water from Packs of Granular Material.* The Hague : Society of Petroleum Engineers, 1951. p. 544.
20. **Chuoke, R. L., van Meurs, P. and van der Poel, C.** *The instability of Slow, Immiscible, Viscous Liquid-Liquid Displacements in Permeable Media.* Houston, Texas, Amsterdam, The Netherlands : SPE, AIME 1959. Petroleum Transactions. T.P. 8073.
21. **Araktingi, U. G. and Orr Jr., F. M.** *Viscous Fingering in Heterogeneous Porous Media.* Stanford University. Stanford : Society of Petroleum Engineers, 1992. p. Vol 1. No. 1.

22. **Gilje, Eli.** *Simulation of viscous instabilities in miscible and immiscible displacement.* Department of Chemistry, University of Bergen. Bergen : University of Bergen, 2008. Master Thesis.
23. **Homsy, G.M.,.** *Viscous Fingering in Porous Medium.* Stanford, California : Annual Review of Fluid Mechanics; Department of Chemical Engineering, Stanford University, Stanford, 1987. pp. 271-311.
24. **Golan, Michael and Curtis H, Whitson.** *Well Performance.* Trondheim : Prentice Hall, 1991. ISBN 0-13-946609-6.
25. **Cossé, R.** *Basics of Resevoir Engineering.* [trans.] R. Cossé Le gisement. Paris : Institut francais du pétrole, 1993. Vol. Éditions Technip. ISBN 2-7108-0630-4.
26. **Fanchi, John R.** *Principles of Applied Reservoir Simulation.* 3rd edition. Burlington : Gulf Professional Publishing, Elsevier, 2006. ISBN 10: 0-7506-7933-6.
27. **Martel, Richard, et al.** *Displacement and sweep efficiencies in a DNAPL recovery test using micellar and polymer solutions injected in a five-spot pattern.* INRS-Eau, Terre et Environnement, Institut national de la recherche scientifique, Université du Québec. Québec : Journal of Contaminant Hydrology, ScienceDirect, 2002, revised and accepted 2004. 75 (2004) 1-29.
28. **Guliyev, Ruslan.** *Simulation Study of Areal Sweep Efficiency Versus a Function of Mobility Ratio and Aspect Ratio for Staggered Line-Drive Waterflood Pattern.* Petroleum Engineering, Texas A&M Univeristy. Texas : Office of Graduate Studies, 2008. Master Thesis.
29. **Ebrahimi, Arian.** *Analysis of Waterflood in the Valendis Horizon of Suderbruch Oil Field.* Clausthal University of Technology, Institute of Petroleum Engineering. Clausthal-Zellerfeld : Clausthal University of Technology, 2009. Seminar thesis.
30. **Mott, Robert L.** *Machine Elements in Mechanical Design 4th edition in SI units.* Uni of Dayton. s.l. : Pearson Prentice Hall. ISBN 0-13-197-644-3.
31. **Irgens, Fridtjof.** *Fasthetslære, 6th ed.* s.l. : Tapir, 1999. ISBN 82-519-1522-1.
32. **Irgens, Fritjof.** *Statikk, 7th ed.* s.l. : Tapir, 2005. ISBN 82-519-2067-1.
33. **Papatzacos, Paul Georg.** *ÅMA150 Mathematical Modelling.* H-2008. Lecture Notes.
34. **Time, Rune.** *MPE 490 Flerfasestrømning i rør.* V-2009. s. Chapter 6, Lecture Notes.
35. **Microsoft.** *Help Tool in Microsoft Excel 2010.* 2010. pp. Search for Goal Seek and What-If Analysis.
36. **Electronics, Gibson Medical.** *Gibson 305 Piston Pump.* Villiers le Bel, France : s.n.
37. **200, PAAR PHYSICA Rheometer US.** *Manual.*
38. **AS, Dipl Ing Houm.** *Anton Paar, DMA 4500/5000 Density/Spesific/Gravity/Consentration Meter - Instruction Handbook.* Grefsen, Oslo : s.n.
39. **Rabenjafimanantsoa, S Myhren.** *Laboratory exsercises in Reservoir engineering.* s.l. : University of Stavanger, 2010.
40. **du Noüy, Pierre Lecomte.** *An Interfacial Tensiometer for Universal Use.* s.l. : The Journal of General Physiology, 1925.
41. **Oil, Esso Imperial.** Product Data Sheet, White Oil, Marcol83, Primol, Bayol35. *Esso Imperial Oil.* [Online] Esso, 2009. [Cited: 30 3 2010.] http:www.imperialoil.ca/Canada-English/Files/Products_Lubes/IOCAENWPOESWhiteoil.pdf.
42. **AS, Esso Norge.** *Helse,-Miljø- og Sikkerhetsdatablad.* Oslo : Esso Norge AS, 2002. N-63-L5891.
43. **Mobile, Exxson.** *Sikkerhetsdatablad - Marcol 82.* Oslo : Exxson Mobile, 2008.
44. **Outmans, H. D.** *Nonlinear Theory for Frontal Stability and Viscous Fingering in Porous Media.* Union Oil Company of California. Brea, California : Society of Petroleum Engineers, SPE 183, 1962. Member AIME.
45. **Satter, Abdus, Iqbal, Ghulam M. and Buchwalter, James L.** *Practical Enhanced Reservoir Engineering.* Tulsa : PennWell Corporation, 2007. ISBN-10: 1-59370-056-3.
46. **Wiggins, Michael L.** *Inflow and Outflow Performance.* NN. U. of Oklahoma : NN, NN. Vol. IV. NN.

APPENDIX A

Table A- 1 Measured Flow, Qreal, and Pressure Drop, dp/dx, for absolute permeability calculation

Q_{inn}		Q_{real}	Pressure		Permeabilitet, k		
q [ml/h]	q [m^3/s]	q [m^3/s]	dP [bar]	dP [Pa]	[m^2]	[D]	[D]
0	0	0	0	0	0	0	
60	1,67E-08	1,71E-08	0,011	1100	4,01E-11	40,65	52,23
80	2,22E-08	2,36E-08	0,015	1485	4,10E-11	41,50	
100	2,78E-08	2,86E-08	0,017	1700	4,34E-11	43,99	
120	3,33E-08	3,32E-08	0,020	2000	4,28E-11	43,37	
140	3,89E-08	3,76E-08	0,023	2254	4,30E-11	43,61	
160	4,44E-08	4,44E-08	0,025	2546	4,49E-11	45,53	
180	5,00E-08	4,99E-08	0,029	2885	4,46E-11	45,17	
200	5,56E-08	5,61E-08	0,032	3162	4,57E-11	46,33	
400	1,11E-07	1,13E-07	0,062	6162	4,73E-11	47,88	
800	2,22E-07	2,24E-07	0,122	12192	4,73E-11	47,95	
1000	2,78E-07	2,97E-07	0,154	15408	4,97E-11	50,36	

APPENDIX B - VISCOSITY MEASUREMENTS

Bayol

The viscosity was measured with Physica viscosity meter.

Table B- 1 Measured viscosity of Bayol

d(gamma)/dt	Meas. Pts.	Time	Shear Stress	Viscosity	Speed	Torque
1/s		[s]	[Pa]	[Pa·s]	[1/min]	[µNm]
1,5	1	10	0,008	0,00504	0,26	0,3
1,5	2	20	0,013	0,00869	0,26	0,5
3,1	1	30	0,028	0,00897	0,54	1,0
3,1	2	40	0,030	0,00955	0,54	1,1
5,1	1	50	0,024	0,00476	0,89	0,9
5,1	2	60	0,006	0,00126	0,89	0,2
10,2	1	70	-0,016	-0,00157	1,78	-0,6
10,2	2	80	0,030	0,00297	1,78	1,1
51,1	1	90	0,051	0,00101	8,90	1,9
51,1	2	100	0,048	0,00094	8,90	1,8
102	1	110	0,081	0,00079	17,80	3,0
102	2	120	0,077	0,00076	17,80	2,9
153	1	130	0,154	0,00100	26,60	5,8
153	2	140	0,142	0,00093	26,60	5,3
340	1	150	0,328	0,00096	59,20	12,3
340	2	160	0,328	0,00097	59,20	12,3
511	1	170	0,500	0,00098	89,00	18,7
511	2	180	0,527	0,00103	89,00	19,7
1021	1	190	1,050	0,00103	178,00	39,4
1021	2	200	1,050	0,00103	178,00	39,2

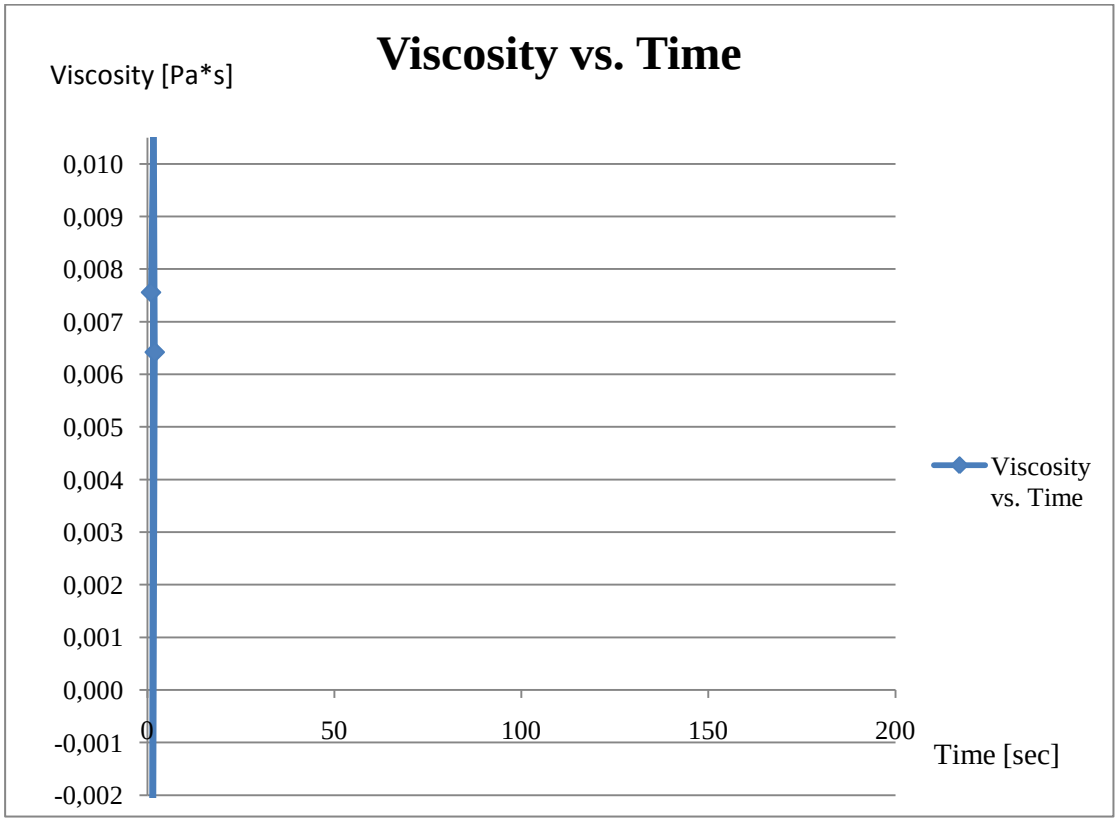

Plot B- 1 Viscosity measurements

The plot shows the measured viscosity over a time of 200sec. The viscosity is on the y-axis and the time is on the x-axis. Between the first measurement, μ = 0.00504Pa*s at t = 10sec to μ = 0.00100Pa*s at t= 130 sec, the variation in viscosity is varying.

Probably the reason for the large variation of viscosity is because of low velocities and a large uncertainty in measurement instruments. The viscosity became more stable for higher shear rates. The viscosity used for first calculation of permeability, was calculated to be 0.00099088Pa*s. This value is an average number between the viscosities for the eight last shear rates given in **Error! Reference source not found.**. The result of the absolute permeability (21.12D) was lower than the permeability of oil (31D), which gave a relative permeability larger than one.

The second viscosity measurement was done by using another steering tool.

below shows the most relevant measured viscosities for given shear rates. The viscosity used for permeability calculation was measured to be, μ = 0.00245. This number is an average viscosity from the numbers in the tables below.

Table B- 2 gives an overview of viscosities measured with MK24 coned plate

Shear Rate	Time	Shear Stress	Viscosity	Speed	Torque
[1/s]	[s]	[Pa]	[Pa·s]	[1/min]	[μNm]

153	10	0,37	0,00245	26	41
153	20	0,37	0,00244	26	41
153	30	0,37	0,00244	26	41
153	40	0,38	0,00245	26	41
153	50	0,37	0,00245	26	41
340	60	0,83	0,00244	57	92
340	70	0,83	0,00245	57	92
340	80	0,83	0,00244	57	92
340	90	0,83	0,00244	57	92
340	100	0,83	0,00244	57	92
511	110	1,26	0,00246	85	139
511	120	1,26	0,00246	85	139
511	130	1,25	0,00244	85	138
511	140	1,24	0,00243	85	137
511	150	1,25	0,00244	85	138
1020	160	2,51	0,00246	170	277
1020	170	2,53	0,00248	170	279
1020	180	2,52	0,00246	170	278
1020	190	2,51	0,00246	170	277
1020	200	2,53	0,00248	170	279
1020	210	2,51	0,00246	170	277
1020	220	2,52	0,00246	170	278
1020	230	2,53	0,00247	170	279
1020	240	2,51	0,00245	170	277
1020	250	2,52	0,00247	170	278

Average viscosity = 0.0024528Pa*s
Viscosity used for permeability calculation, μ_{oil} = 0.00245Pa*s
The viscosity used for permeability calculation is more accurate and will be used for calculation.

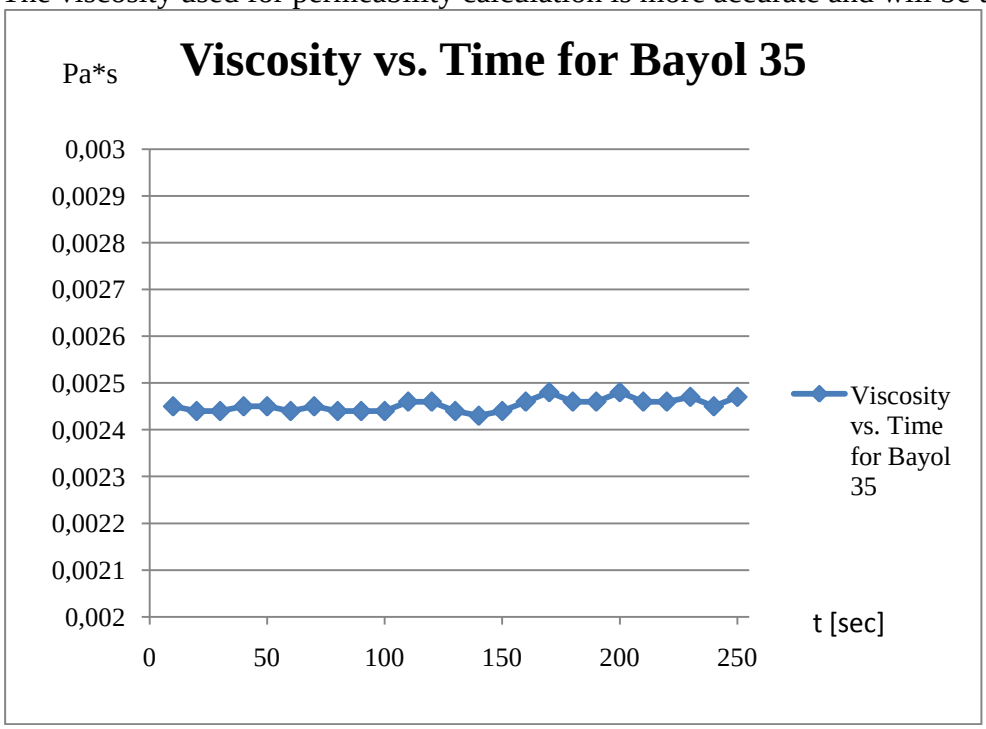

Plot B- 2 More accurate viscosity measurements. There are fewer variations in viscosity and the average viscosity can be used in further applications

Ionized Water

Table B- 3 Ionized water

Shear Rate	Shear Stress	Viscosity	Speed	Torque
[1/s]	[Pa]	[Pa·s]	[1/min]	[µNm]

1020	1,28	0,00125	170	141
1020	1,30	0,00127	170	143
1020	1,29	0,00126	170	142
1020	1,28	0,00125	170	141
1020	1,30	0,00127	170	143
1020	1,28	0,00125	170	141
1020	1,28	0,00126	170	142
1020	1,30	0,00127	170	143
1020	1,28	0,00125	170	141
1020	1,29	0,00126	170	142

Average viscosity = 0.001259Pa*s
Viscosity used for permeability calculation, μ_w = 0.00126Pa*s

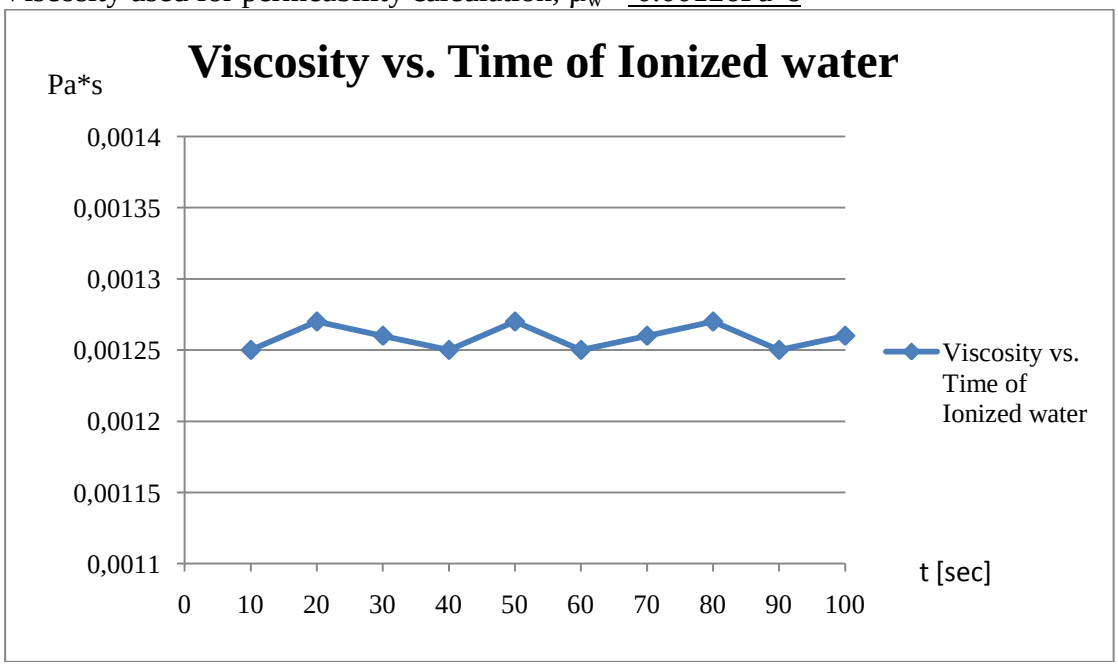

Plot B- 3 Viscosity measured vs. time for ionized water

Marcol82

Table B- 4 Viscosity, shear stress for Marcol82

Marcol 82		
Shear Stress [Pa]	Viscosity [cP]	Viscosity [Pa·s]
0,1	100	0,1
0,1	100	0,1
0,1	100	0,1
0,1	100	0,1
0,1	100	0,1
0,1	44,4	0,0444
0,1	46,1	0,0461
0,1	46,1	0,0461
0,1	46,4	0,0464
0,1	45,8	0,0458
0,2	40	0,04
0,2	40	0,04
0,2	40	0,04
0,2	40	0,04

0,2	40	0,04
0,3	31	0,031
0,3	31,8	0,0318
0,3	32,2	0,0322
0,3	32,3	0,0323
0,3	32,8	0,0328
1,6	31,4	0,0314
1,6	31,4	0,0314
1,6	31,4	0,0314
1,6	31,4	0,0314
1,6	31,4	0,0314
2,8	27,5	0,0275
2,8	27,5	0,0275
2,8	27,5	0,0275
2,8	27,5	0,0275
2,8	27,5	0,0275
4,9	28,8	0,0288
4,9	28,8	0,0288
4,9	28,8	0,0288
4,9	28,8	0,0288
4,9	28,8	0,0288
9,5	27,9	0,0279
9,5	27,9	0,0279
9,5	27,9	0,0279
9,5	27,9	0,0279
9,5	27,9	0,0279
14,1	27,6	0,0276
14,1	27,6	0,0276
14,1	27,6	0,0276
14,1	27,6	0,0276
14,1	27,6	0,0276
27,9	27,4	0,0274
27,9	27,3	0,0273
27,9	27,3	0,0273
27,8	27,2	0,0272
27,8	27,2	0,0272

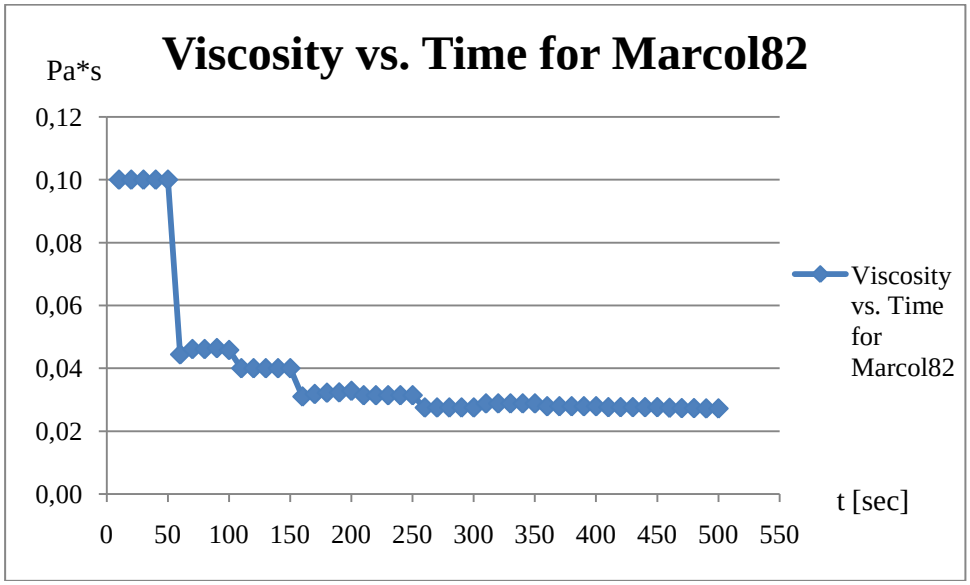

Plot B- 4Viscosity vs. time for Marcol82

APPENDIX C - 1D DISPLACEMENT OF OIL IN POROUS MEDIUM

Figure C 1 The visualization of 1D displacement in vertical upward flow

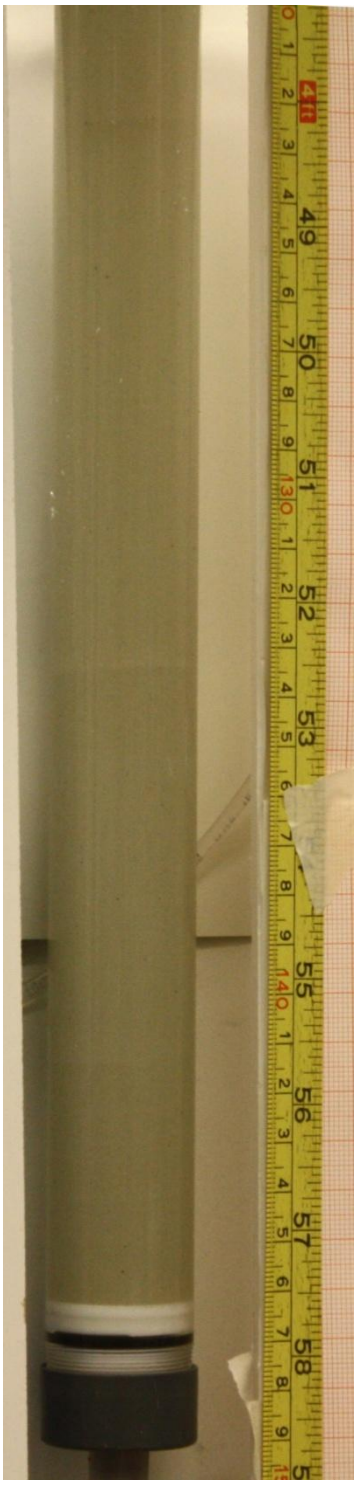

Start test, 14:39

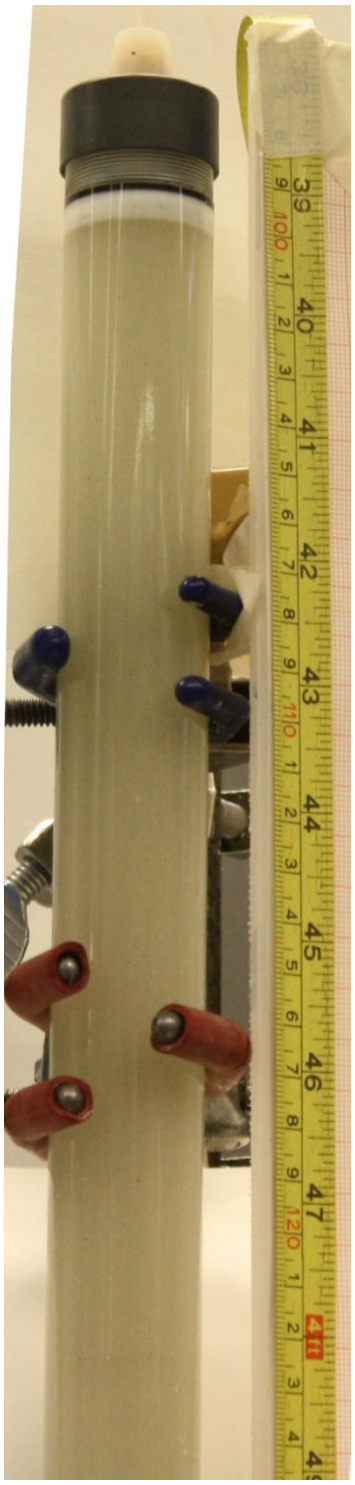

Test cell after test start, 14:39

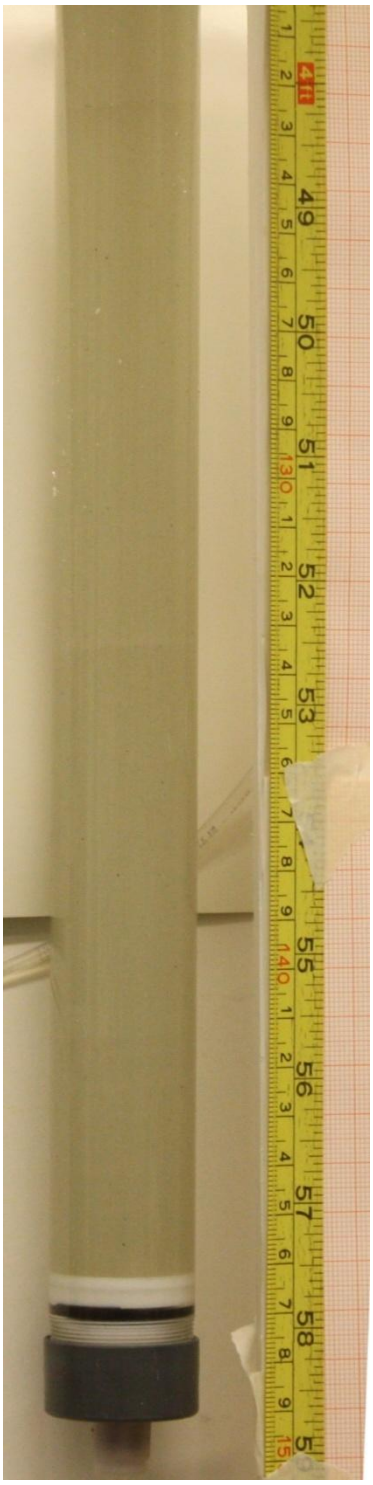

Displacing oil. Just before injection of water, 14:56

Production point

16.03.2010 15:28
Injection of water. White area is viscous fingering. The arrow shows the displacement distance.

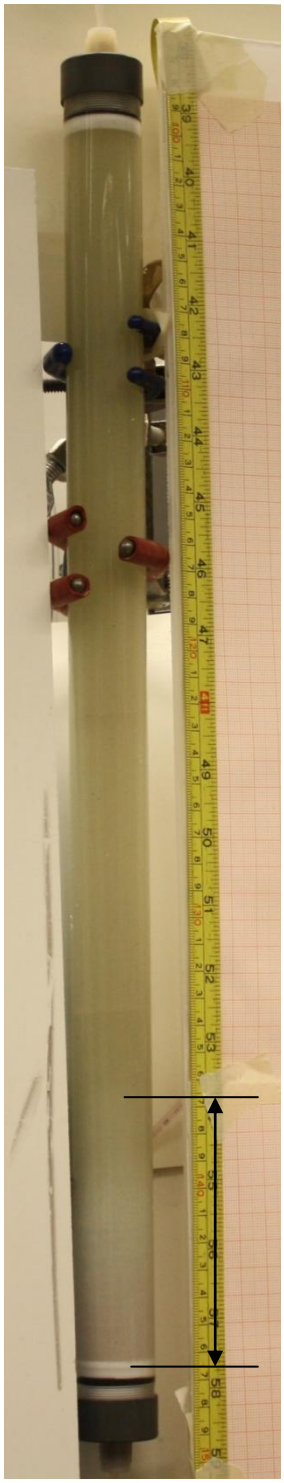

16.03.2010 15:28
Two minutes after injection

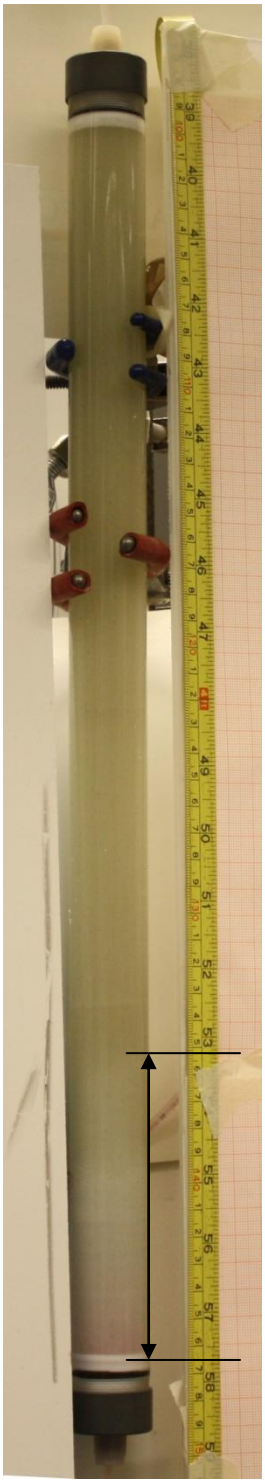

16.03.2010 15:29
Three minutes after injection. Can see some red water

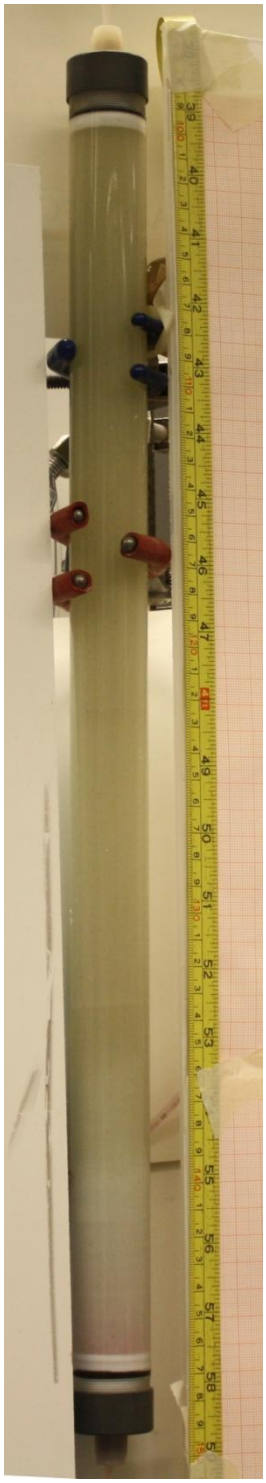

16.03.2010 15:29
Three minutes after injection. Can see some more red water injected.

16.03.2010 15:32

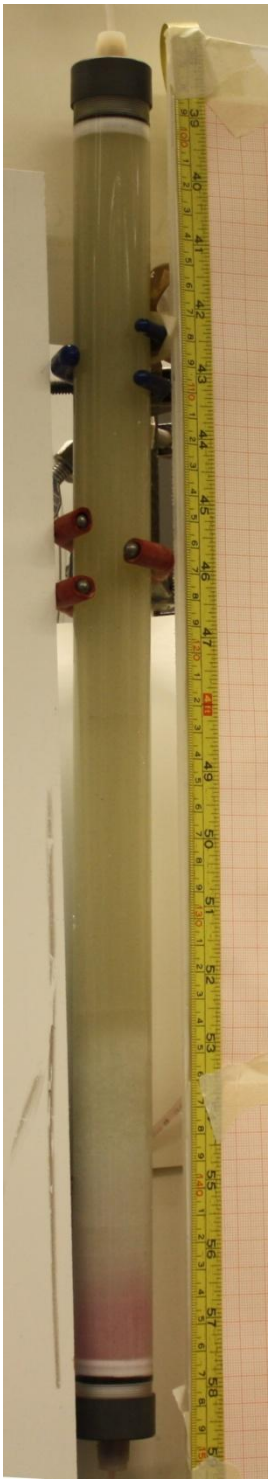

16.03.2010 15:29
More red water injected after three minutes. From the shape of the displacement it might look like piston like displacement.

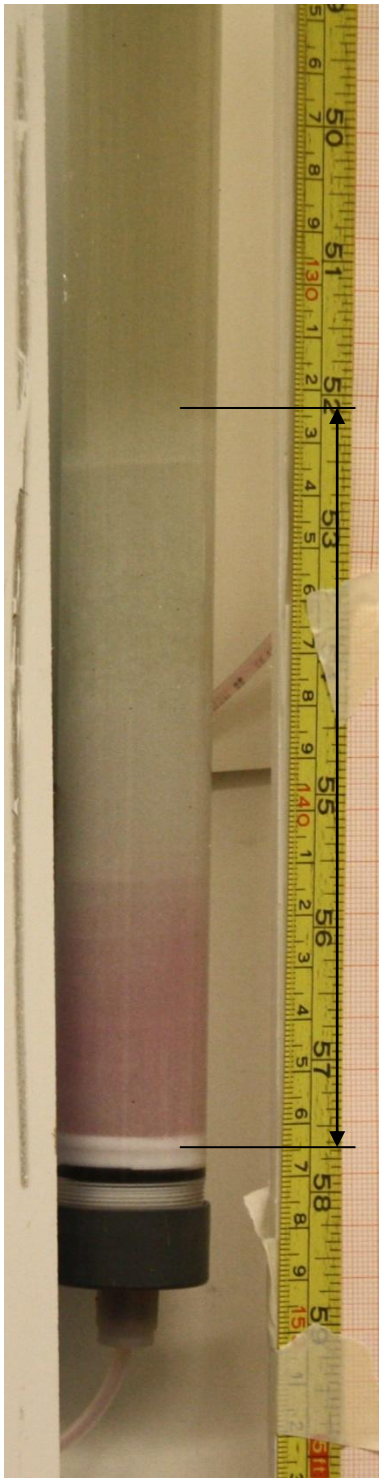

16.03.2010 15:32
Six minutes after injection. Oil displaced 14.2cm in six minutes.

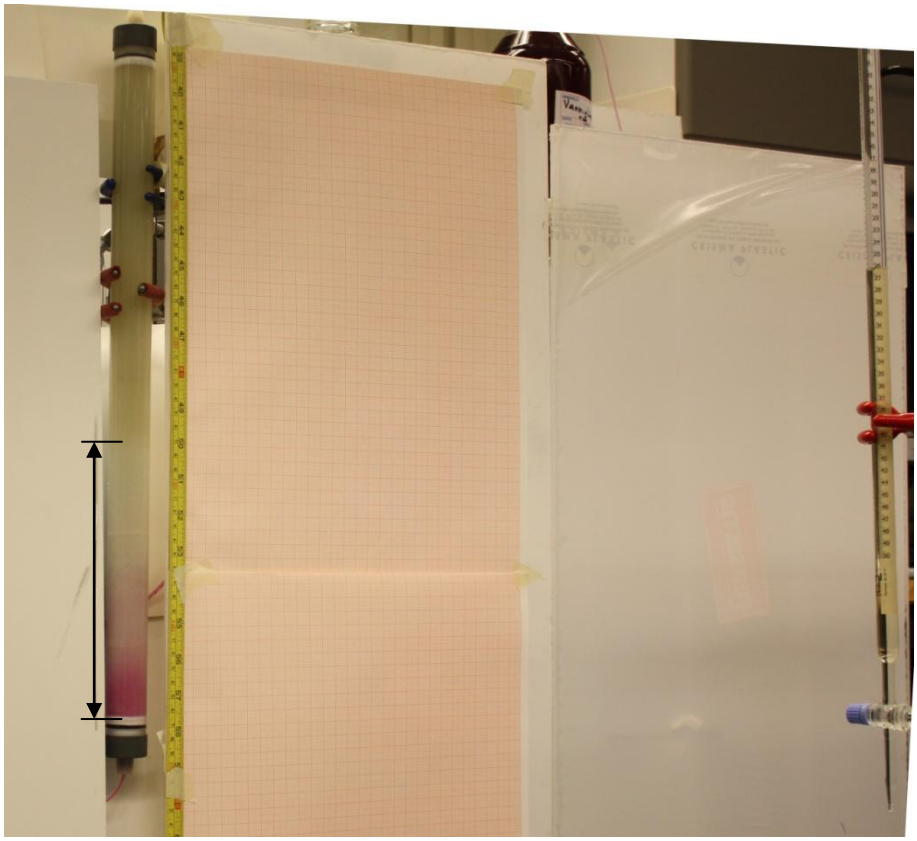

16.03.2010 15:35 Displaced oil and produced oil after 9 min. Can see strong red water in the bottom of the model.

16.03.2010 15:37
11 min.

16.03.2010 15:42
16 min.

16.03.2010 15:44
18 min.

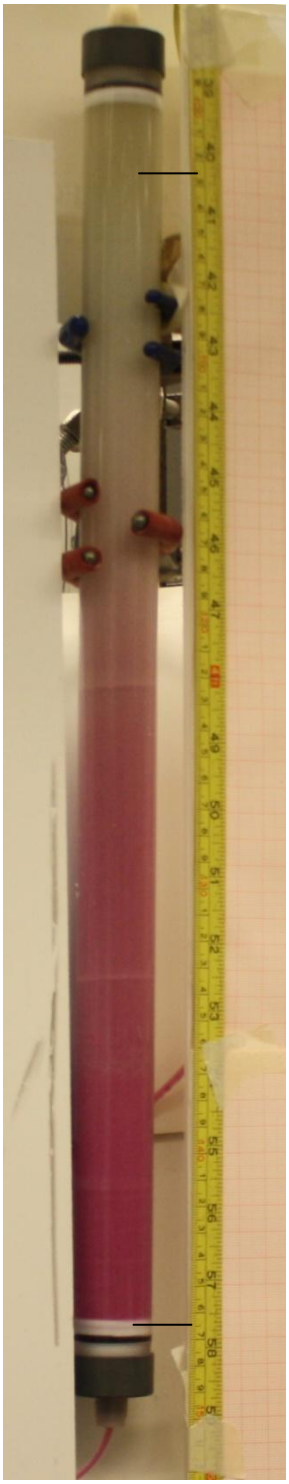

16.03.2010 15:45
19 min

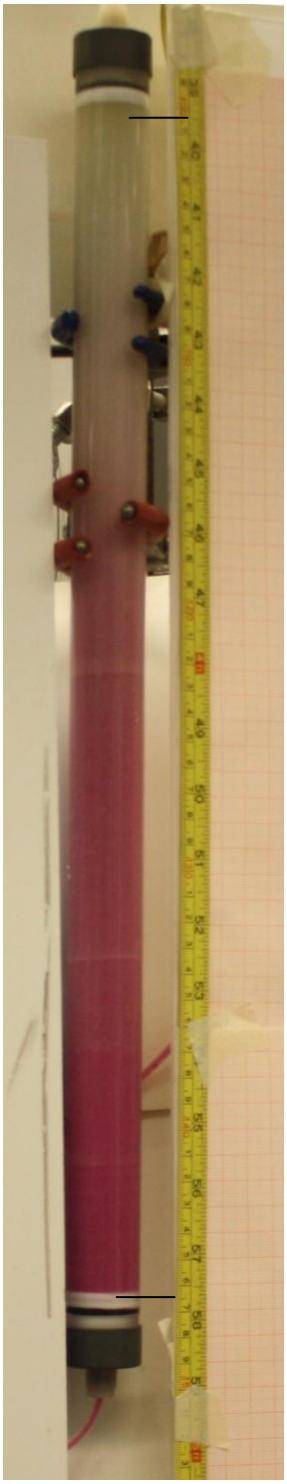

16.03.2010 15:47
21 min

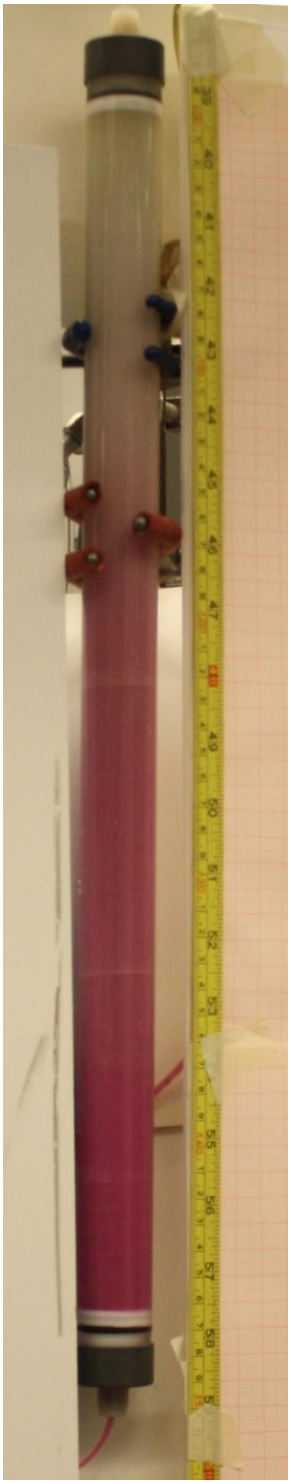

16.03.2010 15:48
Breakthrough after 22 min.

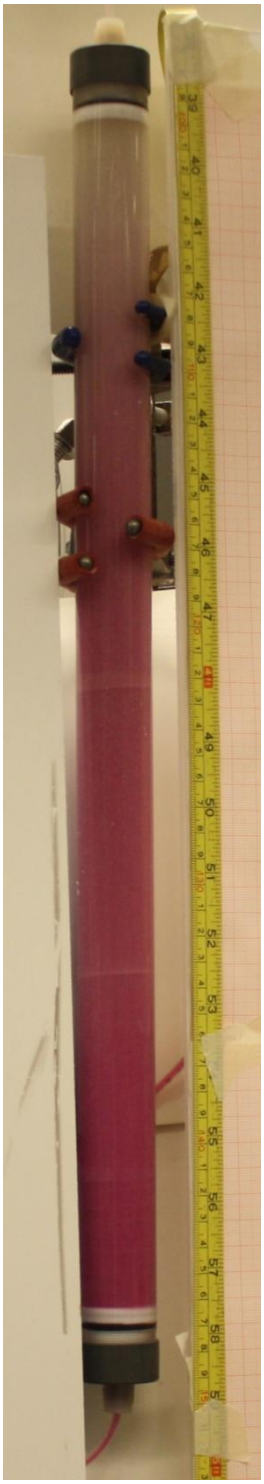

16.03.2010 15:51

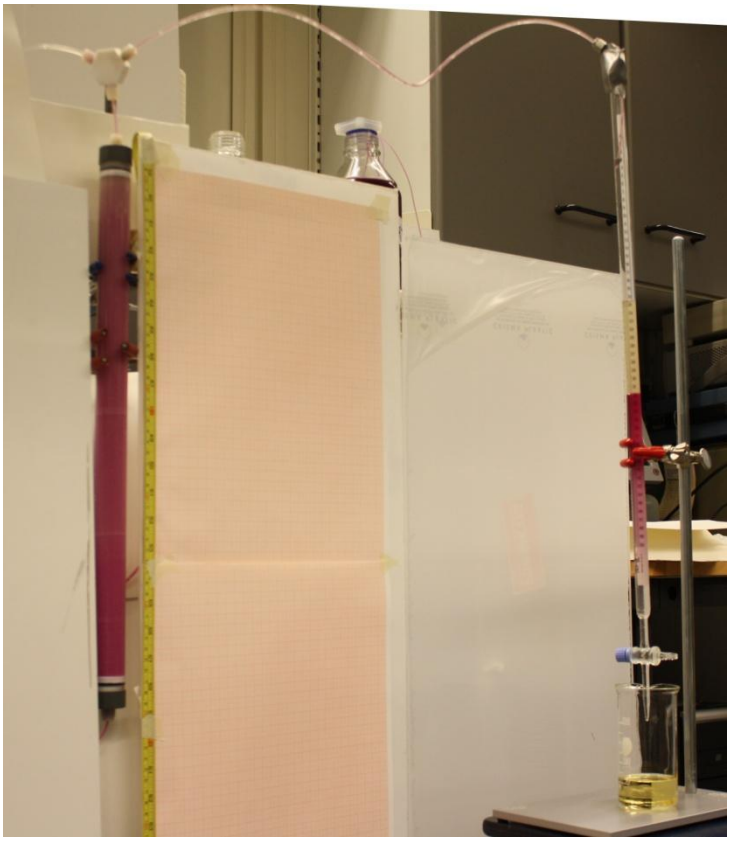

16.03.2010 15:57 production of oil and producing water

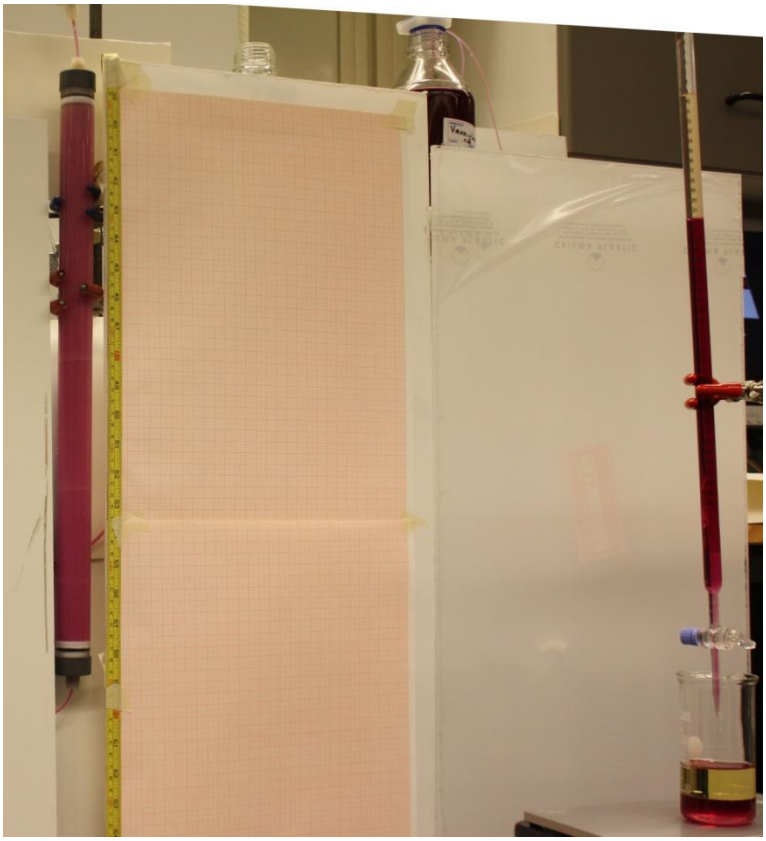

16.03.2010 16:13 Produced water

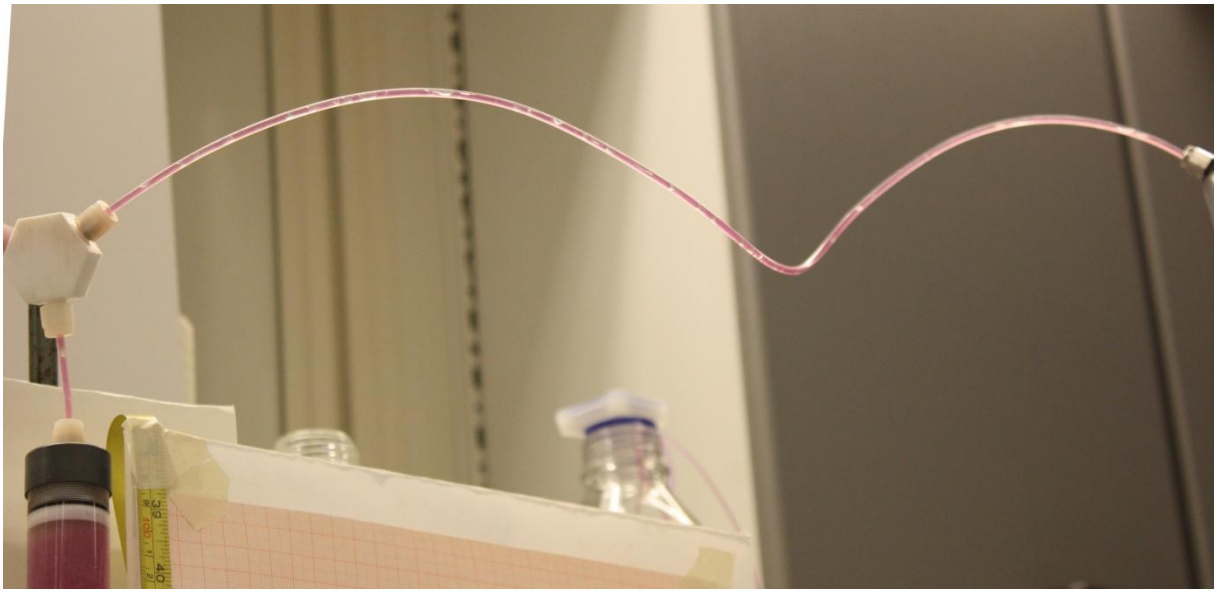

16.03.2010 16:20 Low capillary pressure in the tube

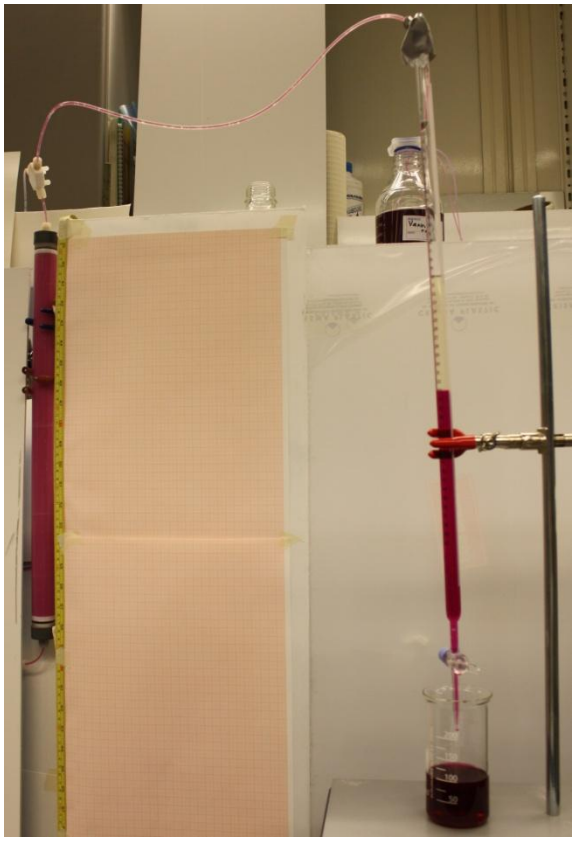

16.03.2010 16:21

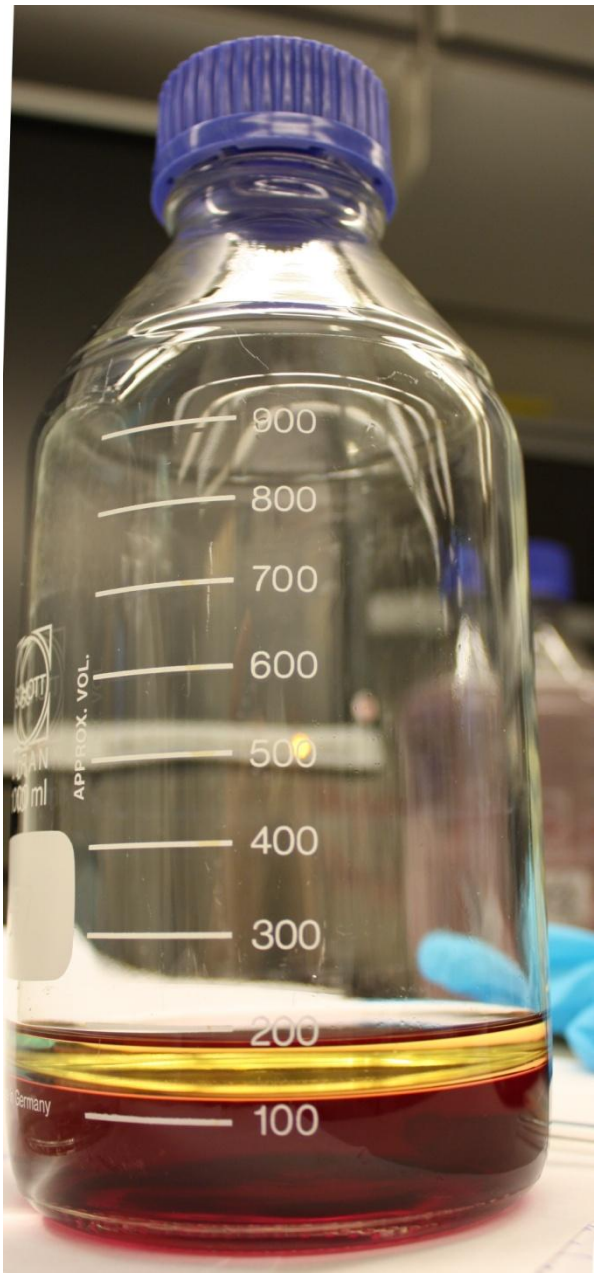

16.03.2010 17:03 Produced oil

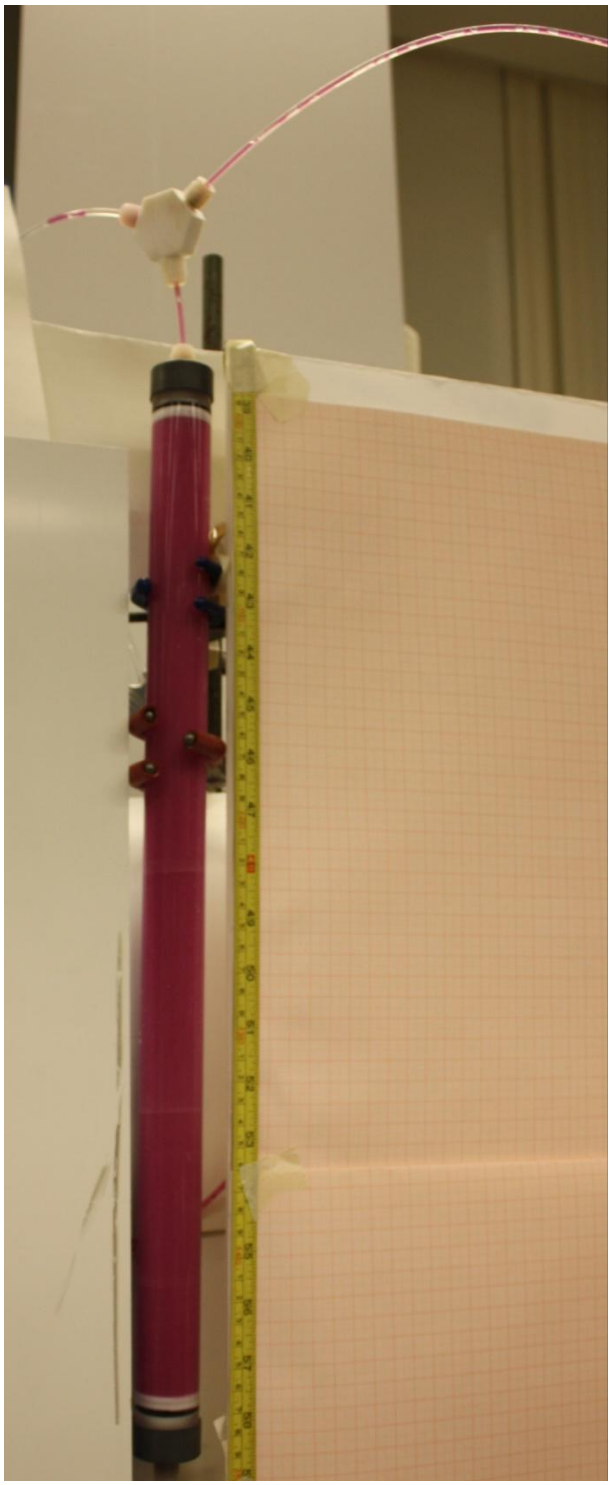

16.03.2010 19:20 Water saturated model with residual oil

APPENDIX D - CALCULATION OF PRODUCED OIL AND WATER BEFORE AND AFTER BREAKTHROUGH

q [ml/h]	Time [min]	Oil Produced [ml]	Water Produced [ml]	Oil total [ml]
200	0	40,8	0	
200	4	25	0	
200	7	14	0	
400	22	83,27567	2	Water break through
400	24	10,5	13,3	10,5
400	29	12	28,5	12
400	32,5	10	40	10
400	44,5	13,5	36,5	13,5
400	46	12,5	0	
400	55	12,3	2	
400	57	12	15	
400	60	12,9	11,8	
400	65	13,4	28,3	13,4
400	68	10	40	
400	75	13,9	15	13,9
400	80	13	37	
400	88	13,3	8,4	
400	95	14,4	30,3	
200	96,5	13	37	14,4
50	102,5	8,7	4,9	
50	176,5	8,6	11,2	
50	182,5	7,8	15	
50	187,5	8	20	
50	194	7,7	39	0,9
Produced water after breakthrough [ml]			288	
Produced oil after breakthrough [ml]				3,5
Produced oil total	Before + after breakthrough			86,77567

APPENDIX E - PRODUCTION DECLINE CURVE

Breakthrough time, produced oil at breakthrough and after breakthrough											
q_{real} [ml/h]	q_{real} [cm^3/s]	Time [min]	Δt [min]	Distance of displaced oil, h [cm]	Δh [cm]	Area/s [cm^2/s]	Area, A [cm^2]	Volume, V [cm^3]	V_{op} [cm^3]	Front velocity [cm/s]	Total volume of oil produced, V_t
400	0,11	0	0	0,0	0,0	0,02498	4,45	0,00	0,00	0,000	0,00
400	0,11	2	2	9,8	9,8	0,02498	4,45	43,60	17,44	0,082	17,44
400	0,11	3	1	11,3	1,5	0,02498	4,45	6,67	2,67	0,025	20,11
400	0,11	6	3	14,2	2,9	0,02498	4,45	12,90	5,16	0,016	25,27
400	0,11	9	3	18,8	4,6	0,02498	4,45	20,46	8,19	0,026	33,45
400	0,11	11	2	25,3	6,5	0,02498	4,45	28,92	11,57	0,054	45,02
400	0,11	16	5	36,5	11,2	0,02498	4,45	49,83	19,93	0,037	64,95
400	0,11	18	2	40,9	4,4	0,02498	4,45	19,57	7,83	0,037	72,78
400	0,11	19	1	43,9	3,0	0,02498	4,45	13,35	5,34	0,050	78,12
400	0,11	21	2	45,0	1,1	0,02498	4,45	4,89	1,96	0,009	80,07
400	0,11	22	1	46,8	1,8	0,02498	4,45	8,01	3,20	0,030	83,28
400	0,11	23	1						0,00		3,00
400	0,11	24	1								0,00

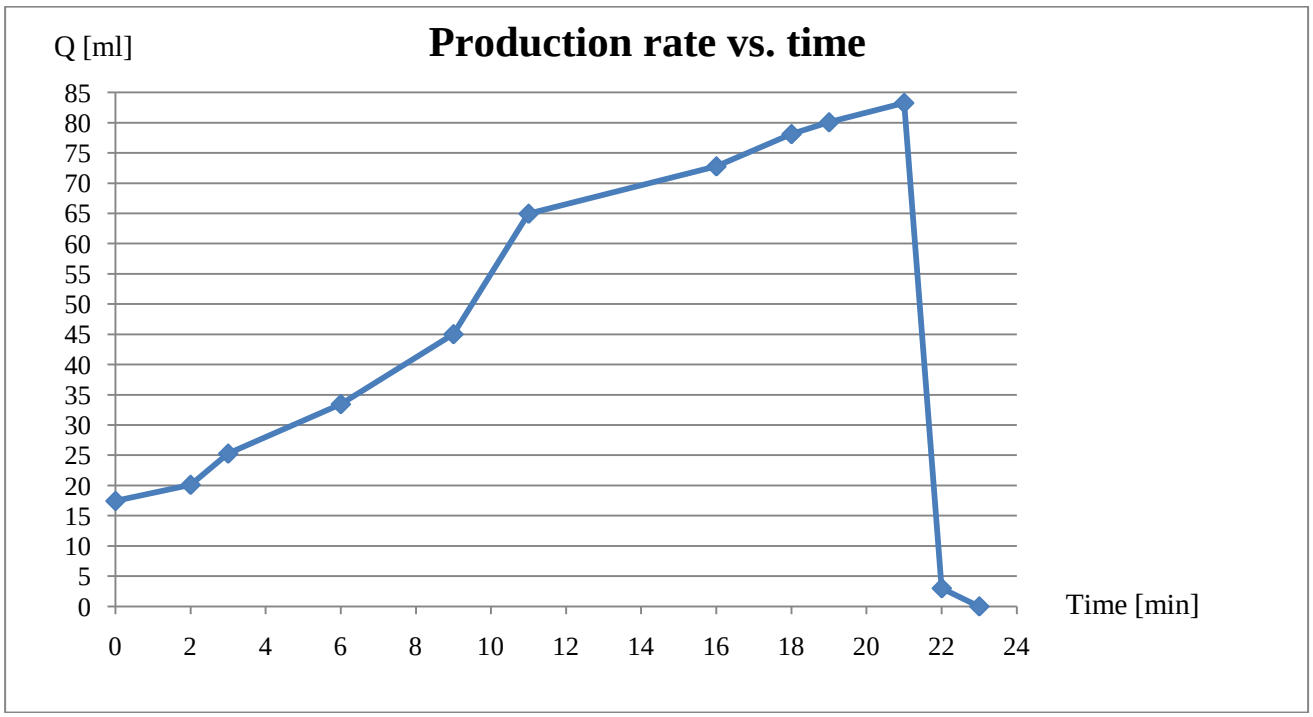

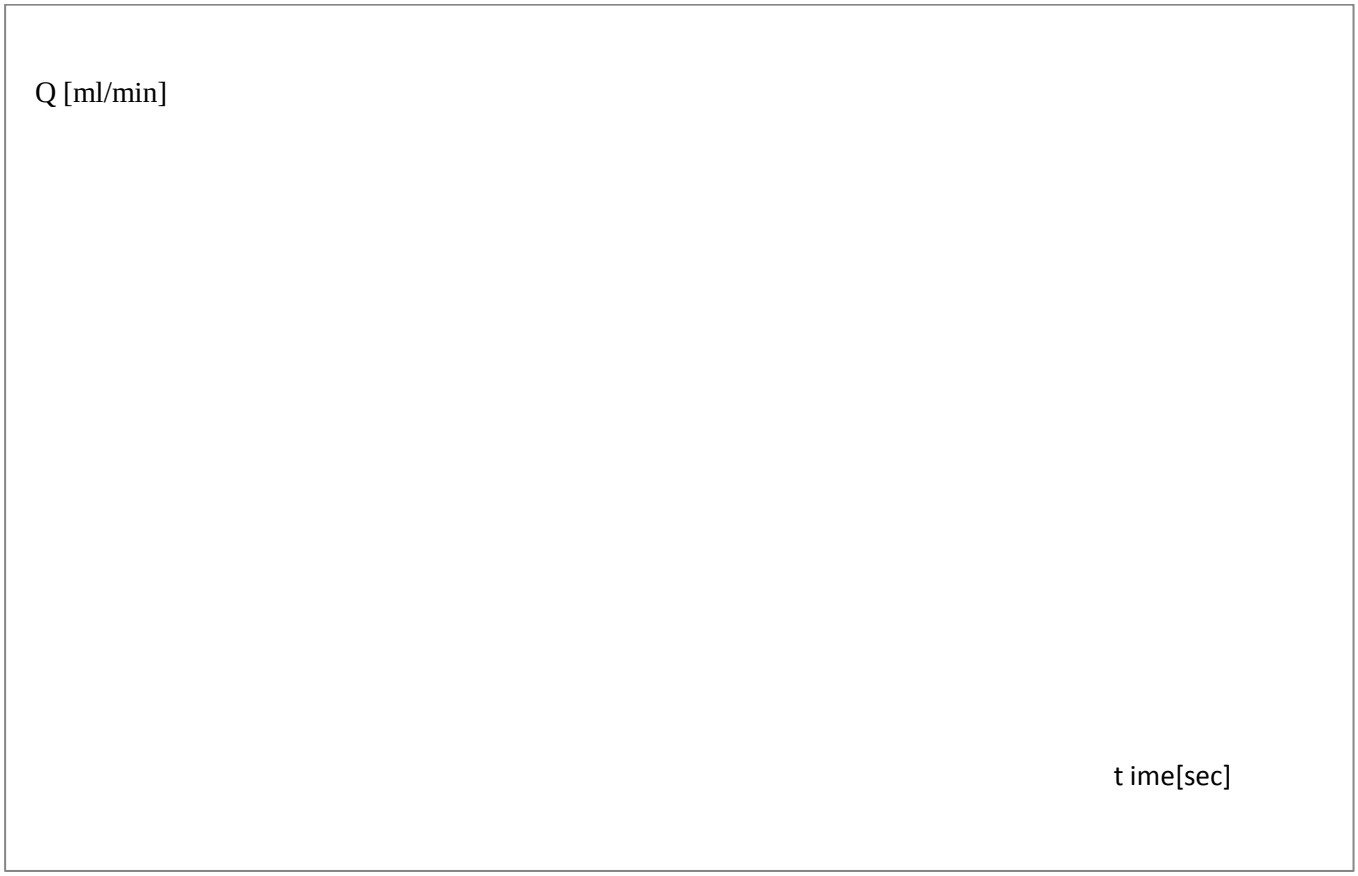

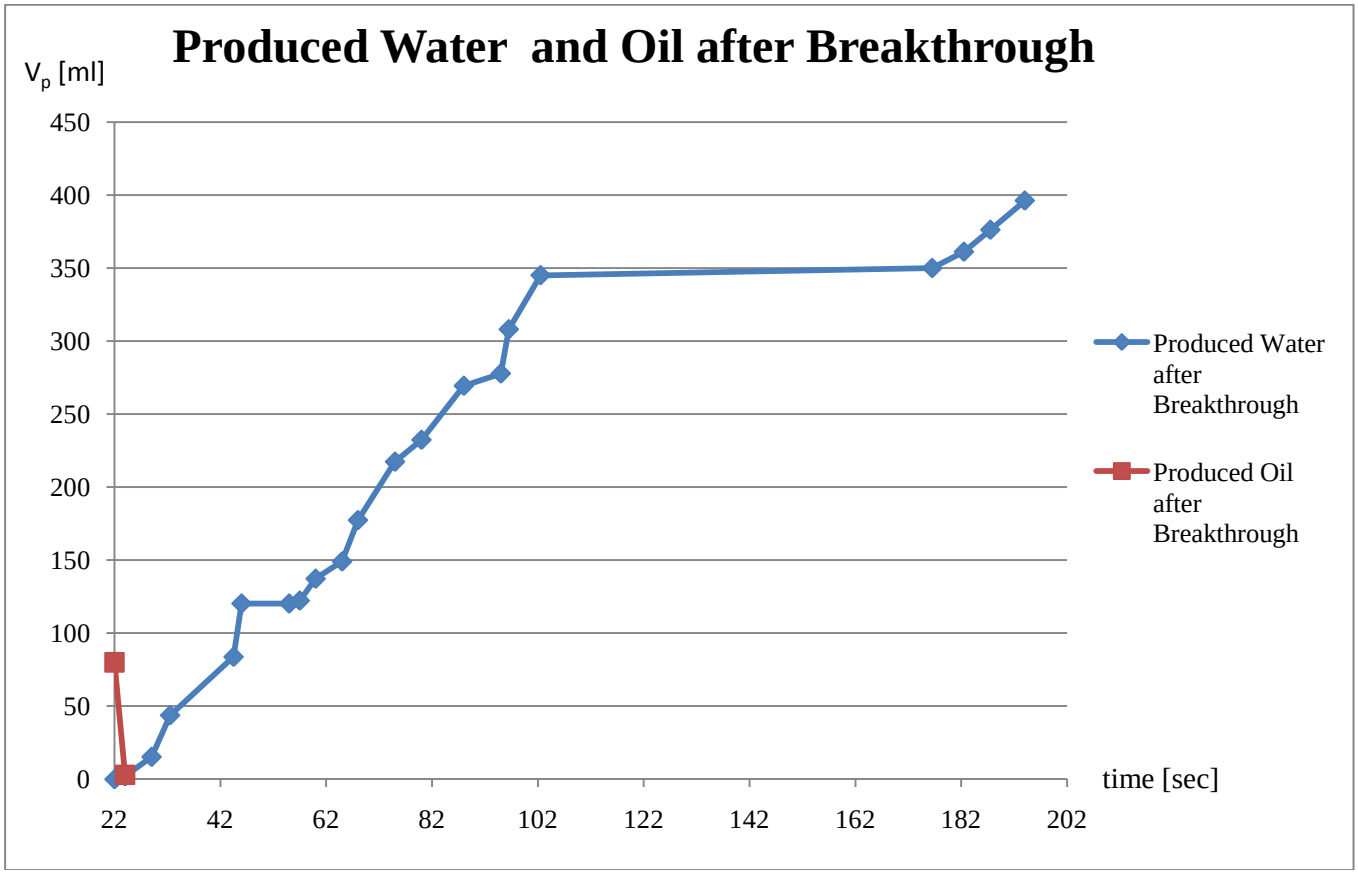

Production Rate Decline

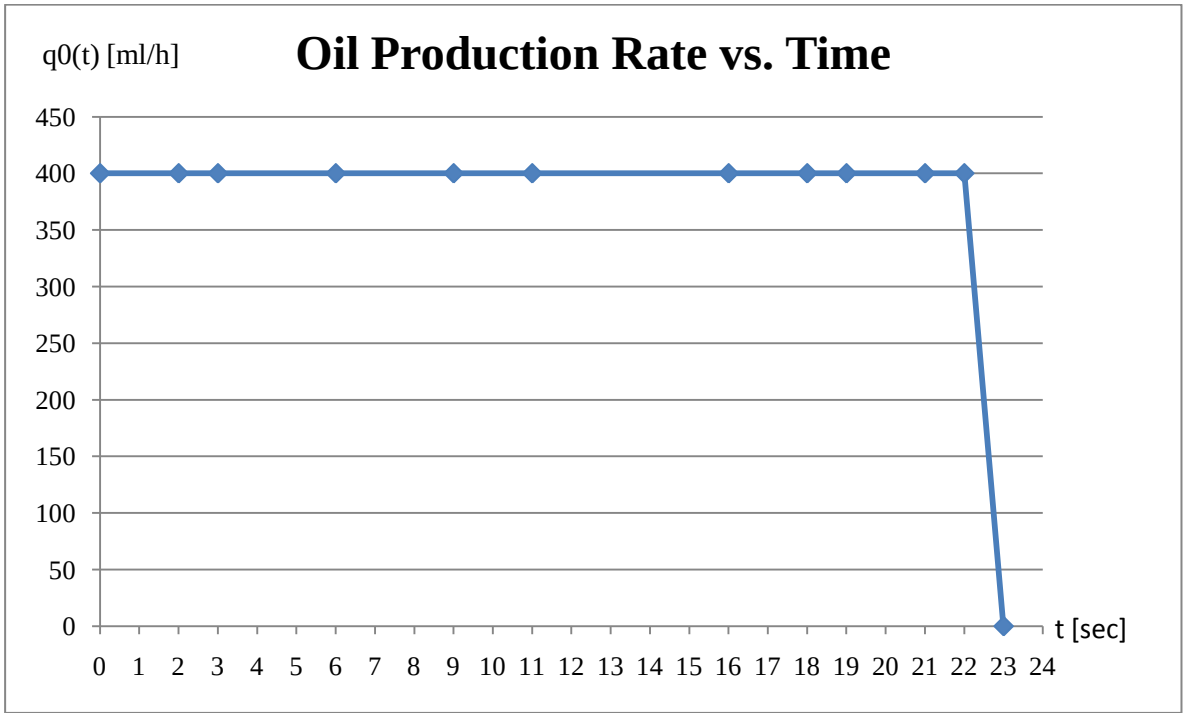
Oil Production Rate vs. Time
q0(t) [ml/h]
450
400
350
300
250
200
150
100
50
0
0 1 2 3 4 5 6 7 8 9 10 11 12 13 14 15 16 17 18 19 20 21 22 23 24
t [sec]

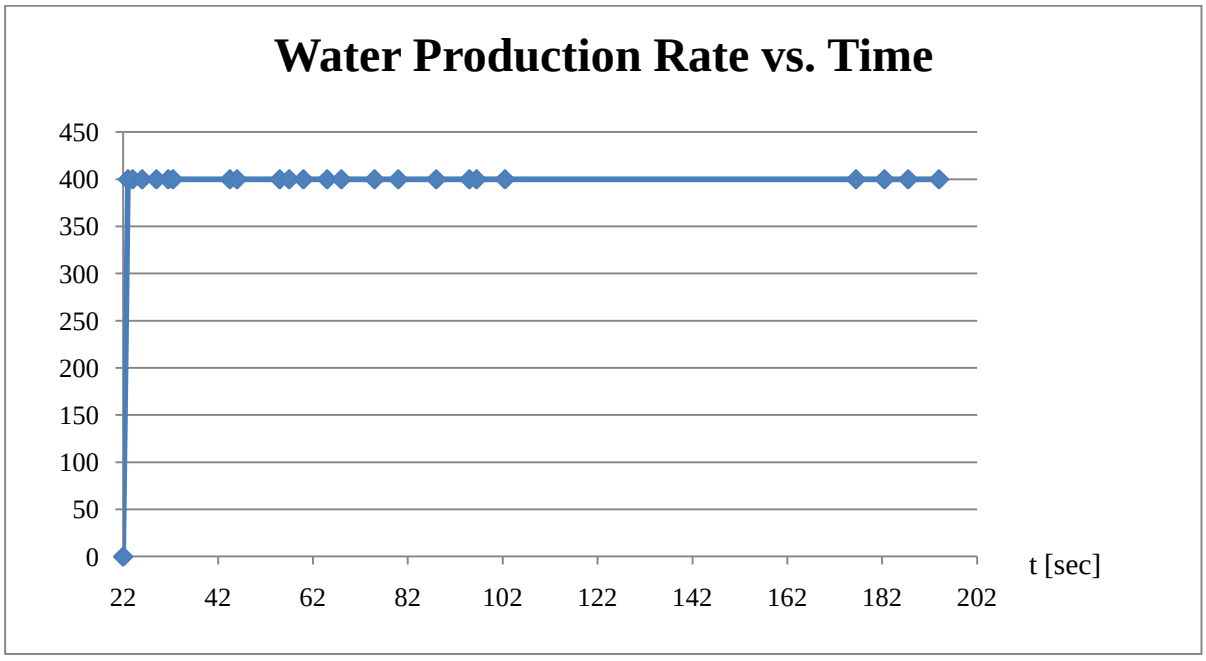
Water Production Rate vs. Time
450
400
350
300
250
200
150
100
50
0
22 42 62 82 102 122 142 162 182 202
t [sec]

APPENDIX F - GOAL SEEK

Input data for Goal Seek to calculate pressure drop, flow rates for the different inlet tubes and total flow rate.

Input data:		
Lap, [m]:	0,965	*Length from A to Perforation*
Lbp, [m]:	0,765	*Length from B to Perforation*
Lcp, [m]:	0,560	*Length from C to Perforation*
Ldp, [m]:	0,390	*Length from D to Perforation*
Lep, [m]:	0,170	*Length from E to Perforation*
H, [m]:	0,300	*Height of pipe*
Dpipe, [m]:	0,00635	*ID pipe*
Wgravel, [m]:	0,0150	*Width of gravel pack*
Hgravel, [m]:	0,0150	*Height of gravel pack*
Permeability, [m2]:	5,15E-11	*NB! Assumed to be constant*
Pinn_vann, [Pa]:	47 000	*Inlet pressure (gauge)*
Pinn_olje, [Pa]:	47 000	*Inlet pressure (gauge)*
P_ut, [Pa]:	0	*Discharge pressure (gauge)*
g, [m/s2]:	9,81	*Gravity*
ρ_vann, [kg/m3]:	991,41	*Density water*
ρ_olje, [kg/m3]:	847,38	*Density oil*
μ_vann, [Pas]:	1,260E-03	*Viscosity water*
μ_olje, [Pas]:	2,720E-02	*Viscosity oil*
Calculations:		
A_pipe, [m]:	3,17E-05	*Area pipe*
A_gravel, [m]:	2,25E-04	*Area gravel pack*
V_water_pipe_a, [m/s]:	0,001	*Fluind velocinty in pipe a*
V_water_gravel_ap, [m/s]:	0,000	*Fluind velocinty in gravel from a-p*
V_oil_pipe_b, [m/s]:	0,001	*Fluind velocinty in pipe b*
V_oil_gravel_bp, [m/s]:	0,000	*Fluind velocinty in gravel from b-p*
V_oil_pipe_c, [m/s]:	0,001	*Fluind velocinty in pipe c*
V_oil_gravel_cp, [m/s]:	0,000	*Fluind velocinty in gravel from c-p*
V_oil_pipe_d, [m/s]:	0,002	*Fluind velocinty in pipe d*
V_oil_gravel_dp, [m/s]:	0,000	*Fluind velocinty in gravel from d-p*
V_oil_pipe_e, [m/s]:	0,004	*Fluind velocinty in pipe e*
V_oil_gravel_ep, [m/s]:	0,000	*Fluind velocinty in gravel from e-p*

Re_water:	3,07E+00	*Reynolds number water*
Re_oil:	1,71E-02	*Reynolds number oil*
f_water:	1,92E-01	*Friction factor water*
f_oil:	1,07E-03	*Friction factor oil*
DP_h_water, [Pa]:	2 918	*Hydrostatic pressure drop - water*
DP_h_oil, [Pa]:	2 494	*Hydrostatic pressure drop - oil*
DP_f_water_a, [Pa]:	0	*Friction based pressure drop water*
DP_f_oil_b, [Pa]:	0	*Friction based pressure drop olje - pipe b*
DP_f_oil_c, [Pa]:	0	*Friction based pressure drop olje - pipe c*
DP_f_oil_d, [Pa]:	0	*Friction based pressure drop olje - pipe d*
DP_f_oil_e, [Pa]:	0	*Friction based pressure drop olje - pipe e*
DP_d_water_ap, [Pa]:	44 082	*Darcy pressure drop "water" a-p*
DP_d_oil_bp, [Pa]:	44 506	*Darcy pressure drop oil b-p*
DP_d_oil_cp, [Pa]:	44 506	*Darcy pressure drop oil c-p*
DP_d_oil_dp, [Pa]:	44 506	*Darcy pressure drop oil d-p*
DP_d_oil_ep, [Pa]:	44 506	*Darcy pressure drop oil e-p*
Dp_a-p, [Pa]:	47 000	*Calculated pressure drop*
Dp_b-p, [Pa]:	47 000	*Calculated pressure drop*
Dp_c-p, [Pa]:	47 000	*Calculated pressure drop*
Dp_d-p, [Pa]:	47 000	*Calculated pressure drop*
Dp_e-p, [Pa]:	47 000	*Calculated pressure drop*
Dp_a-p, [Pa]:	47 000	*"Real" pressure drop*
Dp_b-p, [Pa]:	47 000	*"Real" pressure drop*
Dp_c-p, [Pa]:	47 000	*"Real" pressure drop*
Dp_d-p, [Pa]:	47 000	*"Real" pressure drop*
Dp_e-p, [Pa]:	47 000	*"Real" pressure drop*

(assumes that oil will flow through gravel pack
until water break through - oil viscosity is therefore used)

q_"water"_a-p:	1,9E-08 m3/s	1,2E-06 m3/min	1,2 milliliter / min	*OK - 'Goal Seek' is used to verify calculation*
q_oil_b-p:	2,5E-08 m3/s	1,5E-06 m3/min	1,5 milliliter / min	*OK - 'Goal Seek' is used to verify calculation*
q_oil_c-p:	3,4E-08 m3/s	2,0E-06 m3/min	2,0 milliliter / min	*OK - 'Goal Seek' is used to verify calculation*
q_oil_d-p:	4,9E-08 m3/s	2,9E-06 m3/min	2,9 milliliter / min	*OK - 'Goal Seek' is used to verify calculation*
q_oil_e-p:	1,1E-07 m3/s	6,7E-06 m3/min	6,7 milliliter / min	*OK - 'Goal Seek' is used to verify calculation*

Result - Qtot: 14,3 milliliter / min

APPENDIX G - VISUALIZATION OF DISPLACEMENT IN HORIZONTAL GRAVEL PACK

Figure G- 1 Visualization of displacement

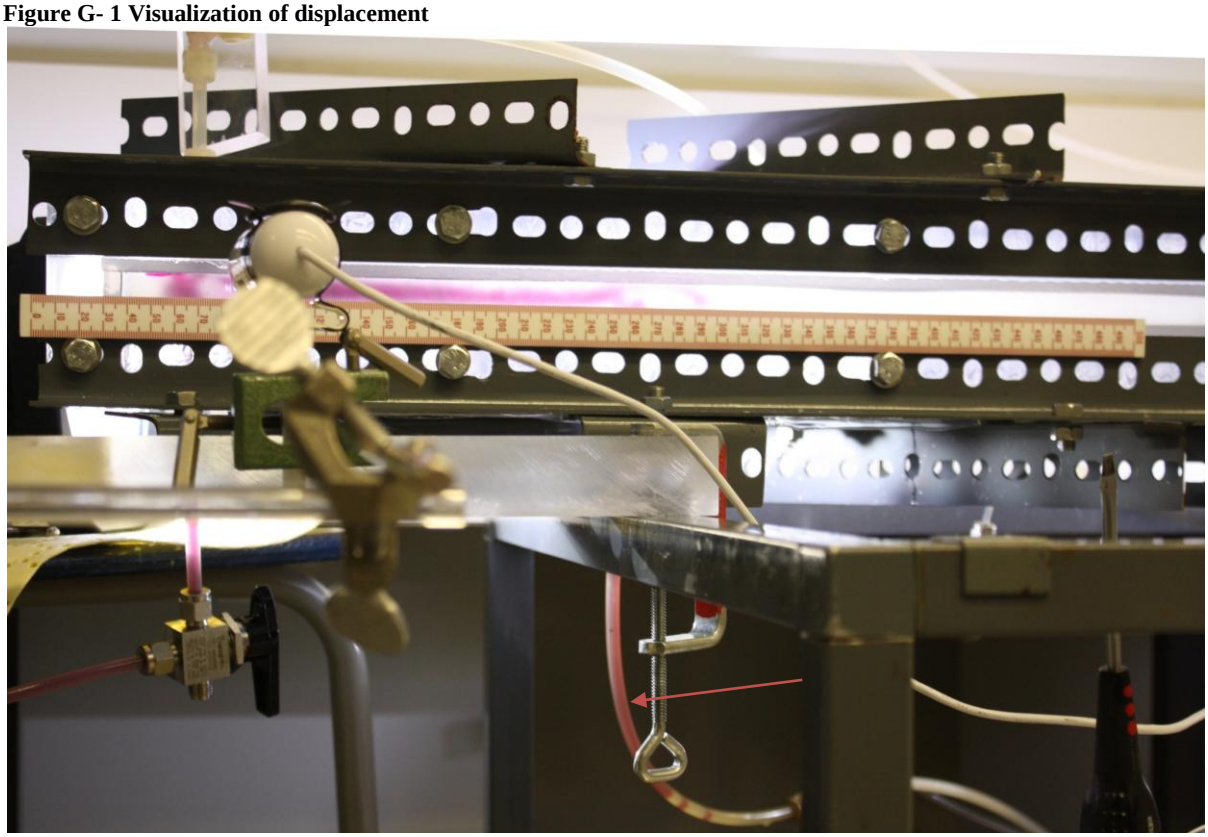

10. June 2010, 10:47:12 Water has started fingering through the gravel pack.

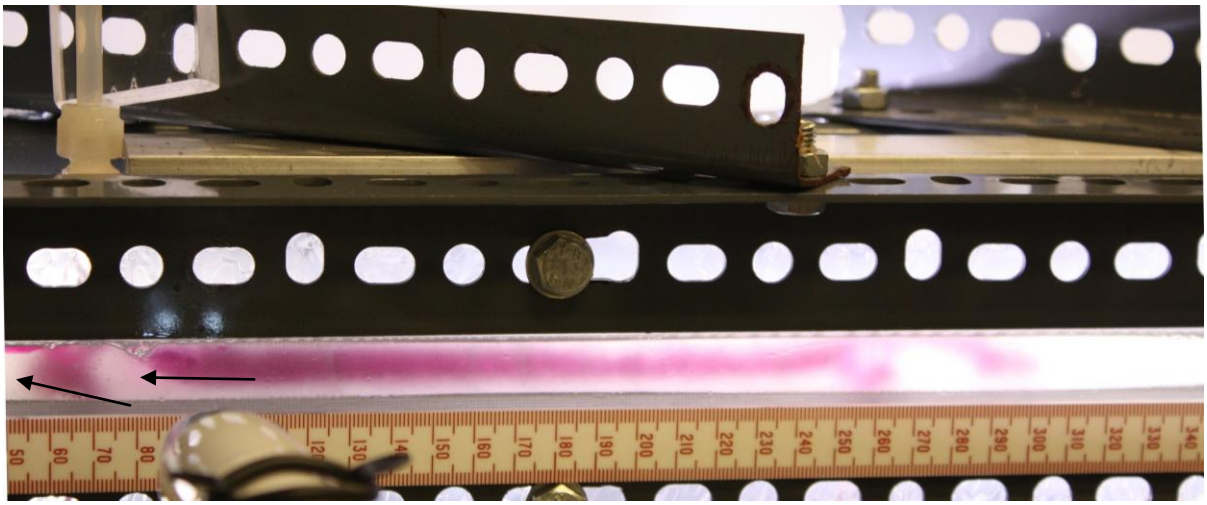

10. June 2010, 10:47

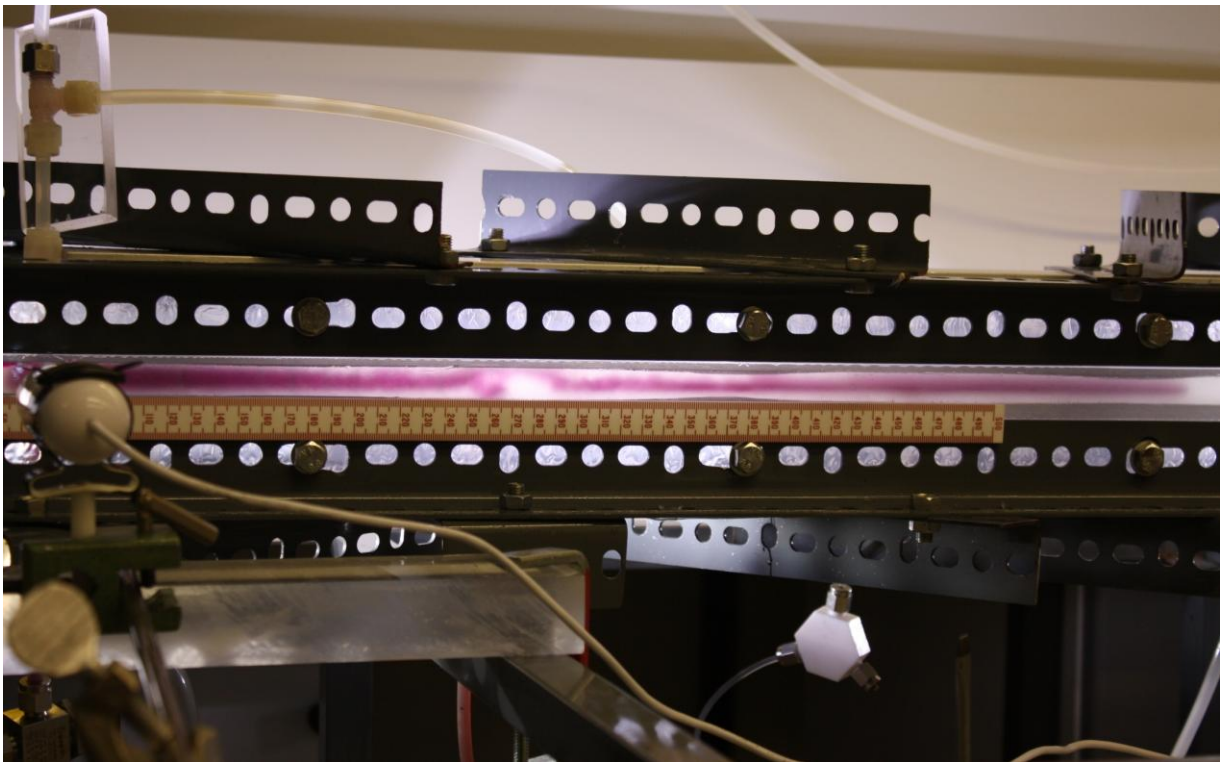

10. June 2010, 10:54:58

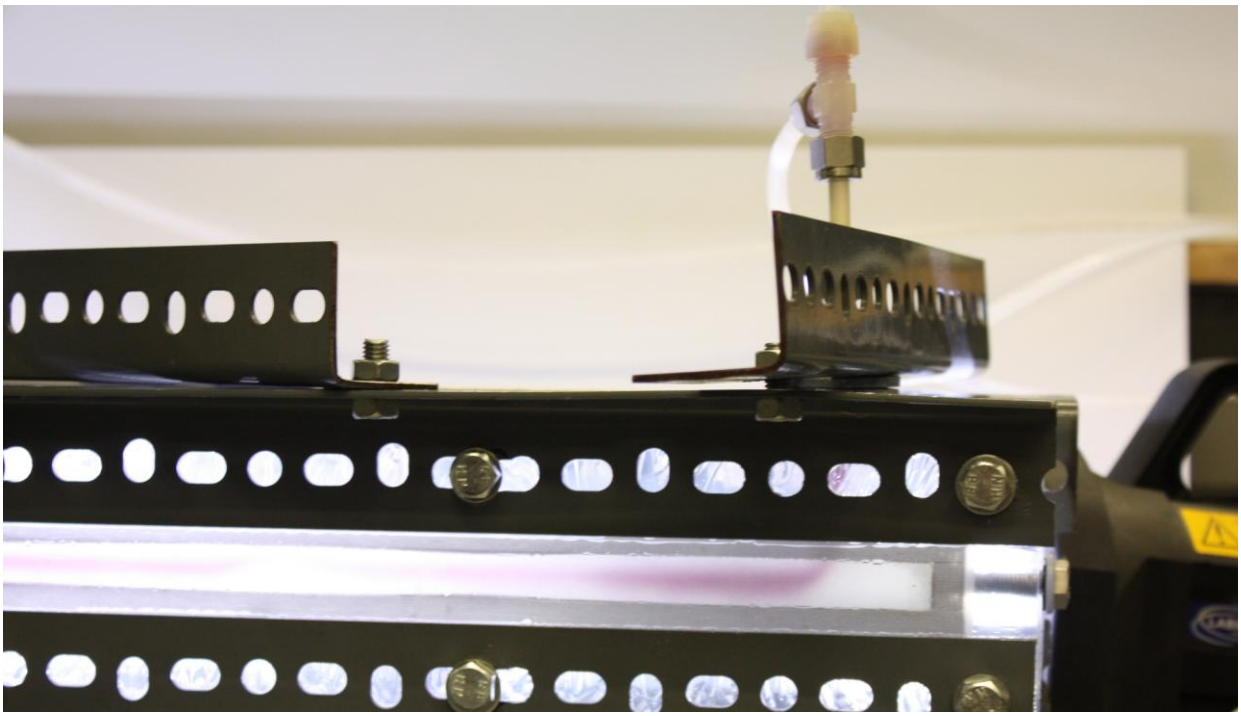

10. June 2010, 10:58:14 Breakthrough

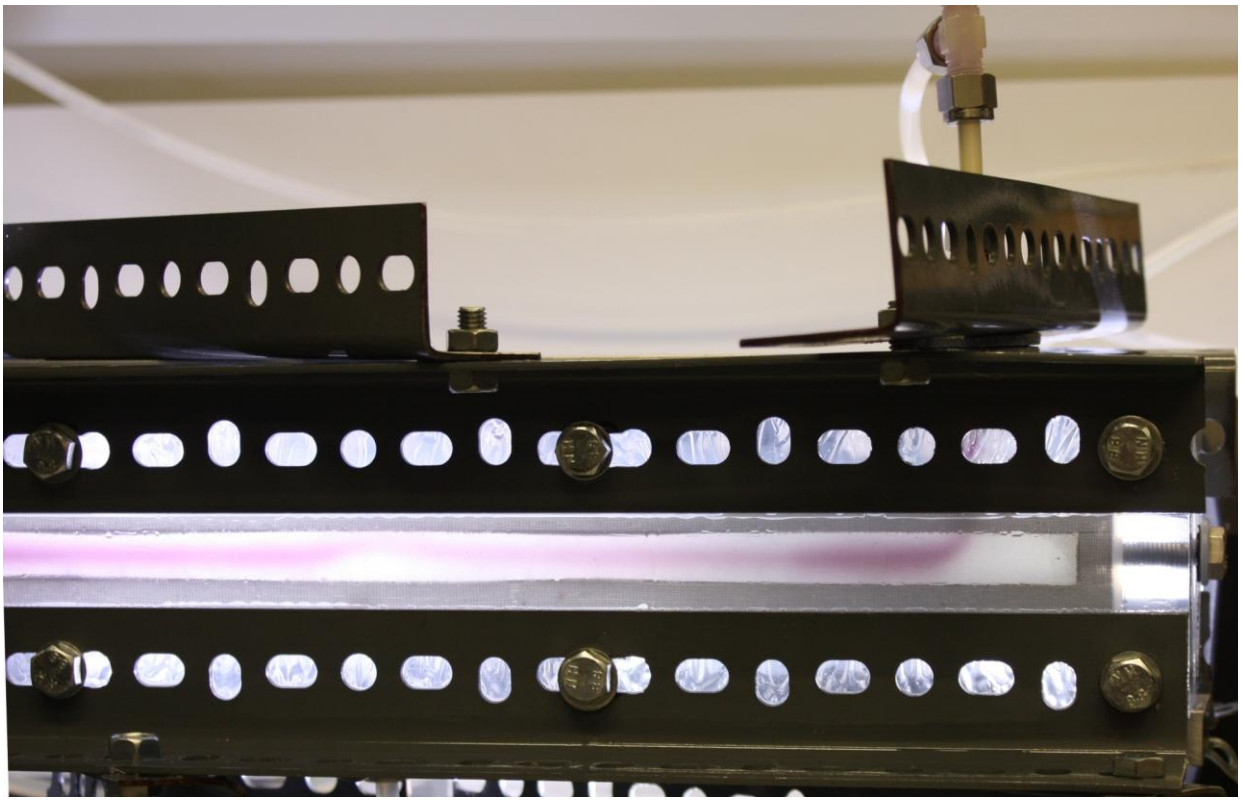

10. June 2010, 11:00:24
10. June 2010, 11:01:36

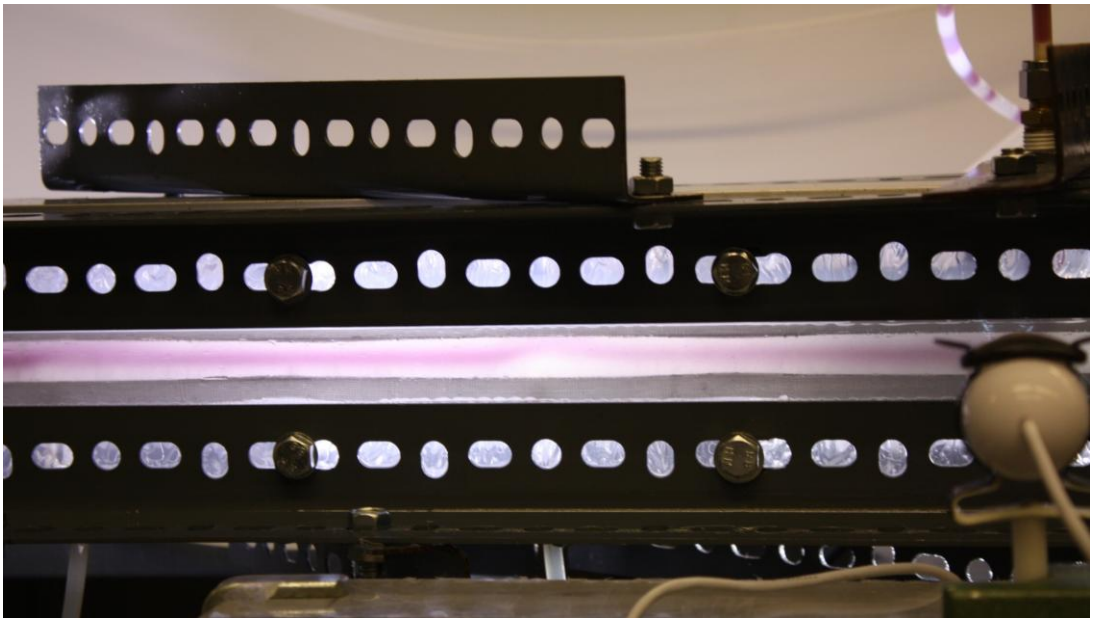

10. June 2010, 11:02:14

10. June 2010, 11:15:50

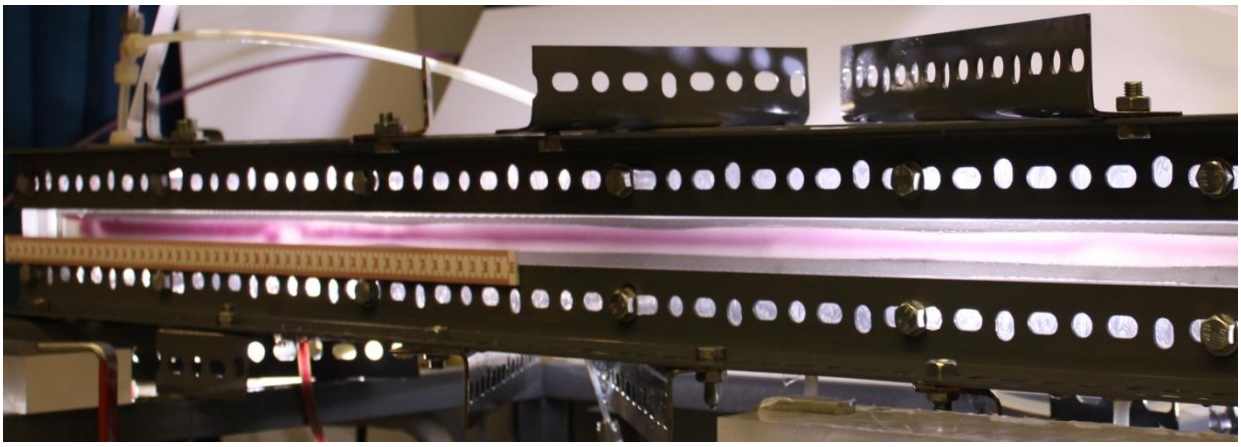

10. June 2010, 11:16:20

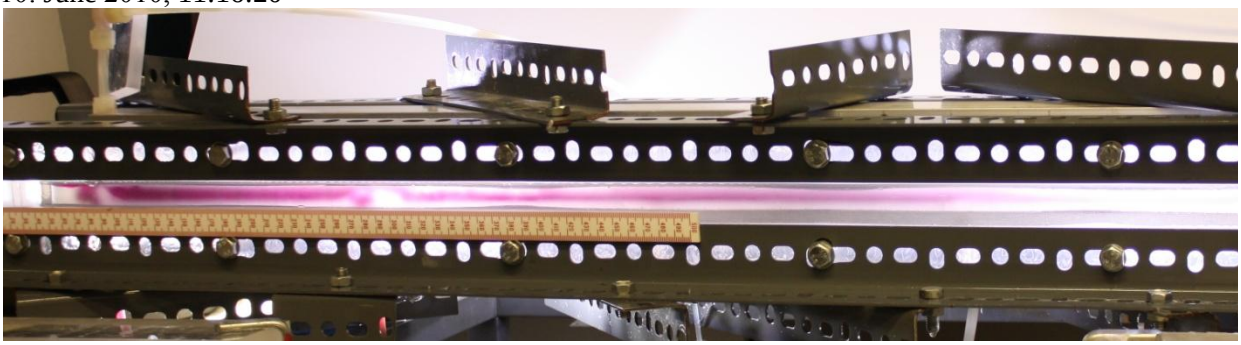

10. June 2010, 11:17:58

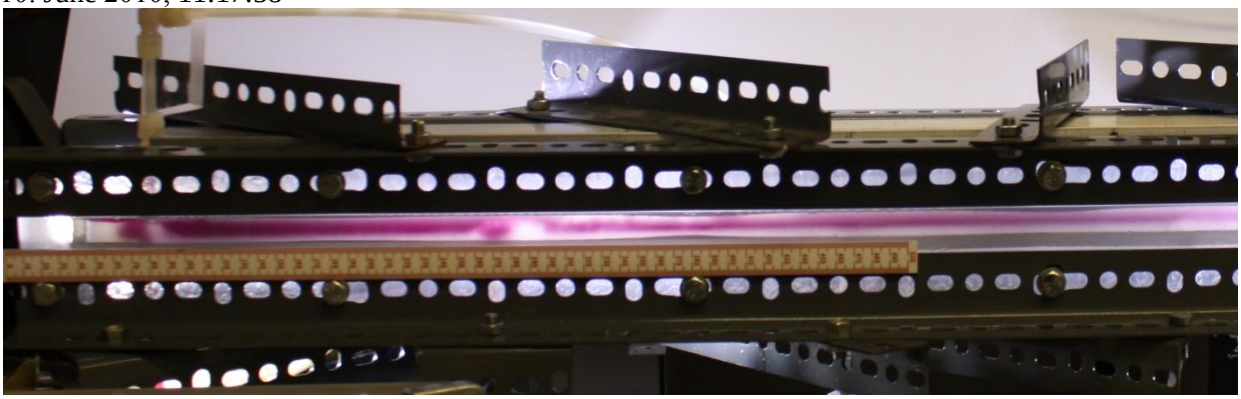

10. June 2010, 11:26:20

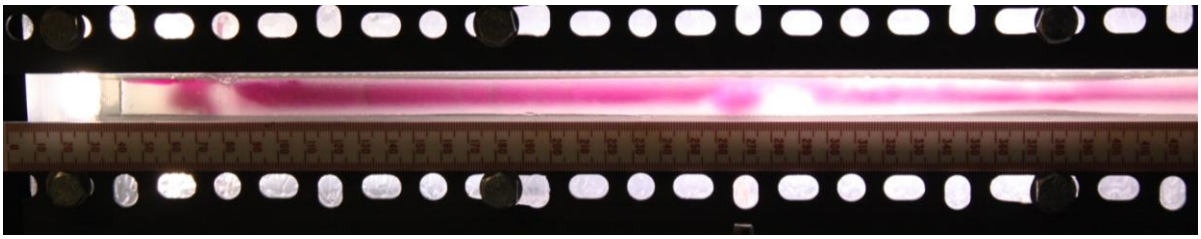

10. June 2010, 11:27:06

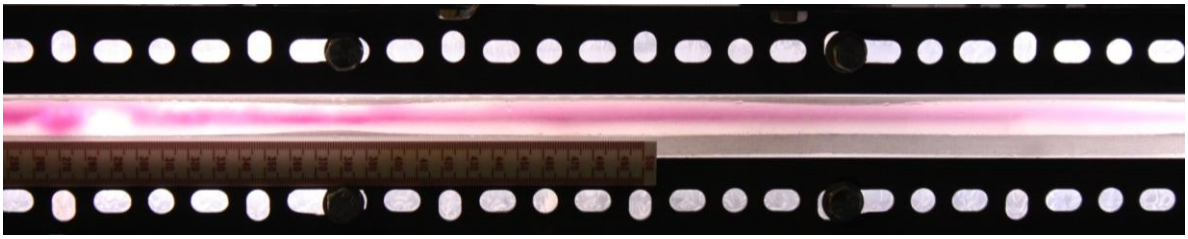

10. June 2010, 11:27:12

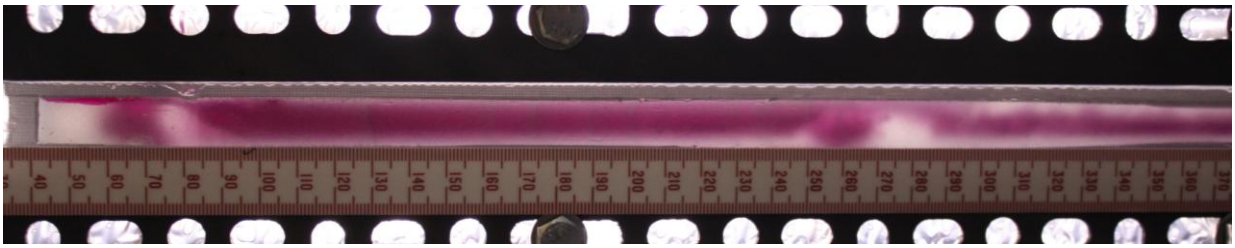

10. June 2010, 11:27:44

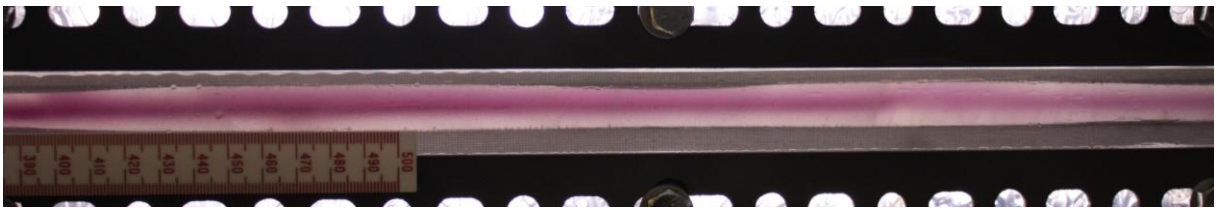

10. June 2010, 11:27:52

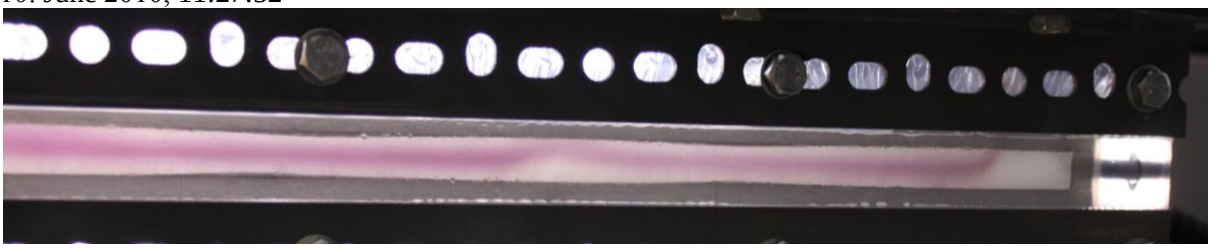

10. June 2010, 11:27:56

10. June 2010, 11:29:30

Inlet tubes from water and oil (formation)

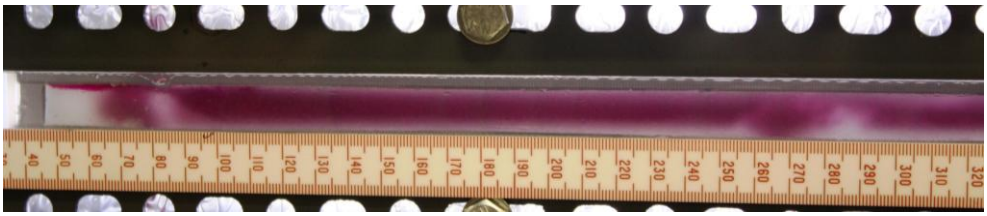

10. June 2010, 11:41:22

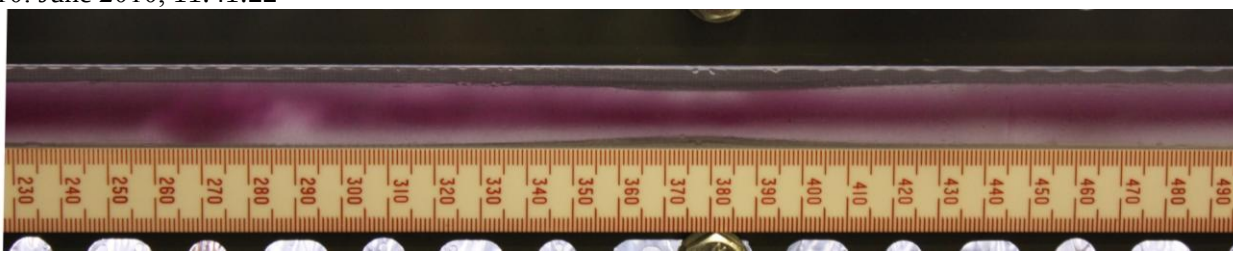

10. June 2010, 11:41:26

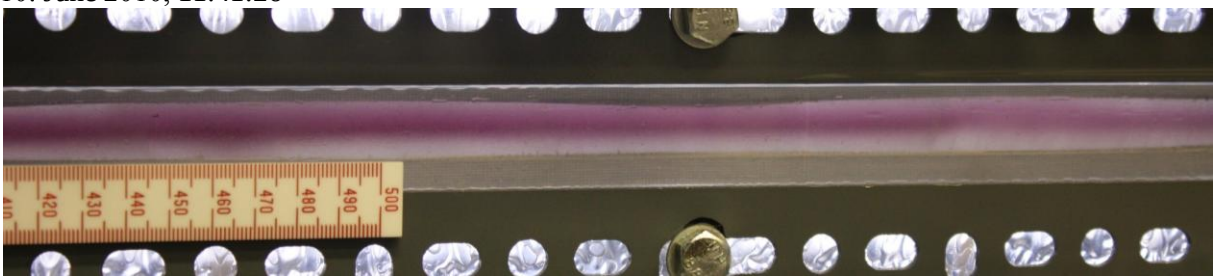

10. June 2010, 11:41:28

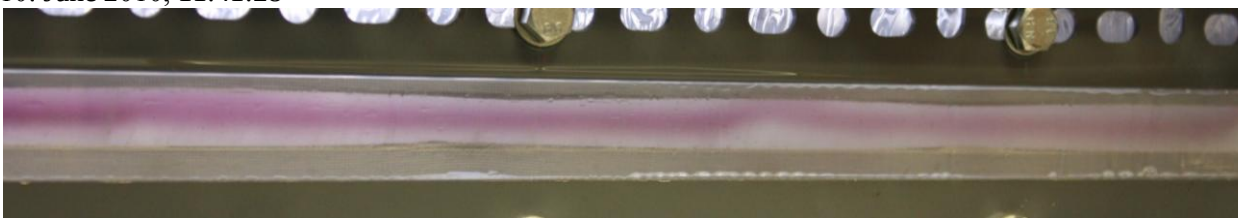

10. June 2010, 11:41:30

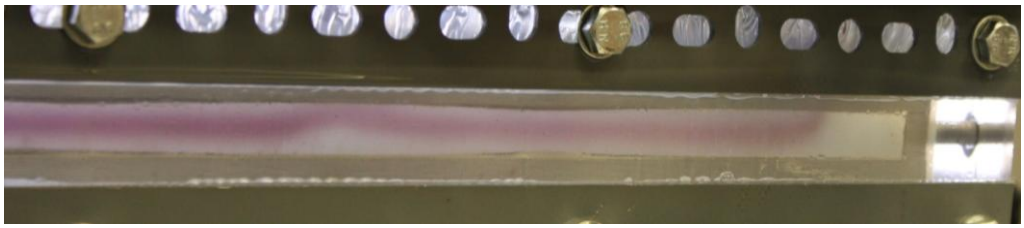

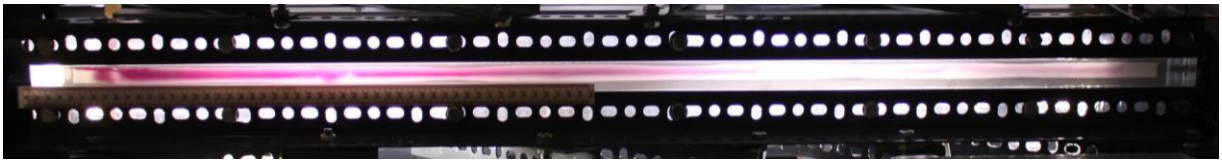

10.June 2010, 12.09

Saturation and Permeability Differences in different horizontal layers

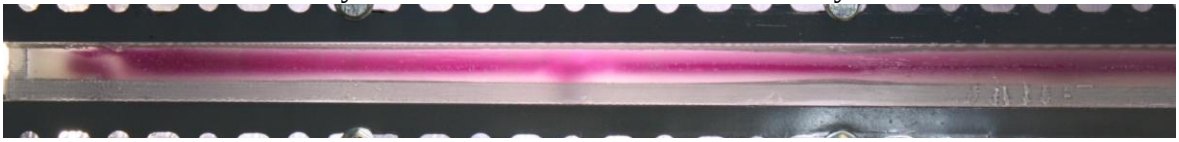

10. June 2010, 12:27:58

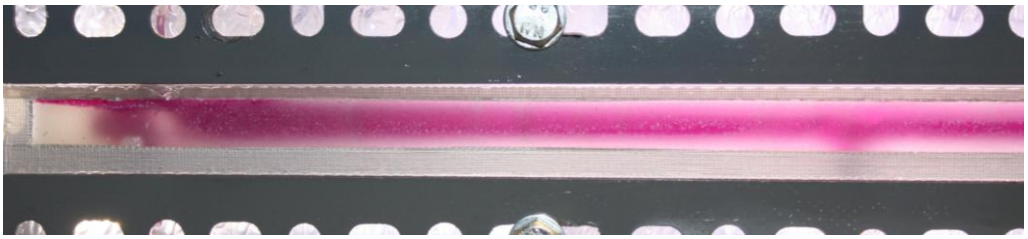

10. June 2010, 13:23:38

10. June 2010, 13:24:12

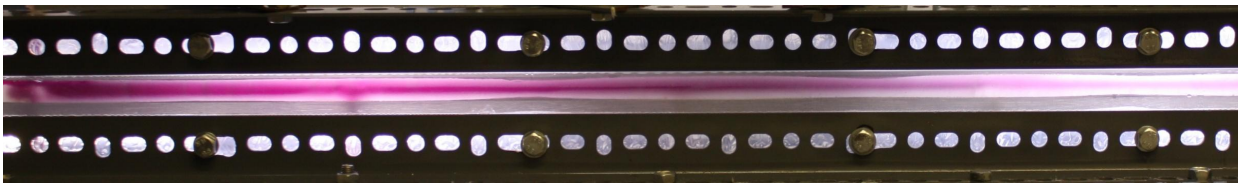

10. June 2010, 13:24:20

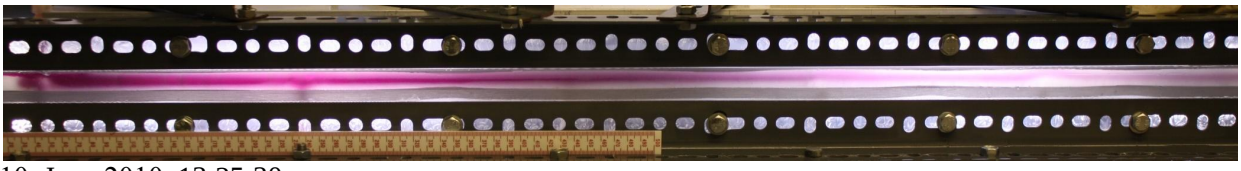

10. June 2010, 13:25:30

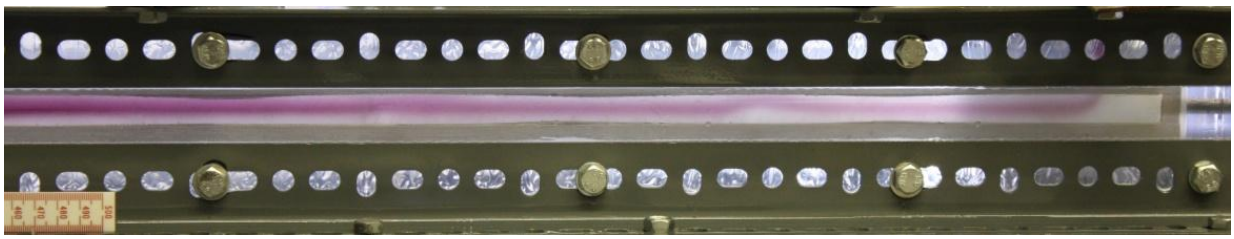

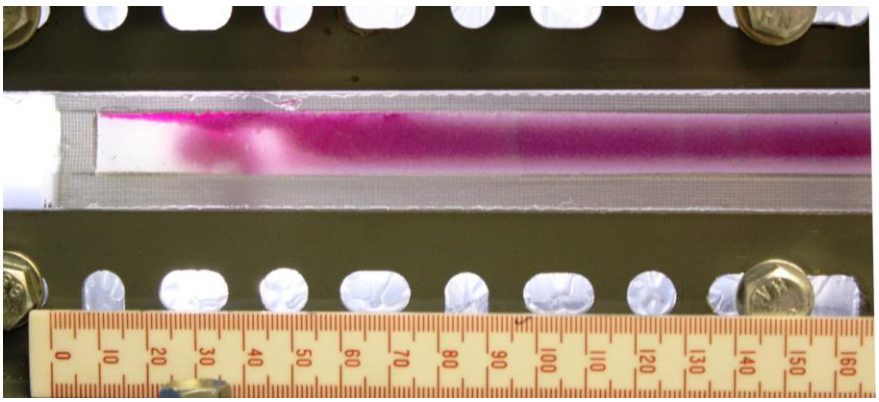

10. June 2010, 13:25:52

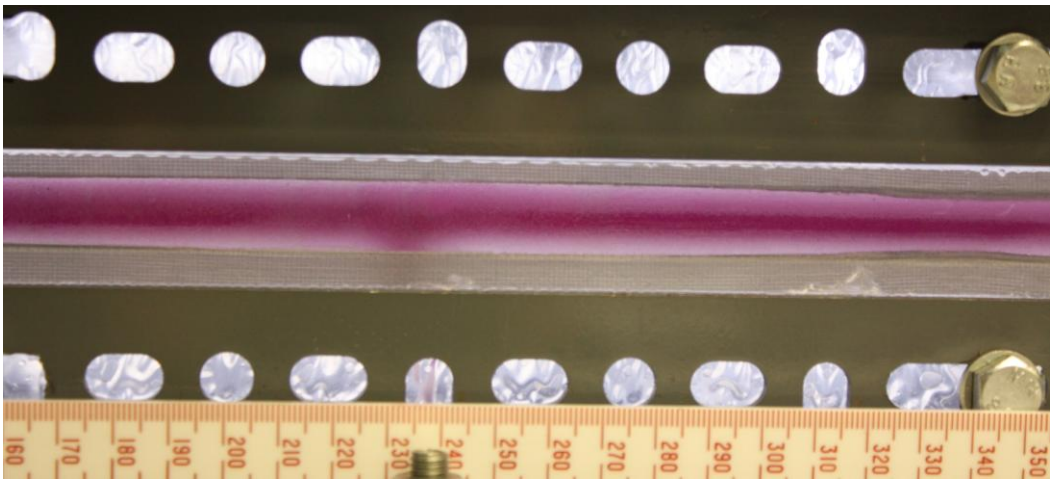

10. June 2010, 13:26:00

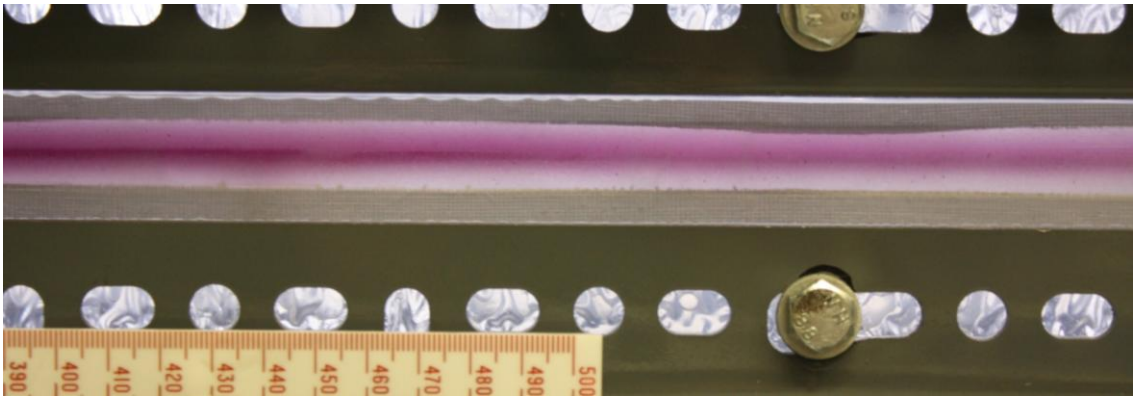

10. June 2010, 13:26:08

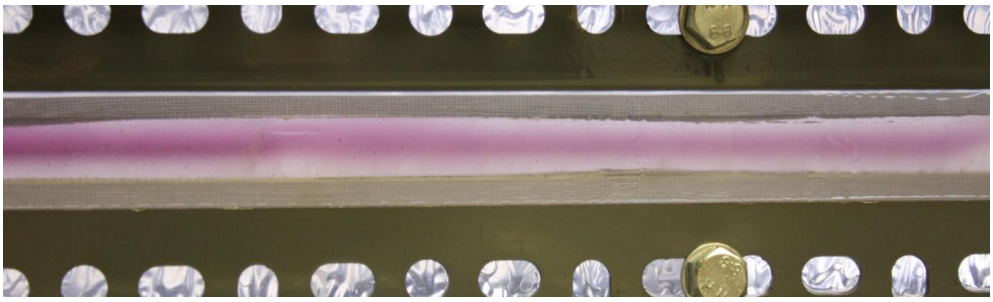
10. June 2010, 13:26:12

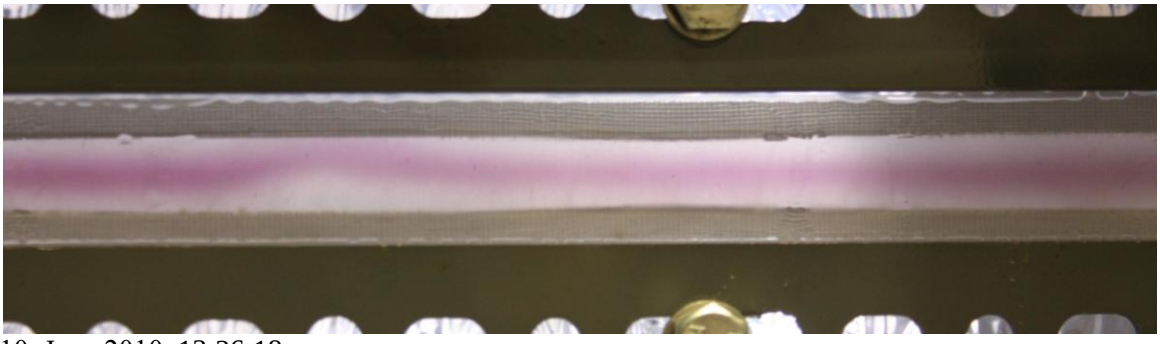
10. June 2010, 13:26:18

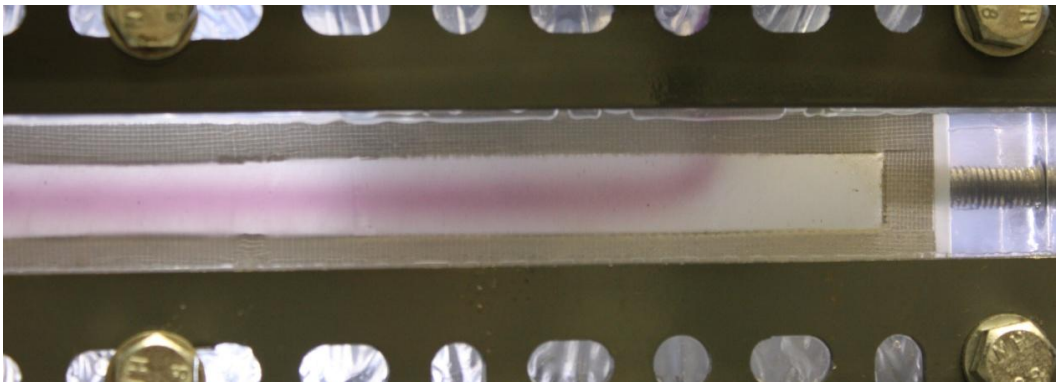

10. June 2010, 13:26:20

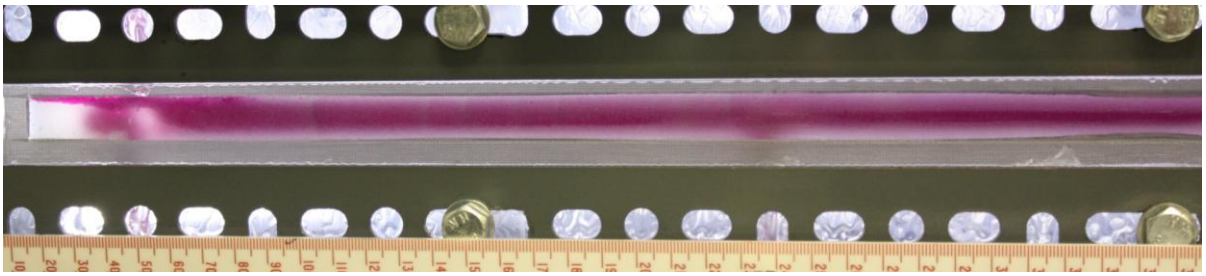

10. June 2010, 13:26:52

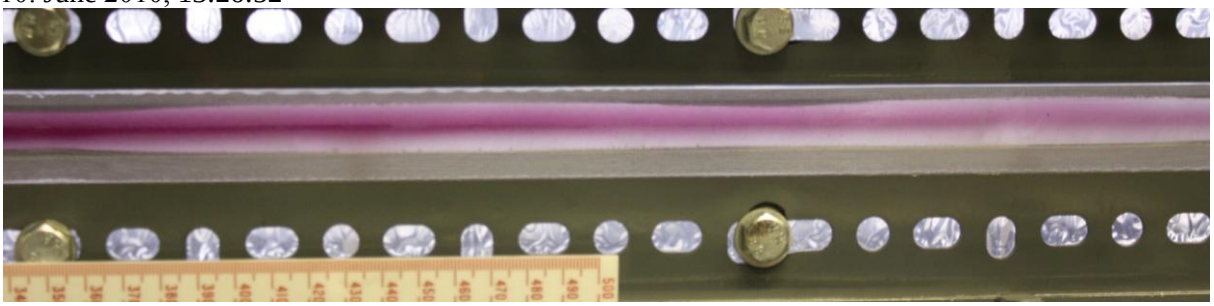

10. June 2010, 13:26:56

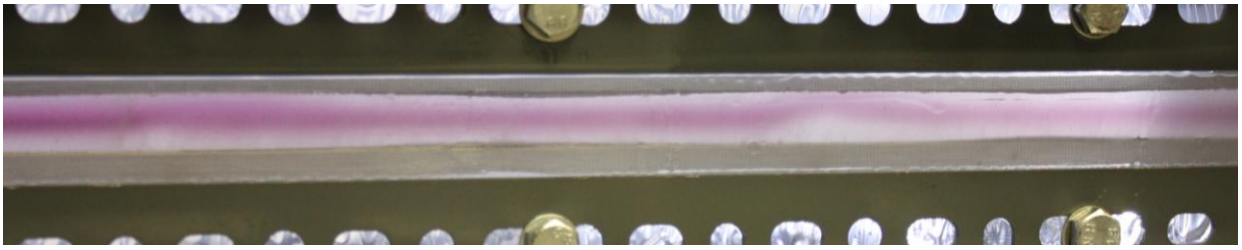

10. June 2010, 13:27:00

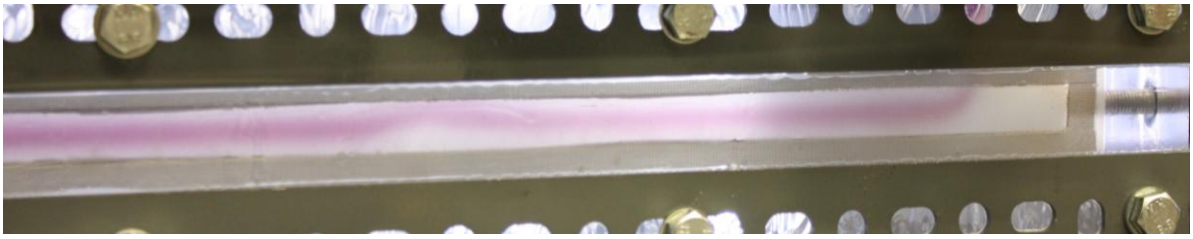

10. June 2010, 13:27:04

Small “gravitation segregation” in the production tube.

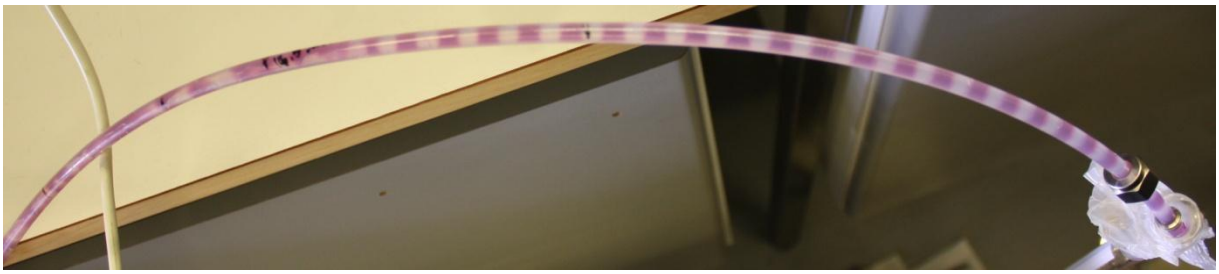

10. June 2010, 16:03:08

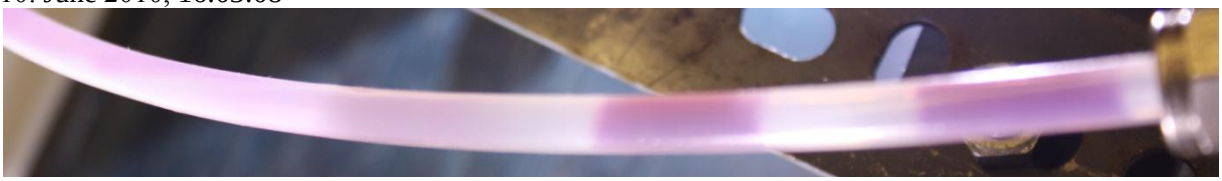

10. June 2010, 16:02:46

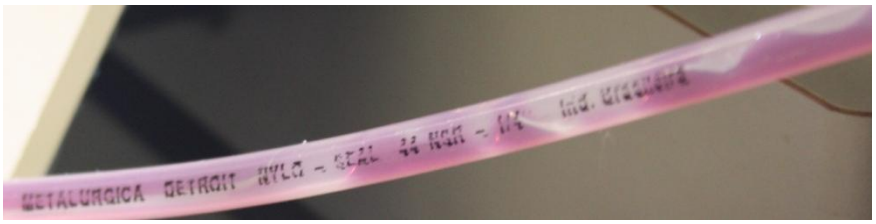

10. June 2010, 13:30:16

Vertical Permeability and Saturation Layers

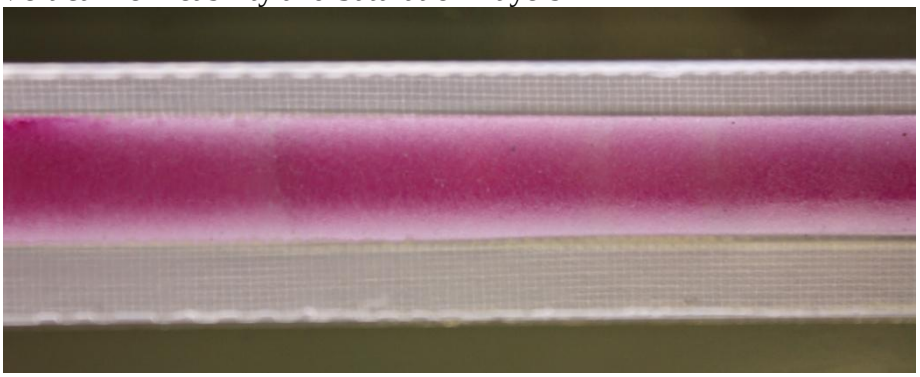

10. June 2010, 13:31:38

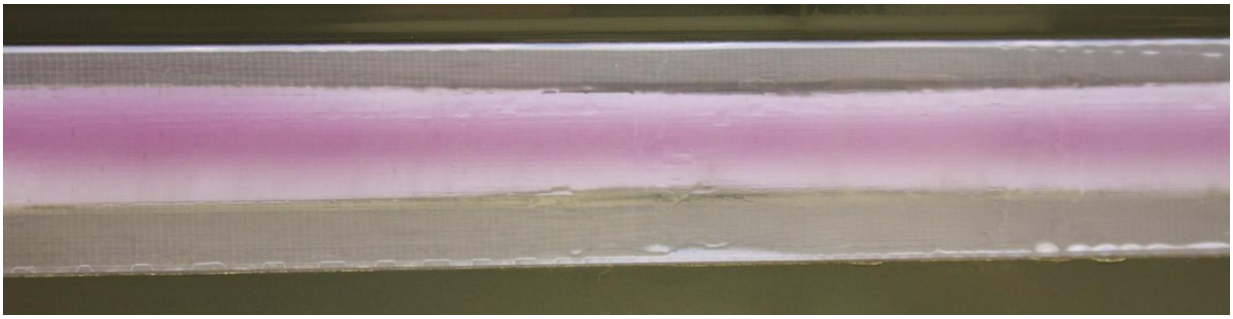

10. June 2010, 13:32:44

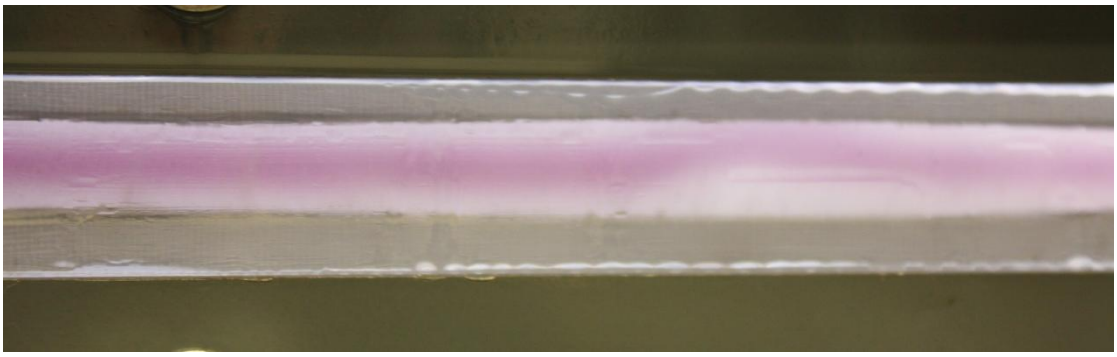

10. June 2010, 13:32:46

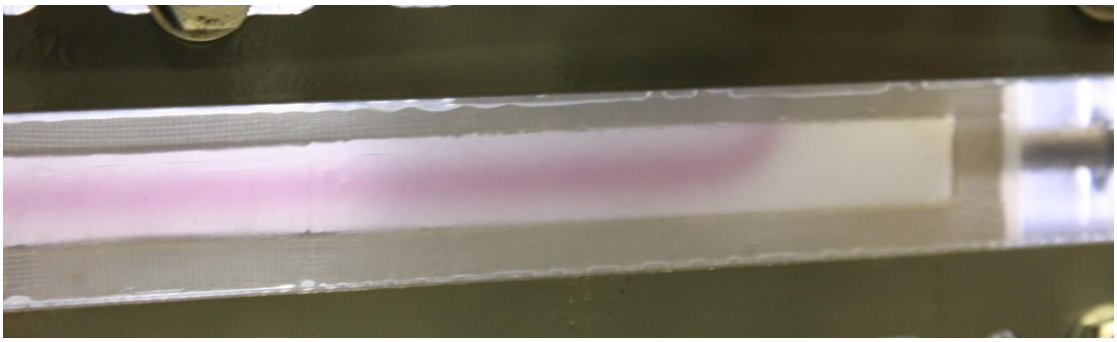

10. June 2010, 13:32:50

10. June 2010, 13:33:04

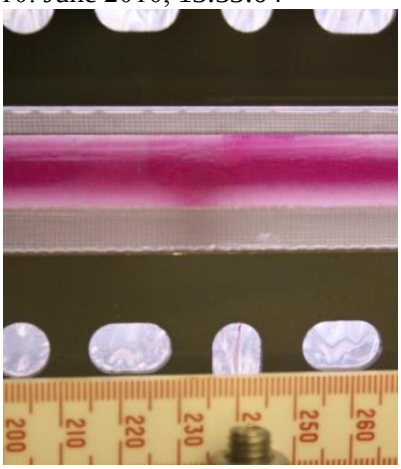

10. June 2010, 15:57:44

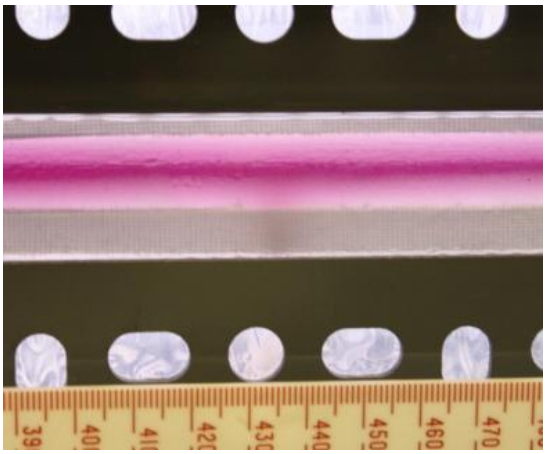

10. June 2010, 15:58:14

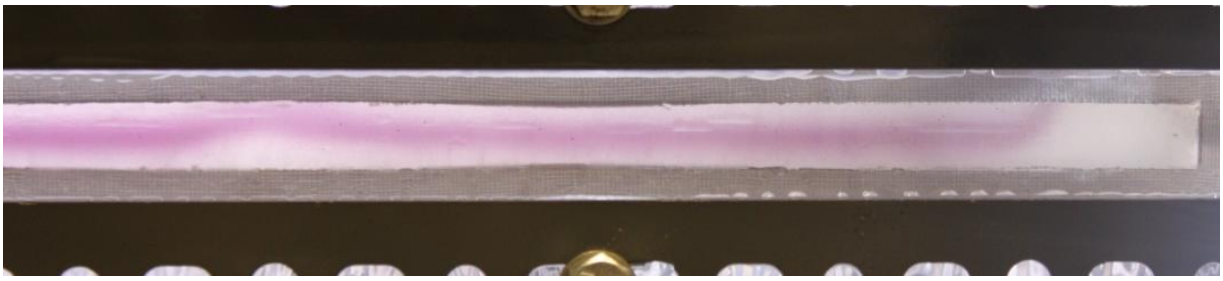

10. June 2010, 16:02:16

10. June 2010, 19:18:40

11. June 2010, 11:11:12

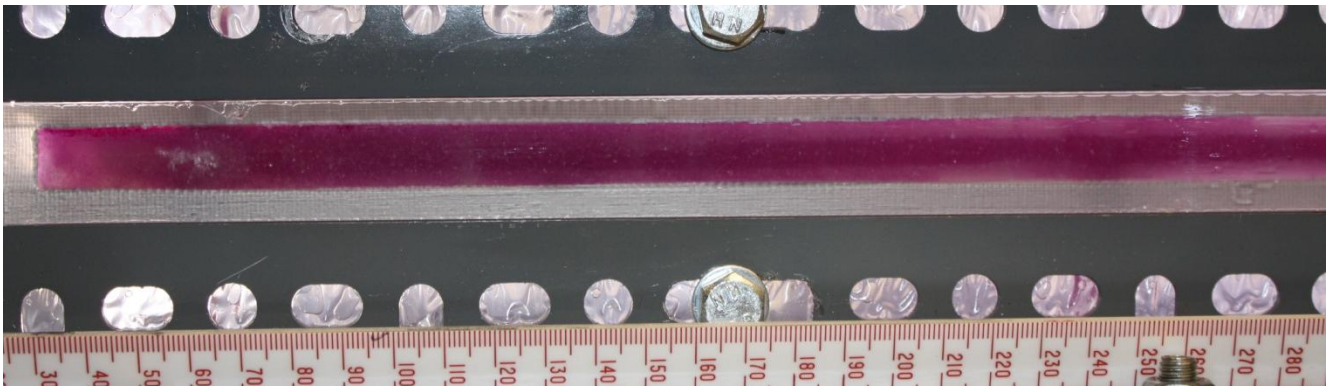

11. June 2010, 15:28:12

11. June 2010, 15:29:34

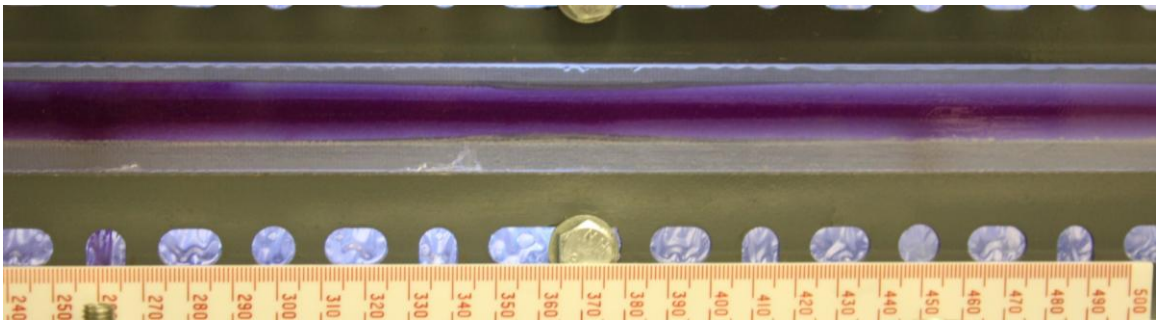

12. June 2010, 15:23:48

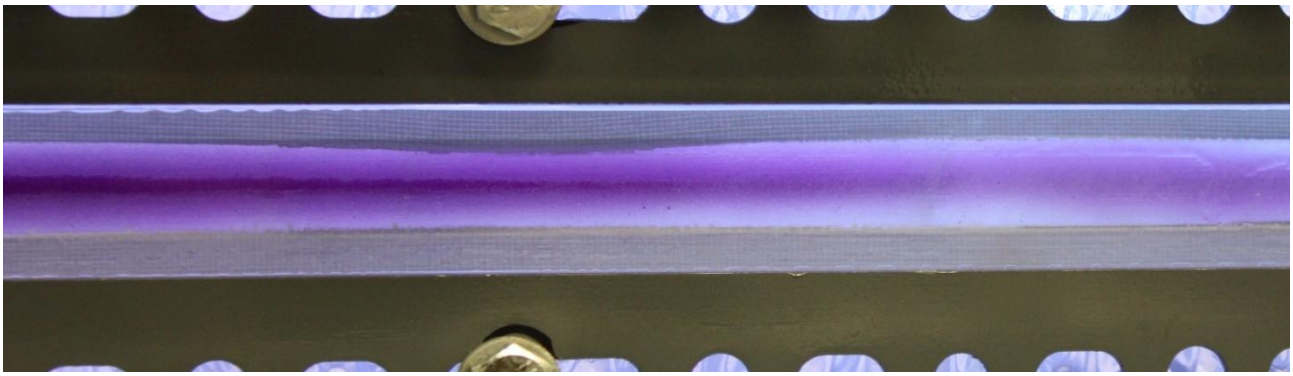

12. June 2010, 15:23:56

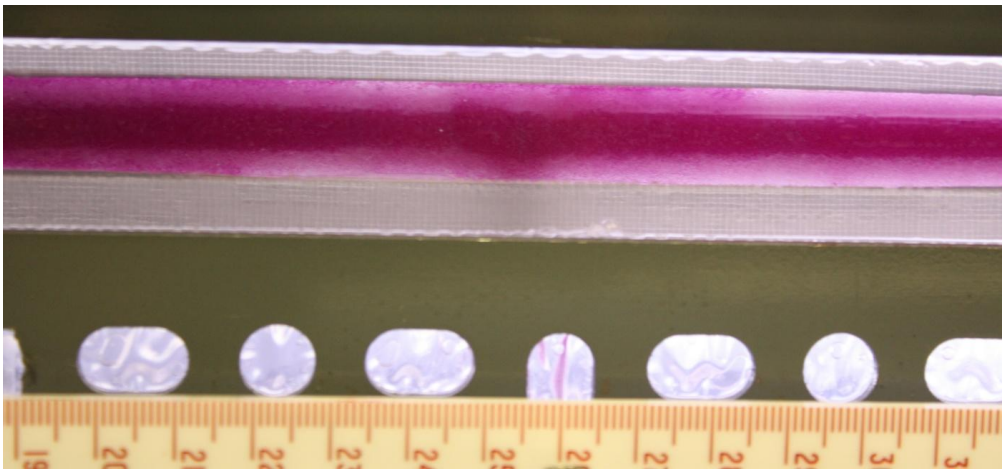

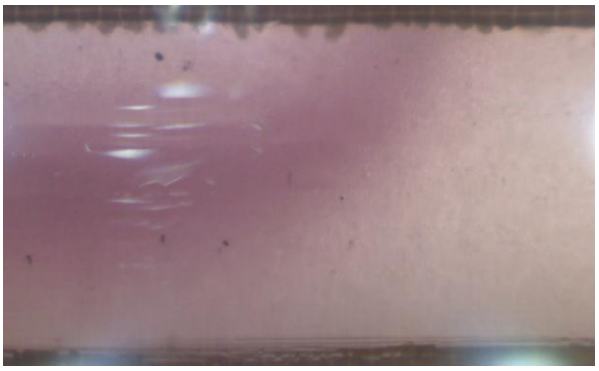

10. June 2010, 15:51:56

10. June 2010, 15:53:38

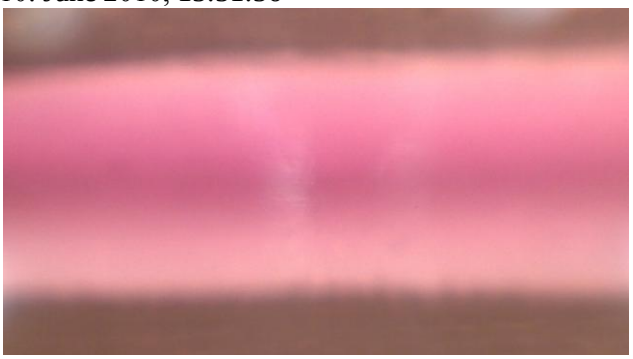

10. June 2010, 16:10:40

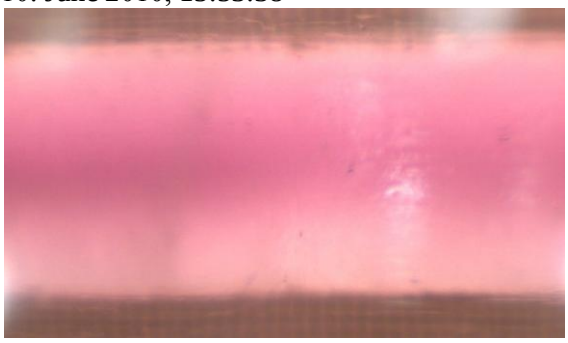

10. June 2010, 16:11:10

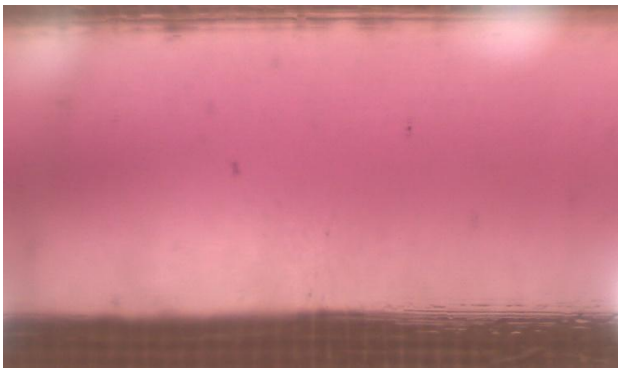

10. June 2010, 16:10:40

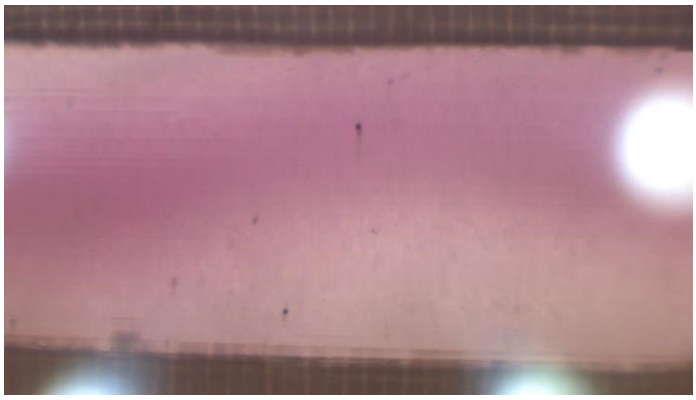

10. June 2010, 16:12:52

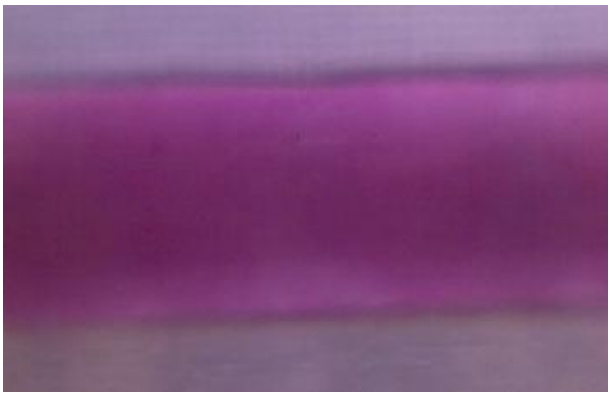

13. June 2010, 20:35:10

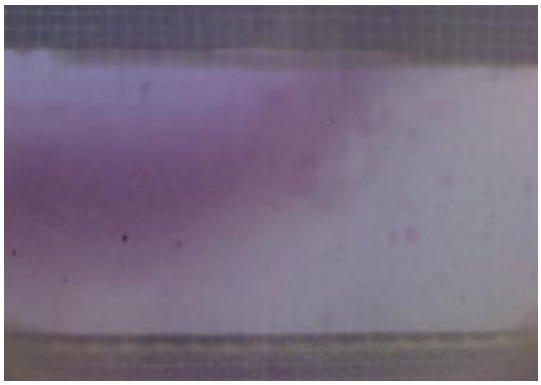

13. June 2010, 20:44:16

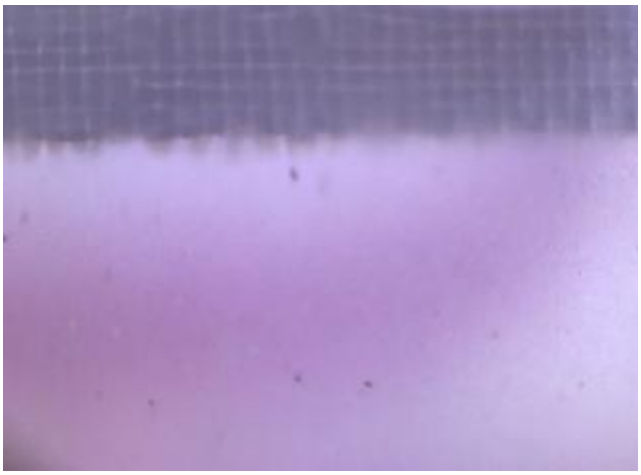

11. June 2010, 15:09:54

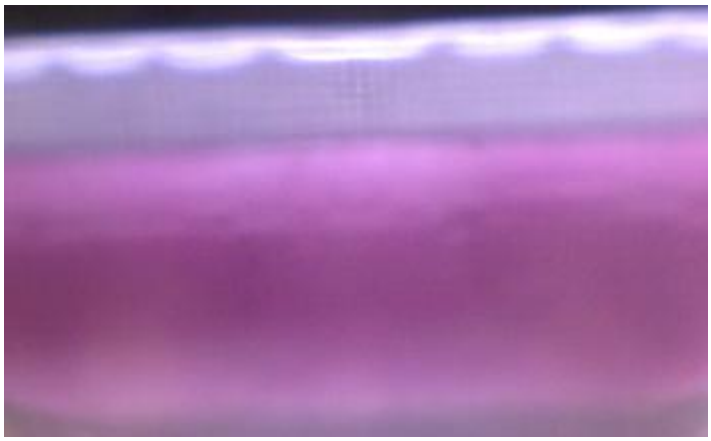

At the first oil injection tube

13. June 2010, 20:38:46 Between second and third oil injection tube

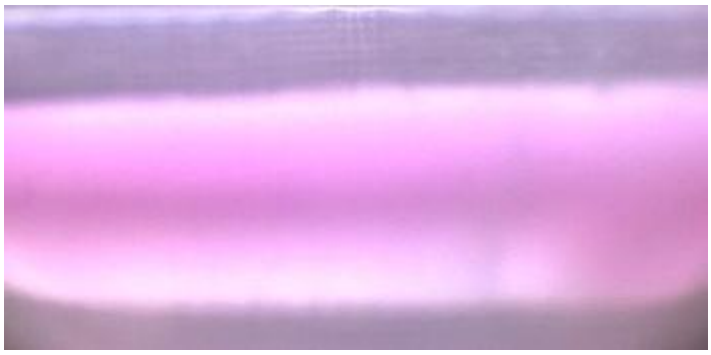

13. June 2010, 20:40:38 In between third and fourth injection tub

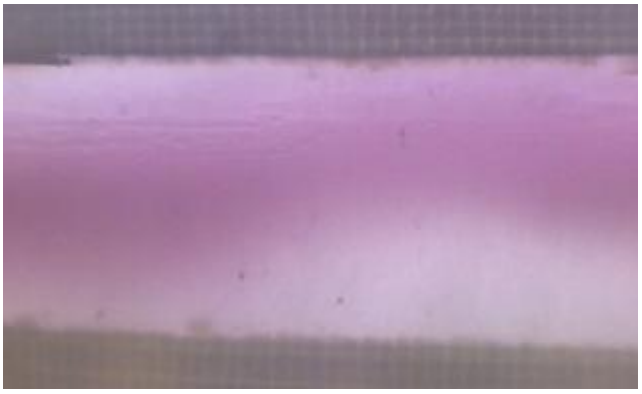

13. June 2010, 20:42:22 At the fourth oil injection tube

11. June 2010, 15:11:58 Four cm from the first oil injection tube

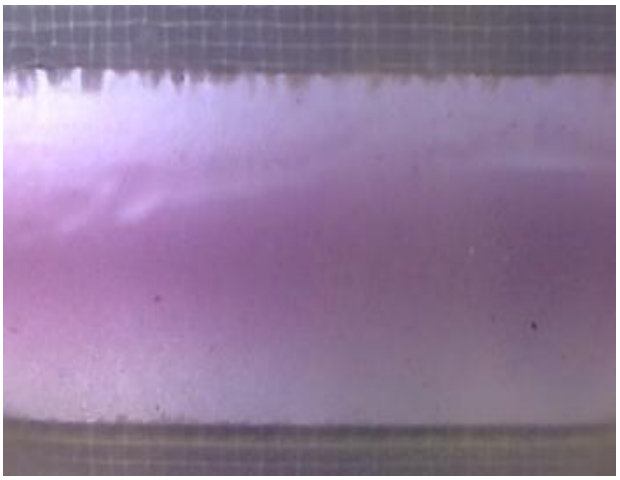

13. June 2010, 20:43:40 10 cm from outlet

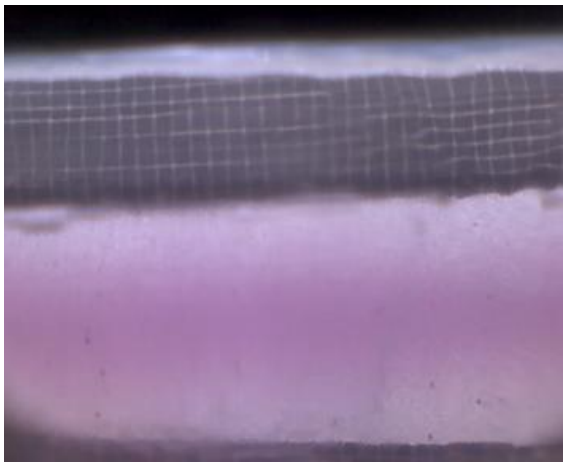

11. June 2010, 15:07:36 8 cm from oulet

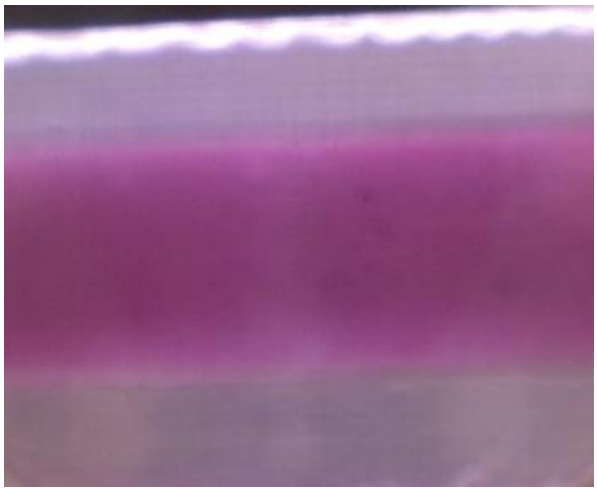

13.June 2010 20:36:36Between water injection tube and first oil injection tube

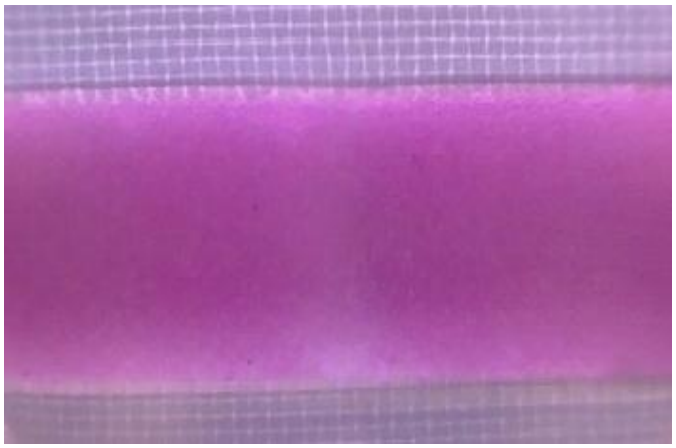

11. June 2010, 15:14:04 Close to water injection tube

Oil Produced at breakthrough of water

APPENDIX H - DATA FOR DISPLACEMENT IN GRAVEL PACK

Table H 1

Measured data for horizontal displacement in gravel pack				
Date	**P [bar]**	**T [°C]**	**dP [bar]**	**Time [sec]**
10:37:06	0,17	22,73	0,19	0,00
10:37:21	0,18	22,74	0,21	0,25
10:37:36	0,23	22,74	0,26	0,50
10:37:51	0,27	22,75	0,30	0,75
10:38:06	0,31	22,74	0,34	1,00
10:38:21	0,34	22,76	0,37	1,25
10:38:36	0,37	22,74	0,40	1,50
10:38:51	0,39	22,75	0,42	1,75
10:39:06	0,41	22,75	0,44	2,00
10:39:21	0,43	22,75	0,46	2,25
10:39:36	0,44	22,75	0,47	2,50
10:39:51	0,45	22,75	0,48	2,75
10:40:06	0,46	22,74	0,48	3,00
10:40:21	0,46	22,74	0,48	3,25
10:40:36	0,46	22,74	0,48	3,50
10:40:51	0,45	22,75	0,48	3,75
10:41:06	0,44	22,74	0,47	4,00
10:41:21	0,43	22,75	0,45	4,25
10:41:36	0,42	22,76	0,44	4,50
10:41:51	0,41	22,76	0,44	4,75
10:42:06	0,41	22,76	0,43	5,00
10:42:21	0,38	22,77	0,41	5,25
10:42:36	0,36	22,75	0,39	5,50
10:42:51	0,34	22,77	0,37	5,75
10:43:06	0,34	22,77	0,36	6,00
10:43:21	0,33	22,78	0,36	6,25
10:43:36	0,32	22,77	0,35	6,50
10:43:51	0,32	22,76	0,35	6,75
10:44:06	0,32	22,77	0,34	7,00
10:44:21	0,31	22,77	0,34	7,25
10:44:36	0,31	22,77	0,34	7,50
10:44:51	0,31	22,78	0,33	7,75
10:45:06	0,30	22,78	0,33	8,00
10:45:21	0,31	22,77	0,34	8,25
10:45:36	0,32	22,77	0,35	8,50
10:45:51	0,33	22,78	0,36	8,75
10:46:06	0,34	22,78	0,37	9,00
10:46:21	0,35	22,77	0,37	9,25
10:46:36	0,35	22,78	0,38	9,50

10:46:51	0,36	22,78	0,38	9,75
10:47:06	0,36	22,79	0,39	10,00
10:47:21	0,36	22,79	0,39	10,25
10:47:36	0,36	22,78	0,39	10,50
10:47:53	0,36	22,78	0,39	10,75
10:48:06	0,36	22,78	0,39	11,00
10:48:21	0,36	22,78	0,39	11,25
10:48:36	0,36	22,78	0,38	11,50
10:48:51	0,36	22,79	0,38	11,75
10:49:06	0,35	22,79	0,38	12,00
10:49:21	0,35	22,79	0,38	12,25
10:49:36	0,35	22,79	0,38	12,50
10:49:51	0,35	22,79	0,37	12,75
10:50:06	0,34	22,79	0,37	13,00
10:50:21	0,34	22,79	0,37	13,25
10:50:36	0,34	22,79	0,36	13,50
10:50:51	0,33	22,8	0,36	13,75
10:51:06	0,33	22,8	0,36	14,00
10:51:21	0,33	22,79	0,35	14,25
10:51:36	0,32	22,8	0,35	14,50
10:51:51	0,32	22,79	0,34	14,75
10:52:06	0,31	22,8	0,34	15,00
10:52:21	0,31	22,81	0,34	15,25
10:52:36	0,31	22,81	0,33	15,50
10:52:51	0,30	22,82	0,33	15,75
10:53:06	0,30	22,81	0,33	16,00
10:53:21	0,30	22,81	0,32	16,25
10:53:36	0,29	22,81	0,32	16,50
10:53:51	0,29	22,81	0,32	16,75
10:54:06	0,29	22,82	0,31	17,00
10:54:21	0,28	22,81	0,31	17,25
10:54:36	0,28	22,81	0,31	17,50
10:54:51	0,28	22,82	0,31	17,75
10:55:06	0,28	22,83	0,30	18,00
10:55:21	0,27	22,81	0,30	18,25
10:55:36	0,27	22,82	0,29	18,50
10:55:51	0,26	22,83	0,29	18,75
10:56:06	0,26	22,83	0,28	19,00
10:56:21	0,25	22,82	0,28	19,25
10:56:36	0,25	22,82	0,27	19,50
10:56:51	0,24	22,82	0,26	19,75
10:57:06	0,22	22,82	0,24	20,00
10:57:21	0,20	22,82	0,22	20,25
10:57:36	0,19	22,81	0,21	20,50
10:57:51	0,19	22,83	0,21	20,75

APPENDIX I - PRODUCTION OF OIL BEFORE AND AFTER BREAKTHROUGH

Information	time [min]	time [sec]	V_{op} [ml]	q_o [ml/min]	q_o [m^3/s]	time [min]	time [sec]	V_t	V_{wp} [ml]	q_w [ml/min]	q_w [m3/s]	qt [ml/min]	q_t[m^3/s]	u_w [m/s]	u_o [m/s]
Start test	0	0	0	0,000	0			0				0,000	0		0
Water into model and Production starts	0	600	14	0,000	0			14				0,000	0		0
	8	480	31	3,850	6,42E-08			31				3,850	6,42E-08		2,85E-04
	15,5	930	41	2,632	4,39E-08			41				2,632	4,39E-08		1,95E-04
	16,32	979	45	2,776	4,63E-08			45				2,776	4,63E-08		2,06E-04
	18,17	1090	51	2,796	4,66E-08			51				2,796	4,66E-08		2,07E-04
Breakthrough, water production	19,12	1147	54	2,814	4,69E-08	0	0	54	0	0,00	0,000E+00	2,814	4,69E-08	0,00E+00	2,08E-04
	21	1260	63	3,014	5,02E-08	2	113	65	2	1,06	3,333E-08	4,078	8,36E-08	1,48E-04	2,23E-04
	23	1380	67	2,904	4,84E-08	4	233	71	5	1,16	7,500E-08	4,064	1,23E-07	3,33E-04	2,15E-04
	29	1740	77	2,648	4,41E-08	10	593	91	14	1,42	2,333E-07	4,065	2,77E-07	1,04E-03	1,96E-04
	31,27	1876	83	2,648	4,41E-08	12	729	104	21	1,73	3,500E-07	4,376	3,94E-07	1,56E-03	1,96E-04
	33,24	1994	84	2,536	4,23E-08	14	847	109	25	1,77	4,167E-07	4,307	4,59E-07	1,85E-03	1,88E-04
	60	3600	148	2,472	4,12E-08	41	2453	238	90	2,20	1,500E-06	4,673	1,54E-06	6,67E-03	1,83E-04
	120	7200	193	1,611	2,68E-08	101	6053	338	145	1,44	2,417E-06	3,048	2,44E-06	1,07E-02	1,19E-04
	180	10800	254	1,413	2,35E-08	161	9653	464	210	1,31	3,500E-06	2,718	3,52E-06	1,56E-02	1,05E-04
	240	14400	299	1,247	2,08E-08	221	13253	574	275	1,25	4,583E-06	2,492	4,6E-06	2,04E-02	9,24E-05
	360	21600	394	1,095	1,83E-08	341	20453	774	380	1,11	6,333E-06	2,210	6,35E-06	2,81E-02	8,11E-05
	420	25200	459	1,094	1,82E-08	401	24053	903	444	1,11	7,400E-06	2,201	7,42E-06	3,29E-02	8,10E-05
	480	28800	533	1,111	1,85E-08	461	27653	1072	539	1,17	8,983E-06	2,281	9E-06	3,99E-02	8,23E-05
	540	32400	578	1,071	1,78E-08	521	31253	1162	584	1,12	9,733E-06	2,192	9,75E-06	4,33E-02	7,93E-05
	600	36000	633	1,056	1,76E-08	581	34853	1272	639	1,10	1,065E-05	2,156	1,07E-05	4,73E-02	7,82E-05
Test end	660	39600	678	1,028	1,71E-08	641	38453	1382	704	1,10	1,173E-05	2,126	1,18E-05	5,21E-02	7,61E-05
						660	39600	1382							

APPENDIX J – ROSEMOUNT DATA LOGGING TOOL SETUP